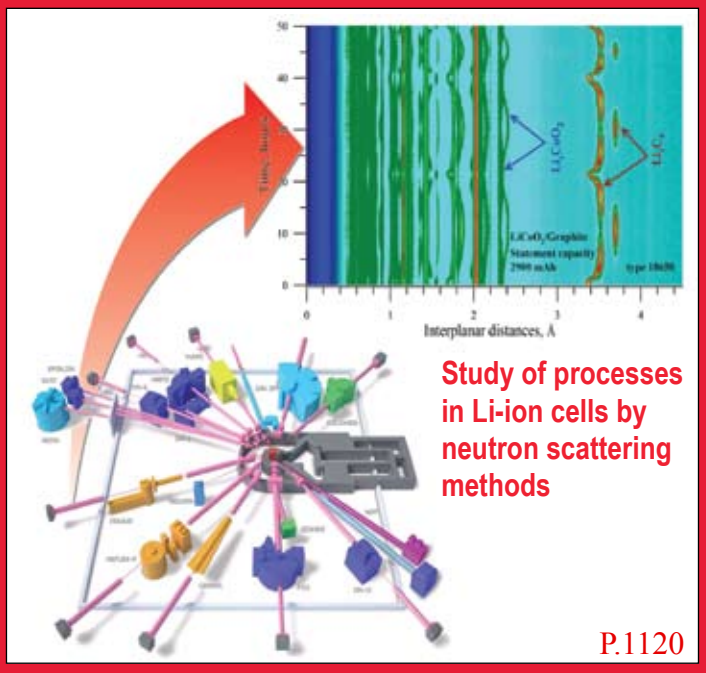
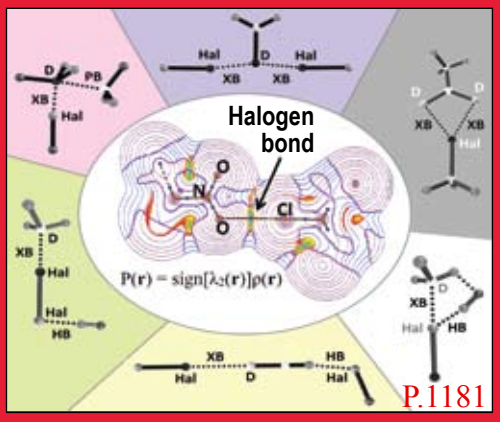
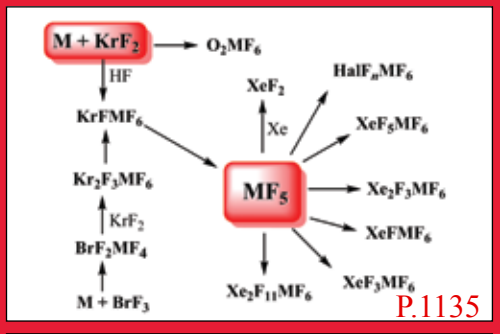
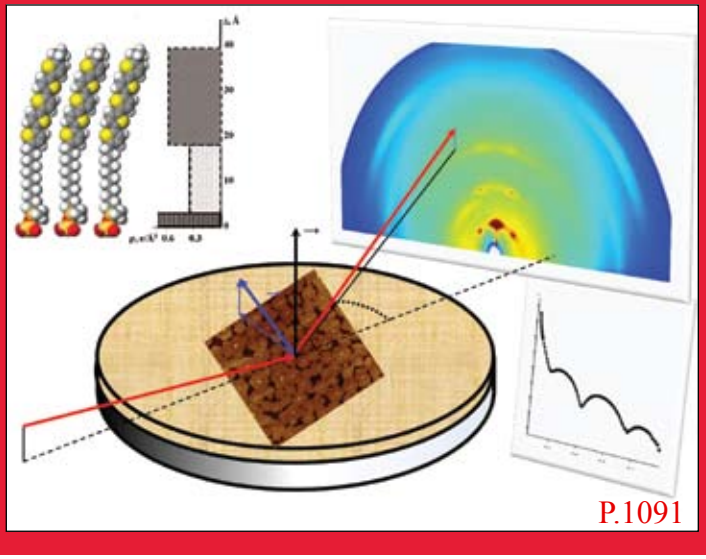
ISSN 0036-021X

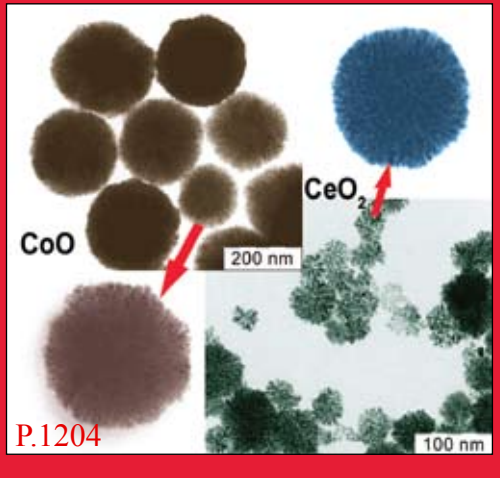
Russian Chemical Reviews











Reviews on current topics in chemistry

International Year of Crystallography

Volume 83 2014 Number 12

 © 2014 Russian Academy of Sciences and Turpion Ltd

DOI 10.1070/RCR4475

Molecular and crystal structures of noble gas compounds

Sh Sh Nabiev, V B Sokolov (deceased), B B Chaivanov

National Research Centre 'Kurchatov Institute'
pl. Kurchatova 1, 123182 Moscow, Russian Federation

Data on the structures of xenon and krypton compounds in various physical states are analyzed and generalized. The structures of simple, coordination, polymeric and clathrate-like compounds of these elements with various types of bonds are considered. Characteristic features of their vibrational spectra are discussed in relation to structural transformations caused by cation – anion interactions, structurally non-rigid intramolecular rearrangements and other factors.
The bibliography includes 332 references.

Contents

I. Introduction 1135
II. Structures of noble gas fluorides, oxyfluorides and oxides 1136
III. Molecular and crystal structures of compounds with Xe – O, Xe – N and Xe – C bonds 1147
IV. Structure of complex xenon and krypton fluorides 1150
V. Structures of the complex compounds of xenon oxyfluorides 1160
VI. Complex compounds with the Xe – metal bonds 1165
VII. Compounds of noble gases as ligands 1166
VIII. Low-temperature matrix-isolated compounds of noble gases 1173
IX. Conclusion 1175

I. Introduction

The ability of noble gases to form chemical compounds discovered in 1962 by Canadian chemist Bartlett† inspired researchers working in various fields of science and technology. Bartlett's sensational discovery [1] crucially changed the traditional views about the inertness of inert gases and about chemical bonding. The long-standing views on the particular stability of the completely filled outermost electron shell of noble gas atoms were violated.

Sh Sh Nabiev Doctor of Physical and Mathematical Sciences, Head of Department at the National Research Centre 'Kurchatov Institute'.
Telephone: (7-499) 196 78 65, e-mail: Nabiev_SS@nrcki.ru
V B Sokolov Doctor of Chemical Sciences, Chief researcher at the same Research Centre
B B Chaivanov Doctor of Chemical Sciences, Deputy Director for Science of the same Research Centre.
Telephone: (7-499) 196 95 27, e-mail: Chaivanov_BB@nrcki.ru
Current research interests of the authors: vibrational and terahertz spectroscopy; molecular struture and dynamics, in particular, of noble gas compounds in various physical states; physics of intermolecular interactions; structural non-rigidity of polyatomic molecules; chemistry and chemical engineering of inorganic fluorine-based oxidants; physics of distributed combustion and explosion of fuel – air mixtures; safety and stability problems of the fuel-and-power sector.

Received 17 June 2014
Uspekhi Khimii **83** (12) 1135 – 1180 (2014); translated by Z P Svitanko

Over two decades after Bartlett's discovery, there appeared hundreds of publications and some reviews and monographs [2 – 9] devoted to the synthesis and physicochemical properties of new compounds of noble gases.‡

Meanwhile, despite the initial Bartlett's assumption that the chemical reaction between Xe and PtF_6 gives the complex $XePtF_6$, attempts to isolate and identify this compound failed. More recent Bartlett's studies (see Refs 11 – 13) showed that the product was actually a mixture of $XeF \cdot PtF_6$, PtF_5 and $XeF \cdot Pt_2F_{11}$. However, as it has been noted,[14, 15] this misinterpretation of the product by no means diminishes the importance of the outstanding Bartlett's discovery, which was assigned in a monograph [16] to the ten most significant experimental results in the history of chemistry.

The development of noble gas chemistry in Russia was started by experimental studies of the reaction between

† Neil Bartlett (1932 – 2008) is a Professor of Chemistry at the University of California, Berkeley, an outstanding inorganic chemist of the second half of the 20th century, the author of two sensational discoveries in chemistry:
— synthesis of the first true chemical compound of a noble gas, xenon ($Xe^+PtF_6^-$);
— molecular oxygen oxidation process ($O_2 + PtF_6^-$).

‡ A virtually complete list of references covering the synthesis of simple compounds of noble gases, studies of their physicochemical properties, structural and spectroscopic parameters over the period from 1962 to 1976 is presented in a monograph by Hawkins.[10]

xenon and fluorine carried out in 1964 at the Kurchatov Institute of Atomic Energy (currently the National Research Centre 'Kurchatov Institute') under supervision of Academician V A Legasov.§ The compounds XeF_2, XeF_4, XeF_6 and KrF_2 were synthesized for the first time, and as soon as 1965, the *Souzkhimreaktiv* (USSR Chemicals) company started the sales of xenon fluorides. As a result, many research centres of the country have received a new fluorinating reagent, xenon difluoride, which was safe and convenient to handle.[17]

Noble gas compounds, in particular, binary xenon fluorides XeF_n ($n = 2$, 4, 6) and krypton fluorides KrF_2 have acquired wide use in both fundamental and applied research as fluoroxidizers [18] for low-temperature inorganic synthesis of fluorine-containing compounds,[6–8,19] for the synthesis of organofluorine (fluoroaromatic, -aliphatic and -heteroorganic) compounds,[20–22] as sources of fluorine for chemical and excimer lasers [23] and components of cathode materials in chemical cells.[24]

Studies of the unique properties of noble gas fluorides in non-aqueous solvents [25–27] resulted in further development and more precise definition of many statements of the fluorine chemistry, reactivity and complexation theories, *etc*. Description of these properties can be found in a number of encyclopaedias.[28–31]

The beginning of the third millennium was marked by a sharp enhancement of the interest in compounds of noble gases, which was called 'a renaissance in noble gas chemistry' by eminent chemist Christie.[32] Binary and complex noble gas fluorides started to be used in various nanotechnologies:[33] for the manufacture of carbon nanostructures and their derivatives: graphene, graphane and fluorographene,[34,35] for ion plasma etching of semiconductor materials,[36] in particular, in selective gas-phase etching of silicon and germanium used in microelectromechanical systems (MEMS).[37] With the use of noble gas fluorides, it became possible to synthesize new simple and coordination compounds of many elements, including fluorides of transition metals in higher oxidation states.[38–41]

Noble gas compounds may serve as vivid examples to illustrate virtually any modern theory of chemical bonding.[42–44] Studies of the properties of elements in high oxidation states provide the unique opportunity for comparing the structural data for molecules that are coordinated in different fashions.[38,45–47] Note that most of these compounds crystallize as several polymorphs;[48] therefore, these data help to understand the nature of polymorphism of molecular and ionic crystals.

Several reviews published in the last decade [22,47,49–56] were devoted to various aspects of noble gas chemistry. The review of Liebman and Deakyne [49] is mainly concerned with the synthesis of complex compounds containing $[NgO]^+$ and $[NgO_2]^+$ cations (Ng = Kr, Xe) and $[Xe_2]^+$ cations. Brisdon [50] considered the general regularities of the synthesis of complexes and coordination compounds of halogens and xenon. Tramsek and Zemva [51] presented a detailed account of the methods for synthesis and physicochemical and spectroscopic (IR, Raman, NMR) properties of xenon difluoride coordination compounds. The reviews by Grochala and coworkers [52,53] are focused on the methods of synthesis, identification and structure and stability calculations for the hydrohalides HNgX (Ng = Ar, Kr, Xe; X = F, Cl, Br, I) and compounds with the Xe–N, Xe–C, Xe–Cl, Kr–O and Kr–N bonds. A number of papers [22,54,55] are actually annual author's reviews of the results of synthesis and identification of some krypton and xenon compounds for the period of 2010 to 2012. A recent publication [56] is mainly devoted to analysis of the data on the properties of organometallic and metal oxide coordination compounds of krypton and xenon. Our previous review [47] was limited, for a number of reasons, to brief consideration of structural features of only binary and complex krypton and xenon fluorides.

Note that over the last 30 years, no reviews presenting a detailed analysis of the structural parameters of simple and complex noble gas compounds in all physical states were published. The latest review [9] that examined the structural and spectroscopic characteristics of cations and anions in noble gas complexes in considerable detail was published in 1984.

This review presents systematic analysis of most reliable data on the structures of compounds of noble gases in various physical states published in the last 15 years. The structures of simple, coordination, polymeric and clathrate-like compounds of noble gases with different types of bonds are considered. Details of vibrational spectra of these compounds related to their structural transformations caused by cation–anion interactions, structurally non-rigid intramolecular rearrangements and other factors are discussed.

II. Structures of noble gas fluorides, oxyfluorides and oxides

II.1. Brief characterization of noble gas fluorides, oxyfluorides and oxides

Most of noble gas compounds (fluorides, oxyfluorides and oxides) were discovered in the period from the mid-1960 to the early 1970s;[2–7] their physicochemical properties have been studied for all physical states (Table 1). However, some simple compounds of noble gases and a considerable number of complex compounds involving noble gas fluorides have not yet been prepared in a pure state, which is due to cumbersome synthesis, unusually high chemical reactivity and thermodynamic instability.

Binary xenon and krypton fluorides are colourless transparent crystalline solids with a strong smell, stable in a dry atmosphere up to 600–800 K. In open air, lower xenon and krypton fluorides (XeF_2 and KrF_2) are slowly hydrolyzed to give hydrogen fluoride. Hydrolysis of XeF_4 and XeF_6 also gives off hydrogen fluoride and results in the formation of crystalline xenon trioxide XeO_3, which is characterized in the solid state as an explosive compound with a critical mass of not more than 30 mg. Purified XeO_2F_2 exists as colourless crystals and on melting, it forms a colourless liquid. Xenon dioxydifluoride is more stable than XeO_3 but, similarly to the oxide, it is explosive. In a moist atmosphere, XeO_2F_2 is rapidly hydrolyzed to XeO_3 and it also reacts with XeF_6 to give $XeOF_4$. Xenon oxytetrafluoride is also formed upon controlled hydrolysis of XeF_6 or upon the reaction of XeF_6 with SiO_2; at room temperature, this is a colourless transparent liquid. Xenon tetroxide is formed upon the reactions of perxenates (for example, Na_4XeO_6,

§ V A Legasov (1936–1988) is a world renowned scientist in the use of nuclear physical and plasma methods for the synthesis and studies of properties of new compounds in abnormally high oxidation states.

Table 1. Molecular constants of some noble gas fluorides, oxyfluorides and oxides.[31, 47]

Compound	Bond	Bond length /Å	Angle	Value of the angle /deg	Type of structure	Point group of symmetry [a]
Xenon and krypton fluorides						
XeF_2	Xe–F	1.979 ± 0.015	F–Xe–F	180	Linear	$D_{\infty h}$
KrF_2	Kr–F	1.889 ± 0.01	F–Kr–F	180	"	$D_{\infty h}$
XeF_4	Xe–F	1.94 ± 0.01	F–Xe–F	90.0 ± 0.02	Planar square	D_{4h}
	F–F	2.77 ± 0.02				
XeF_6	Xe–F(1)	1.941			Distorted octahedron	C_{3v}
	Xe–F(2)	1.850				
	F(1)–F(1)	3.108				
	F(2)–F(2)	2.535				
	F(1)–F(2)	2.498				
Xenon oxyfluorides and oxides						
$XeOF_4$	Xe–F	1.90 ± 0.05	F–Xe–F	172.4	Square pyramid	C_{4v}
	Xe–O	1.703 ± 0.15	O–Xe–F	91.8		
XeO_2F_2	Xe–F	1.899 ± 0.03	F–Xe–F	174.7	Bisphenoid	C_{2v}
	Xe–	1.714 ±0.04	O–Xe–O	105.7		
XeO_3	Xe–	1.760 ± 0.03	O–Xe–O	103.0	Trigonal pyramid	C_{3v}
XeO_4	Xe–	1.736 ± 0.02	O–Xe–O	109.0	Tetrahedron	T_d
	O···O	2.832				

[a] Hereinafter symmetry.

Ba_2XeO_6) with concentrated sulfuric acid at 293 K. At room temperature, XeO_4 is a gaseous, highly potent explosive, which is converted on cooling first to a liquid and then to a solid.

Three thermodynamically unstable xenon oxyfluorides, XeO_3F_2, XeO_2F_4 and $XeOF_6$, are known. Xenon trioxydifluoride was isolated upon the reaction of XeF_6 with Na_4XeO_6 at room temperature.[57] Xenon dioxytetrafluoride is formed upon the reaction of XeO_3F_2 and XeF_6.[58] Xenon oxyhexafluoride has not been isolated in a pure state, but the reaction of $KrF^+Sb_2F_{11}^-$ with $XeOF_4$ at 263 K yielded [59] the complex compound $XeOF_5^+Sb_2F_{11}^-$.

The synthesis and identification of radon compounds are exceptionally difficult due to the high activity of the most stable ^{222}Rn isotope (half-life $\tau_{1/2}$ = 3.825 days);[60] therefore, the information on radon compounds (mainly fluorides) is only qualitative. It is only known that the fluorides RnF_2 and RnF_4 are formed upon reactions of radon with liquid halogen fluorides (ClF, ClF_3, ClF_5, BrF_3, IF_7) at room temperature, with O_2F_2 at 173 K, or under the action of α-radiation in liquid fluorine or solid ClF_3 at 77 K.[61] Radon difluoride is a colourless crystalline solid resembling XeF_2 in the properties. When made to react with fluorine-based oxidants such as O_2SbF_6, Cl_2FAsF_6, $K_2[NiF_6]$ or $N_2F_3Sb_2F_{11}$, radon difluoride forms solid compounds containing the RnF^+ cation. According to estimates,[7, 60, 62] the enthalpies of formation of radon fluorides are as follows:

Fluoride	RnF_2	RnF_4	RnF_6
$-\Delta H^\circ_{298}$ /kJ mol^{-1}	240.3	340	412

The average Rn–F bond energy is 194.7 kJ mol^{-1}.

II.2. Nature of chemical bonds in binary xenon and krypton fluorides

To date, several concepts have been developed to account for the nature of chemical bonds in compounds of noble gases; however, none of these is fully adequate.[63] Therefore, we will dwell on the concepts proposed to describe the nature of bonding in binary xenon and krypton fluorides. According to one concept,[64] xenon fluorides are formed upon excitation of the xenon valence shell

$$Xe(5s^24d^{10}5p^6) \longrightarrow Xe^*(5s^24d^{10}5p^{6-n}\,5d^n)$$

which makes the xenon atom able to form two bonds in XeF_2 (n = 1), four bonds in XeF_4 (n = 2) or six bonds in XeF_6 (n = 3).

Another, most popular, concept based on the Gillespie–Nyholm valence shell electron pair repulsion theory (VSEPR) postulates the formation of three-centre orbitals for four valence electrons.[65, 66] Within this theory, a p-orbital of xenon in XeF_2 partly overlaps with a p-orbital of fluorine, thus forming bonding, non-bonding, and antibonding orbitals, which are filled by four valence electrons. Other orbitals form the second (XeF_4) and third (XeF_6) three-centre bonds.[65]

The bond in KrF_2 is usually described in terms of delocalized molecular orbitals constructed by combination of krypton and fluorine p_σ-orbitals.[5] One filled $4p_\sigma$ orbital of krypton and two $2p_\sigma$ orbitals of fluorine are considered.[67] Calculations carried out by Sokolov and Prusakov [5] demonstrated that the charges on the fluorine, xenon and krypton atoms are described by equivalent formulas, $Xe^{+1.58}(F^{-0.79})_2$ and $Kr^{+0.94}(F^{-0.47})_2$, indicating a higher degree of covalency for the bonds in KrF_2 than in XeF_2.

II.3. Molecular structures of noble gas fluorides, oxyfluorides and oxides

II.3.a. Xenon and krypton fluorides

The molecular structures of xenon fluorides XeF_n ($n = 2$, 4, 6) were mainly studied by gas phase electron diffraction [68, 69] and vibrational spectroscopy.[70–73] In some cases, NMR, EPR, photoelectron spectroscopy and electric deflection measurements of unfocused electron beam were used.[74, 75] The equilibrium geometric configurations of NgF_n molecules (Ng = Kr, Xe; $n = 2$, 4, 6) were determined and fundamental vibration frequencies were calculated using advanced quantum chemistry techniques (see publications [76, 77] and references cited therein).

The XeF_2 molecule is linear, as indicated by the vibrational spectra of XeF_2, which exhibit three bands

$$\Gamma_{vib} = \sum_g^+(R) + \sum_u^+(IR) + \Pi_u(IR)$$

at $\nu_1 = 516$, $\nu_2 = 213$, $\nu_3 = 560$ cm^{-1} (gas) or $\nu_1 = 496$, $\nu_3 = 547$ cm^{-1} (solid),[70–72, 78] which correspond to the $D_{\infty h}$ symmetry of the structure.

The vibrational spectra of XeF_4 in the gas phase exhibit 6 bands

$$\Gamma_{vib} = A_{1g}(R) + A_{2u}(IR) + B_{1g}(R) + B_{2g}(R) + 2E_u(IR)$$

at $\nu_1(A_{1g}) = 554$, $\nu_2(B_{1g}) = 218$, $\nu_3(A_{2u}) = 291$, $\nu_4(B_{2g}) = 524$, $\nu_6(E_u) = 586$, $\nu_7(E_u) = 161$ cm^{-1} (Refs 70 and 72), which correspond to the D_{4h} symmetry of the structure.

The geometric parameters of the xenon di- and tetrafluoride molecules obtained in electron diffraction experiments [68, 69] support the vibrational spectroscopy data on the linear structure of XeF_2 and square planar structure of XeF_4. The fact that the Xe–F bonds are longer in XeF_2 than in XeF_4 can be attributed to the interaction of axial bonds with three lone electron pairs in equatorial positions. This is consistent with the general rule according to which an increase in the electronegativity of the central atom in a molecule results in shortening of the bonds.[65, 66]

The KrF_2 molecule is also linear. This was shown by gas phase electron diffraction studies [79] and by vibrational spectroscopy.[5, 78, 80] The vibrational spectrum of KrF_2 has three bands at $\nu_1 = 449$, $\nu_2 = 233$, $\nu_3 = 588$ cm^{-1} (gas) and $\nu_1 = 462$, $\nu_3 = 580$ cm^{-1} (solid), corresponding to vibrations of a $D_{\infty h}$-symmetry structure.[78, 80]

The XeF_6 molecule can serve as a vivid example of structurally non-rigid binary hexacoordinate compounds. Out of the 17 known hexafluoride molecules,[81] only this molecule does not form an octahedral configuration.[69, 82]

According to the most widely known concept,[83] the XeF_6 molecule has a distorted octahedral geometry (C_{3v} symmetry). The concept is based on the assumption that the XeF_6 molecule is non-rigid *via* pseudo-rotation,[84] which results in transposition of four fluorine atoms, while the other two fluorine atoms located in the *trans*-positions relative to each other remain intact.

The series of experimental and theoretical studies of the structure of XeF_6 reported in a number of publications [72, 73, 81, 85] demonstrated that the non-rigidity *via* pseudo-rotation is convenient to consider in terms of motion of the lone electron pair, which can occur towards the formation of intermediate structures having the C_{2v} ($C_{3v} \rightarrow C_{2v} \rightarrow C_{3v}$), C_{4v} ($C_{3v} \rightarrow C_{4v} \rightarrow C_{3v}$) or O_h ($C_{3v} \rightarrow O_h \rightarrow C_{3v}$) symmetry.

It was noted [81, 86–88] that the energy barriers for these rearrangements to C_{2v}-, C_{4v}- and O_h-symmetry intermediate structures have not been determined experimentally. However, it is presumed [81, 89] that the $C_{3v} \rightarrow O_h \rightarrow C_{3v}$ transformation is energetically least favourable and the potential maximum for the $C_{3v} \rightarrow C_{4v} \rightarrow C_{3v}$ transformation may be much higher than that for $C_{3v} \rightarrow C_{2v} \rightarrow C_{3v}$. The barrier for the $C_{3v} \rightarrow C_{2v} \rightarrow C_{3v}$ rearrangement can be easily overcome at 300 K at the expense of thermal energy. Detailed investigations of the vibrational spectra of XeF_6 in the gas and solid phases and in cryogenic solutions [72, 73, 81, 85] provided experimental proof for the fact that the XeF_6 molecule has a distorted octahedral structure (C_{3v} symmetry).

Dixon and coworkers [90–92] performed a series of quantum chemical calculations of the equilibrium geometric configurations and the vibrational spectra of XeF_6 with the assumption that it exists as structures with the C_{2v}, C_{3v} and O_h symmetry (Fig. 1). The results of coupled cluster (CC) calculations,[92] in particular, CCSD(T)–F12x ($x = a$, b) calculations [93, 94] with two basis sets (aVTZ and awCVTZ for fluorine and xenon atoms, respectively) demonstrated that the C_{3v}-symmetry structure with the stereochemically active lone electron pair has the lowest energy in the ground state. The energy of this structure is 4.5 kJ mol^{-1} lower than the energy of the C_{2v}-symmetry structure and 7.5 kJ mol^{-1} lower than that of the O_h-symmetric structure. The C_{2v} symmetry corresponds to the transition state between various C_{3v} minima on the potential energy surface of the C_{3v} structure pseudo-rotation, while the O_h symmetry corresponds to the saddle point structure on the route to the C_{2v} transition state.

It was noted [92] that the calculated vibrational frequencies for C_{3v}-symmetry structure are best fitted to the experimental data for gaseous XeF_6. Meanwhile, the calculated heats of formation of XeF_6 amounting to -259.6 ± 5.9 and -267.5 ± 5.9 kJ mol^{-1} at 0 and 298 K, respectively, considerably differ from experimental results obtained in one work [31] (-338.2 kJ mol^{-1}, $T = 298$ K) but are close to the values reported in another publication [47] (-288.1 kJ mol^{-1}, $T = 298$ K).

Thus, the assumption of a non-rigid model for the XeF_6 molecule accounts satisfactorily for not only most of experimental data on the XeF_6 structure [81, 87, 88] but also some characteristic features of the molecule. The latter statement

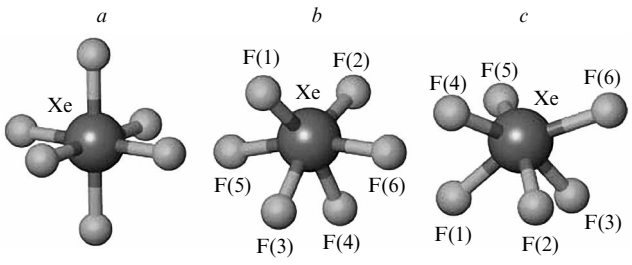


Figure 1. Optimized geometric structures of the O_h (*a*), C_{2v} (*b*) and C_{3v} (*c*) symmetry of the xenon hexafluoride molecule.[92]
Bond lengths/Å: Xe–F = 1.917 (*a*); Xe–F(1) = 1.968, X–F(5) = 1.845, Xe–F(5) = 1.886 (*b*), Xe–F(1) = 1.843, Xe–F(4) = 1.950 (*c*); angles/deg: F(1)–Xe–F(2) = 122.08, F(3)–X(3)–X(4) = 79.08, F(5)–X(3)–F(6) = 164.68 (*b*), F(1)–Xe–F(2) = 82.08, F(4)–Xe–F(5) = 109.33 (*c*).

refers to the absence of bands in the bending mode region in the vibrational spectra of XeF_6 and the absence of an effective dipole moment in the XeF_6 molecule.[81] The fixed dipole moment of XeF_6 may be very low ($\leqslant 10^{-2}$ D) due to interaction between the electron pair and fluorine atoms.[81,88]

II.3.b. Xenon oxyfluorides and oxides

The $XeOF_4$ molecule has a square pyramidal structure (C_{4v} symmetry), which was confirmed by microwave spectroscopy data.[95] The axial oxygen atom is located in the *trans*-position relative to the lone electron pair. The electron diffraction data [96] confirmed the square pyramidal structure for gaseous $XeOF_4$; the Xe–O and Xe–F bond lengths are 1.7109 and 1.9010 Å, respectively, and the O–Xe–F angle is 91.0°. The vibrational spectrum of $XeOF_4$ exhibits nine bands

$$\Gamma_{vib} = 3\,A_1(IR,R) + 2\,B_1(R) + B_2(R) + 3\,E(IR,R)$$

at [70] $\nu_1(A_1) = 926$, $\nu_2(A_1) = 577$, $\nu_3(A_1) = 286$, $\nu_4(B_1) = 225$, $\nu_5(B_1) = 543$, $\nu_6(B_2) = 219$, $\nu_7(E) = 609$, $\nu_8(E) = 362$ and $\nu_9(E) = 161$ cm^{-1}, which correspond to the C_{4v} symmetry of the structure.

According to the VSEPR theory,[65,66] the XeO_2F_2 molecule should be shaped like a trigonal bipyramid (C_{2v} symmetry) in which two oxygen atoms and the lone pair occupy axial positions, while two fluorine atoms are equatorial. However, according to the data of Raman spectroscopy of liquid and solid XeO_2F_2 and IR spectroscopy of xenon dioxydifluoride in an argon matrix,[97] the fluorine atoms in the molecule occupy, conversely, the axial positions, while the oxygen atoms and the lone pair are in the equatorial positions. This gives rise to a bisphenoid structure (C_{2v} symmetry), although a distorted tetrahedral geometry cannot be ruled out either.[29,98] The vibrational spectrum of XeO_2F_2,[97,98] similar to the spectrum of $XeOF_4$, exhibits nine bands

$$\Gamma_{vib} = 4\,A_1(IR,R) + A_2(R) + 2\,B_1(IR,R) + 2\,B_2(IR,R)$$

at $\nu_1(A_1) = 848$, $\nu_2(A_1) = 490$, $\nu_3(A_1) = 333$, $\nu_4(A_1) = 198$, $\nu_5(A_2) = 224$, $\nu_6(B_1) = 905$, $\nu_7(B_1) = 324$, $\nu_8(B_2) = 585$ and $\nu_9(B_2) = 317$ cm^{-1}, which correspond to the C_{2v} symmetry of the structure.

The molecules of $Xe^{16}OF_2$ and $Xe^{18}OF_2$ synthesized by Brock *et al.*[99] by hydrolysis of XeF_4 in HF at 210 K have an unusual T shape (C_{2v} symmetry). The Raman spectra of solid $Xe^{16}OF_2$ show five bands

$$\Gamma_{vib} = 3\,A_1(IR,R) + 2\,B_1(IR,R) + B_2(IR,R)$$

at $\nu(Xe-O) = 749.9$, $\nu_s(XeF_2) = 467.8$, $\rho(XeOF_2) = 298.1$ cm^{-1} (in plane), $\delta(XeF_2) = 256.2$ cm^{-1} (out-of-plane) and $\delta(XeF_2) = 154.0$ cm^{-1} (in plane), which correspond to the C_{2v} symmetry of the structure. No $\nu_{as}(XeF_2)$ mode was observed in the spectra. The band frequencies in the spectrum of $Xe^{18}OF_2$ virtually do not differ from those for $Xe^{16}OF_2$, except for the Xe–O band, which shifts to lower frequency by 712.8 cm^{-1}. Quantum chemical calculation of the equilibrium geometric configurations of $(XeOF_2)_n$ ($n = 1-3$) by CC and density functional theory methods with three-parameter hybrid B3LYP functional demonstrated [99] that the Xe–O and Xe–F bond lengths in the $XeOF_2$ monomer (Fig. 2 *a*) are 1.809 and 1.996 Å, respectively, the latter value being close to the corresponding value for XeF_4 (1.971 Å). The O–Xe–F and F–Xe–F angles are 96.4 and 167.1°, respectively. On going to the $XeOF_2$ dimer and trimer, the Xe–O bond lengths remain almost invariable, while the Xe–F bond lengths and the O–Xe–F and F–Xe–F angles somewhat change. Meanwhile, the bridging Xe···O and Xe···F bonds

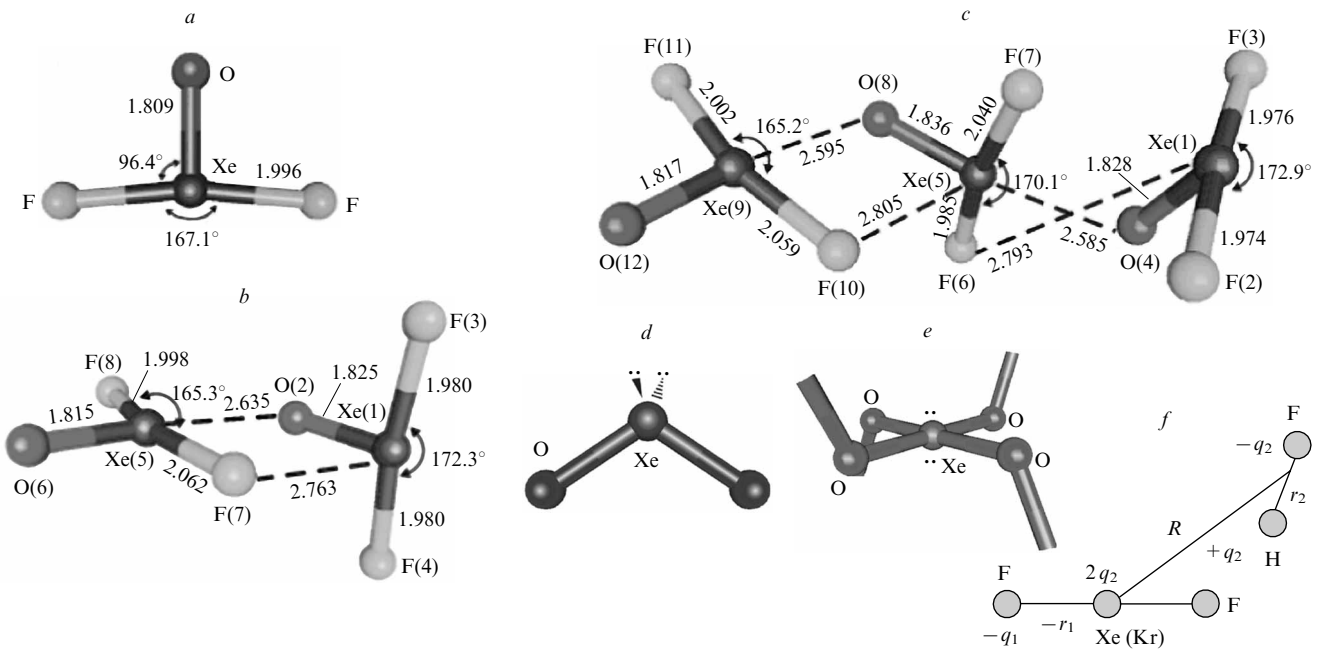


Figure 2. Structures of $XeOF_2$ (*a*), $(XeOF_2)_2$ (*b*), $(XeOF_2)_3$ (*c*) molecules,[99] isolated XeO_2 molecule (*d*) and $(XeO_2)_n$ molecules within a polymer chain (*e*); the bond lengths are given in Å;[100] for *f*, see the text.

Table 2. Experimental frequencies (cm^{-1}) in the Raman spectra of $Xe^{16}O_2$, $Xe^{16}O^{18}O$ and $Xe^{18}O_2$.[100]

$Xe^{16}O_2$	$Xe^{16/18}O_2$	$Xe^{18}O_2$	Group of vibrations	Assignment
632.3 (1)	626.5 sh	625.8 (1)	E	$\nu_{as}(XeO_{trans}-XeO_{trans})$
570.3 (100)	550.9 (100)	542.6 (100)	A_1	$\nu_s(XeO_4)$
			B_2	$\nu_{as}(XeO_{2\,trans}-XeO_{2\,trans})$
283.9 (3)	276.9 (2)	270.0 (3)	B_2	u(XeO_4) out of plane
239.1 (2)	231 sh	226.6 (2)	B_1	$\delta(XeO_{2\,cis}+XeO_{2\,cis})$
227.9 (4)	221.3 (4)	216.9 (6)		
–	–	–	A_2	$\delta(XeO_{2\,trans})$ out of plane
168.9 (13)	165.0 (19)	161.1 (13)	E	$\delta(XeO_{2\,trans})$ in plane
99.5 (14)	99.3 (17)	99.5 (15)	–	lattice vibrations

Note. The following designations of the vibration types are used: ν is stretching, δ is bending, u is umbrella, s is symmetric, as is antisymmetric, sh is shoulder; the numerals in parentheses are relative band intensities.

are noticeably longer than Xe–O and Xe–F (see Figs 2 *b*,*c*).

The oxides $Xe^{16}O_2$, $Xe^{16}O^{18}O$ and $Xe^{18}O_2$ have been prepared[100] by hydrolysis of XeF_4 in $H_2{}^{16}O$ and $H_2{}^{18}O$ and in an $H_2{}^{16}O + H_2{}^{18}O$ equimolar mixture in the presence of 2 M H_2SO_4 at 273 K. According to the VSEPR theory,[65,66] a monomeric XeO_2 molecule should have a bent triatomic structure (see Fig. 2 *d*), which is expected to produce three normal vibrations.[101] However, examination of the Raman spectra of the synthesized oxides $Xe^{16}O_2$, $Xe^{16}O^{18}O$ and $Xe^{18}O_2$ (Table 2) demonstrated that these compounds are chain polymers with an AX_4E_2 type structural unit (flattened tetrahedron with the D_{2d} symmetry; A and X are atoms of different elements, E is the lone pair); in this particular case, this unit is XeO_4 (see Fig. 2 *e*). From the data presented in Table 2, it follows that the vibrational spectrum of XeO_2 incorporated in the polymer chain shows six bands out of the nine bands allowed by the selection rules

$$\Gamma_{vib} = A_1(R) + 2\,A_2(NA) + B_1(IR,R) + 2\,B_2(IR,R) + 3\,E(IR,R)$$

which correspond to the D_{2d} symmetry of the structure (NA is non-active vibration).

According to a publication,[102] the XeO_3 molecule has a trigonal bipyramidal geometry (C_{3v} symmetry). This fact was confirmed by examination of the vibrational spectra of xenon trioxide in the solid phase and in an aqueous solution. According to another work,[103] the vibrational spectrum of XeO_3 shows four bands

$$\Gamma_{vib} = 2\,A_l(IR,R) + 2\,E(IR,R)$$

at $\nu_1(A_1) = 780$, $\nu_2(A_1) = 344$, $\nu_3(E) = 833$, $\nu_4(E) = 317$ cm^{-1} (aqueous solution), $\nu_1(A_1) = 770$, $\nu_2(A_1) = 311$, $\nu_3(E) = 820$, $\nu_4(E) = 298$ cm^{-1} (solid phase), which correspond to the C_{3v} symmetry of the structure. Quantum chemical calculations[104,105] of the vibrational frequencies of XeO_3 performed by the CC method with the Dunning basis set (cc-pv5z) gave the following values: $\nu_1 = 757$, $\nu_2 = 315$, $\nu_3 = 846$, $\nu_4 = 280$ cm^{-1} (Ref. 104) and $\nu_1 = 777$, $\nu_2 = 304$, $\nu_3 = 852$, $\nu_4 = 262$ cm^{-1} (Ref. 105).

An electron diffraction investigation of the molecular structure of gaseous XeO_4 attested to a tetrahedral configuration of the molecule (T_d symmetry).[106] This was confirmed by examination of the vibrational spectra of solid- and gas-phase xenon tetroxide[107] and by quantum chemical calculations.[104,105] The vibrational spectrum of XeO_4 shows four bands

$$\Gamma_{vib} = A_l(R) + E(R) + 2\,F_2(IR,R)$$

at $\nu_1(A_1) = 776$, $\nu_2(E) = 267$, $\nu_3(F_2) = 879$, $\nu_4(F_2) = 306$ cm^{-1} (gas), $\nu_1(A_1) = 774$, $\nu_2(E) = 253$, $\nu_3(F_2) = 868$, $\nu_4(F_2) = 304$ cm^{-1} (solid), which correspond to the T_d symmetry of the structure.

In an estimation of the force constants for the $Xe^{16}O_4$ and $Xe^{18}O_4$ molecule,[107] it was found that, unlike most known tetrahedral molecules,[101] XeO_4 has a negative interaction force constant (-0.18 mdyn $Å^{-1}$). The considerable difference between the force fields of XeO_4 and transition metal tetroxides, in particular, MO_4 type oxides (M = Ru, Os),[108] and the negative sign of the interaction constant attest to a pronounced distinction between the natures of bonds in XeO_4 and in noble metal tetroxides.

II.4. Molecular structures of binary noble gas fluorides in non-aqueous solvents

Non-aqueous solvents are widely used in the chemistry of noble gases; without them, many achievements would have been impossible.[6–9,109]

By analysis of results of experimental studies[5–8,110,111] and physical and chemical properties of non-aqueous solvents,[112] most promising fluorinating agents for the use in non-aqueous solutions were elucidated, namely, XeF_2, KrF_2 and O_2F_2.[5–7,26,113–115] The solubility, high reactivity, the possibility to carry out targeted synthesis and the purity of final products make solutions of KrF_2 most effective media for the preparation of fluorides.[5–7,109,116,117] Using these solutions, it is possible to prepare almost any (with a minor exception) currently known simple and complex fluorides of noble gases and transition elements in higher oxidation states.

Being strong oxidants, noble gas fluorides differ markedly in the chemical properties. This is indicated most clearly in the vibrational spectra of these compounds in non-aqueous fluorinated solvents.[118–120]

A study of the Raman spectra of xenon difluoride dissolved in anhydrous HF showed[118] that, unlike solutions of XeF_2 in acetonitrile[119] or bromine pentafluoride,[118] in this case, the $\nu_1(\Sigma_g^+)$ mode of XeF_2 has a complex contour with several clear-cut maxima. Analysis of the spectral data[18] for a broad range of XeF_2 concentrations in HF (0.2–0.004 mol mol^{-1}) demonstrated that the observed contour of the $\nu_1(\Sigma_g^+)$ line of xenon difluoride can be divided into three components with peaks at 475, 516 and 545 cm^{-1}. The 475 cm^{-1} peak was assigned to a vibration of the bridging Xe···F bond in solvate systems such as $XeF_2-FXe^{\delta+}\cdots FHF^{\delta-}$ formed upon the donor-acceptor interaction between the Lewis base (XeF_2) and Lewis acid (HF). The bands at 516 and 545 cm^{-1} were assigned to the fully symmetric Xe–F mode of the non-bonded XeF_2 molecule and the $\nu_3(\Sigma_u^+)$ mode, which appeared due to distortion of the linear configuration of XeF_2.

Analysis of the Raman spectra of krypton difluoride in an HF solution in the concentration range of 0.30–0.004 mol mol^{-1} at 293–300 K showed [120] that, unlike the spectrum of the XeF_2-HF system, the spectrum of the KrF_2-HF system has one line, which is consistent with the selection rules for $D_{\infty h}$-symmetry linear molecules. Within the framework of semiclassical theoretical views,[120] the intermolecular interaction potentials for NgF_2 (Ng = Kr, Xe) and HF were calculated in terms of a simple electrostatic model (see Fig. 2*f*).

The shift of vibrational frequencies ($\Delta\nu$) of NgF_2 (Ng = Kr, Xe) due to interaction with HF was determined from the expression

$$\Delta\nu = \pm\nu_0 \left[2\left(\frac{\partial^2 U}{\partial r^2}\bigg|_{rl} \Big/ \frac{\partial^2 U_0}{\partial r^2}\bigg|_{rl}\right)\right]^{-1} \quad (1)$$

where U is the potential energy of the intermolecular interaction in the NgF_2-HF system, U_0 is the potential energy of the interatomic interaction in a single linear NgF_2 molecule, θ and φ are the azimuthal and polar angles relative to the Z axis, respectively. Averaging of the shift $\Delta\nu$ over all possible orientations of the NgF_2 and HF molecules gave the statistical mean value, the spectrum of NgF_2 molecules (Ng = Kr, Xe) being represented by a set of δ functions for each selected set of frequencies

$$\delta\left[(\Delta\nu-\nu_0)\left(2\frac{\partial^2 U}{\partial r^2}\Big/\frac{\partial^2 U_0}{\partial r^2}\right)\right]^{-1} = \quad (2)$$

$$= \lim_{t\to 0}\frac{t}{\pi}\left\{\left[(\Delta\nu-\nu_0)\left(2\frac{\partial^2 U}{\partial r^2}\Big/\frac{\partial^2 U_0}{\partial r^2}\right)\right]^2 + t^2\right\}^{-1}$$

According to the calculations, the simulated contour for the KrF_2-HF system is similar to the experimental one, whereas in the case of XeF_2-HF, the simulated and experimental contours are substantially dissimilar. This provides additional evidence for the presence of solvation effects that influence the energy and spectral parameters of the XeF_2-HF system. Apart from the linear solvation, non-linear solvation processes are possible. In highly polar solvents, the latter give rise to areas of local orientational ordering of the molecular structure as a result of interaction of permanent and induced dipoles.[121]

Analysis of the Raman spectra of XeF_4 in an HF solution indicates [122] that, unlike the XeF_2-HF system, in the XeF_4-HF system in the concentration range of 0.0036–0.0014 mol mol^{-1}, interactions between the XeF_4 and HF molecules are nearly absent. This fact confirms the conclusion [110] based on the electrical conductivity data for solutions of XeF_4 in HF and on the ^{19}F NMR spectra about molecular solubility of XeF_4 in HF and chemical stability of this system.

A study of the Raman spectra of the XeF_6-HF system demonstrated [87, 122] that they depend substantially on the XeF_6 concentration in anhydrous HF. This is due to the fact that in concentrated solutions, polymeric forms of xenon hexafluoride exist along with monomeric modifications. According to the views developed in a number of publications,[123–125] the following conclusion was drawn:[122, 126] in a highly polar solvent such as HF,[127] the XeF_6 molecule can be considered as the ionic compound $[XeF_5]^+[F]^-$, whereas polymeric forms of XeF_6 exist as $([XeF_5]^+[F]^-)_2$ dimers and $([XeF_5]^+[F]^-)_4$ tetramers.

The Raman spectra of XeF_6 solutions of various concentrations in anhydrous HF in the frequency range of 450–750 cm^{-1} are presented in Fig. 3, and the frequencies, intensities and preliminary assignment of the bands are in Table 3. It can be seen from these data that over the whole range of XeF_6 concentrations, a polarized band at ~618 cm^{-1} and a depolarized band at ~507 cm^{-1} are observed. According to investigation results,[72, 73, 128] these bands were assigned to the Xe–F vibrations of unionized

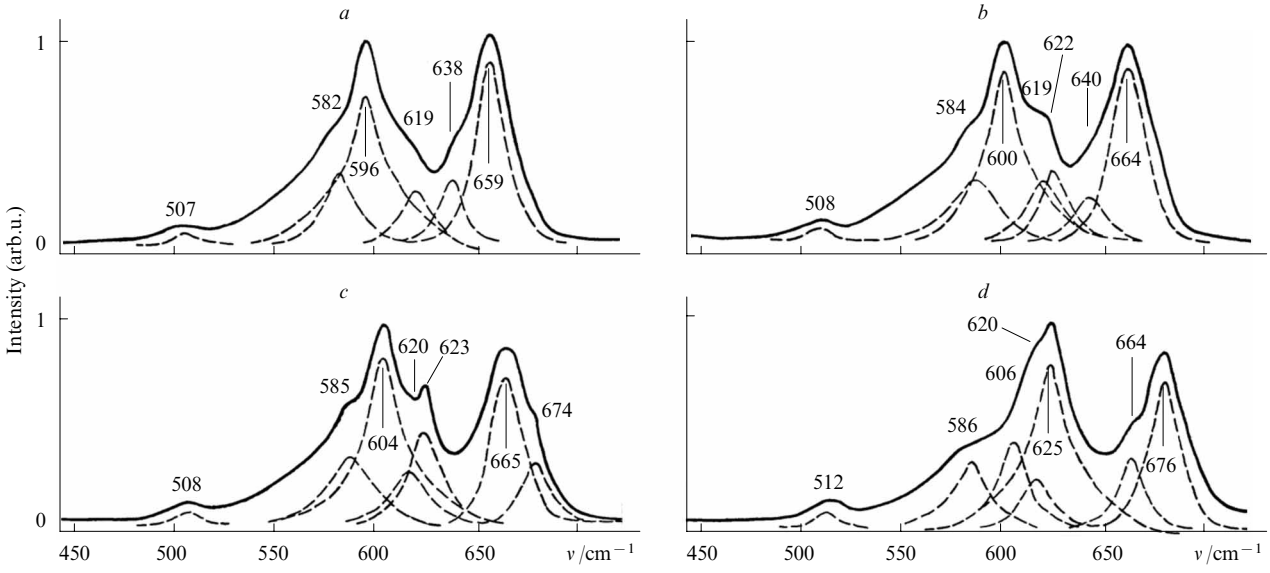


Figure 3. Raman spectra of XeF_6 in anhydrous HF at 293 K in the frequency range of 450–750 cm^{-1} at solution concentrations of 0.12 (*a*), 0.063 (*b*), 0.024 (*c*), 0.0083 (*d*) mol mol^{-1} (see Ref. 122).
The dashed line shows the contributions of individual components found by resolution of the intricate experimental contour.

Table 3. Assignment of the experimental frequencies (cm^{-1}) in the Raman spectra of the XeF_6-HF system at different XeF_6 concentrations ($T = 293$ K).[122]

XeF_6 concentration in anhydrous HF [a]				Assignment
0.120	0.063	0.024	0.0083	
–	–	674 sh, p	674 sh, p	$[XeF_5]^+F^-$
–	–	664 s, p	664 sh, p	$([XeF_5]^+F^-)_2$
659 s, p	–	–	–	$([XeF_5]^+F^-)_4$
638 sh, p	640 w, p	–	–	$[XeF_5]^+[XeF_7]^-$
–	622 sh, p	623 sh, p	625 s, p	$[XeF_5]^+F^-$
619 sh, p	619 sh, p	620 sh, p	620 sh, p	XeF_6
–	619 s, p	604 s, p	605 sh, p	$([XeF_5]^+F^-)_2$
596 s, p	–	–	–	$([XeF_5]^+F^-)_4$
582 sh, p?	584 sh, p	585 sh, p	586 sh, p	$[F_5Xe]^{\delta+}...[FHF]^{\delta-}$
507 w, dp	508 w, dp	508 w, dp	512 w, p	XeF_6
408 w, dp	410 w, dp	410 w, dp	411 vw, dp	$[XeF_5]^+F^-$,
359 w, p	360 w, p	361 w, p	361 w, p	$([XeF_5]^+F^-)_2$ or
206 w, dp	208 w, dp	205 w, dp	200 w, dp	$([XeF_5]^+F^-)_4$

Note. The following designations are used: s is strong, m is medium, w is weak, vw is very weak band; p is polarized and dp is depolarized vibration; sh is shoulder.
[a] in mol mol^{-1}.

XeF_6 molecules. The 596 and 659 cm^{-1} bands (see Fig. 3 *a*) and the 600, 664, 604 and 665 cm^{-1} bands (see Fig. 3 *b*,*c*) were assigned to stretching vibrations of the ionized tetrameric, $([XeF_5]^+[F]^-)_4$, and dimeric, $([XeF_5]^+[F]^-)_2$, modifications of XeF_6; of these, higher-frequency bands are attributable to $(Xe-F)_{ax}$ modes and lower-frequency bands can be assigned to the $(Xe-F)_{eq}$ modes of the $[XeF_5]^+$ cation incorporated in the $([XeF_5]^+[F]^-)_n$ polymeric groups ($n = 2$, 4). Strictly speaking, this assignment cannot be regarded as being sufficiently substantiated, although it is in good agreement with the assignment for the $[Xe_2F_{11}]^+$ cation.[129, 130]

Apart from the xenon hexafluoride tetramer and dimer, the solution may contain the ionic species $[XeF_5]^+[XeF_7]^-$, which have been detected [72, 73] in a study of the IR spectra of solutions of XeF_6 in liquid krypton and xenon. This is supported by the fact that the Raman spectra of concentrated solutions of XeF_6 in HF exhibit a polarized band at about 640 cm^{-1}, which was assigned, in accordance with the data on the vibrational spectra of NO_2XeF_7,[131] to the symmetric $[XeF_7]^-$ stretching mode. Apart from the above-mentioned bands, the Raman spectra recorded over the whole concentration range exhibit a band at ~ 585 cm^{-1} (see Fig. 3 *c*,*d*), which has been assigned to vibration of the bridging Xe···F bond in the solvate systems such as $(XeF_6)_m([F_5Xe]_n^{\delta+}\cdots n[FHF]^{\delta+})$ (the m and n values can vary from 1 to 4; $m+n < 4$), which has been formed upon the donor-acceptor interaction of the Lewis base (XeF_6) and the Lewis acid (HF). Another possible assignment of this band is to the $\nu_4(B_1)$ stretching mode of the $[XeF_5]^+$ cation incorporated in the ionized polymeric form of xenon hexafluoride.[81, 122]

Analysis of the contours of the stretching bands in the Raman spectra of XeF_6 in an HF solution using temporal correlation functions showed the following:[122, 126] if the predominant structural unit in the solution is polymeric, the major contribution to the line contours of the corresponding vibration bands is made by the vibrational dephasing; as the XeF_6 concentration in HF decreases, this contribution decreases and at $\leqslant 0.01$ mol mol^{-1}, the contributions of the vibrational and rotational relaxations virtually coincide. A thorough analysis of the temporal correlation functions for the XeF_6-HF system over a broad concentration range provided the conclusion [88, 122, 126] that the vibrational dephasing time, which slightly depends on the XeF_6 concentration in HF, can serve as a temporal characteristics of the mobility of fluorine atoms during the non-rigid structural rearrangement $C_{3v} \rightarrow C_{2v} \rightarrow C_{3v}$. Using theoretical estimates,[87, 88] the characteristic time of the intramolecular reorientation of the fluorine atoms in XeF_6 was determined for the first time to be 0.35 ± 0.15 ps.

II.5. Crystal structures of simple compounds of xenon and krypton

The crystal structures of binary xenon and krypton fluorides were studied by X-ray diffraction and neutron diffraction techniques.[132–135] The structural parameters of the XeF_n ($n = 2$, 4) and KrF_2 single crystals are summarized in Table 4.

According to the results, XeF_2 has a body-centred tetragonal lattice (space group $I4/mmm$) composed of parallel linear symmetrical F–Xe–F molecules (Fig. 4). It was noted [136] that linear F–Xe–F fragments in which the Xe–F interatomic distances are markedly shorter than the Xe–F distances between the neigbouring fragments can be distinguished in the unit cell of XeF_2. The shortest intermolecular Xe–F distance is 3.64 Å; for each fluorine atom, the closest fluorine atom is located at a distance of 3.02 Å, while the other four fluorine atoms are at a distance of 3.08 Å.

Table 4. Crystallographic parameters of the structures XeF_n ($n = 2$, 4) and KrF_2.

Compound	System	Space group	Unit cell parameters						ρ /g cm^{-3}	T/K	X–F bond length /Å	F–X–F angle /deg	Ref.
			a/Å	b/Å	c/Å	V/Å^3	β /deg	Z					
XF_2	tetragonal	$I4/mmm$	4.2188(7)	4.2188(7)	6.991(2)	124.43(2)	90	2	4.519	100	2.00 ± 0.01	180	136
XF_4	monoclinic	$P2_1n$	5.050	5.922	5.771	–	99.6	2	4.04	–	1.951, 1.954	90 ± 0.1	47
β-KrF_2	tetragonal	$I4/mmm$	6.533	–	5.831	122.5	–	2	3.24	193	1.89(2)	180	137
α-KrF_2	"	$I4/mmm$	4.1790(6)	4.1790(6)	6.489(1)	113.32(3)	90	2	3.570	148	1.894(5)	180	137

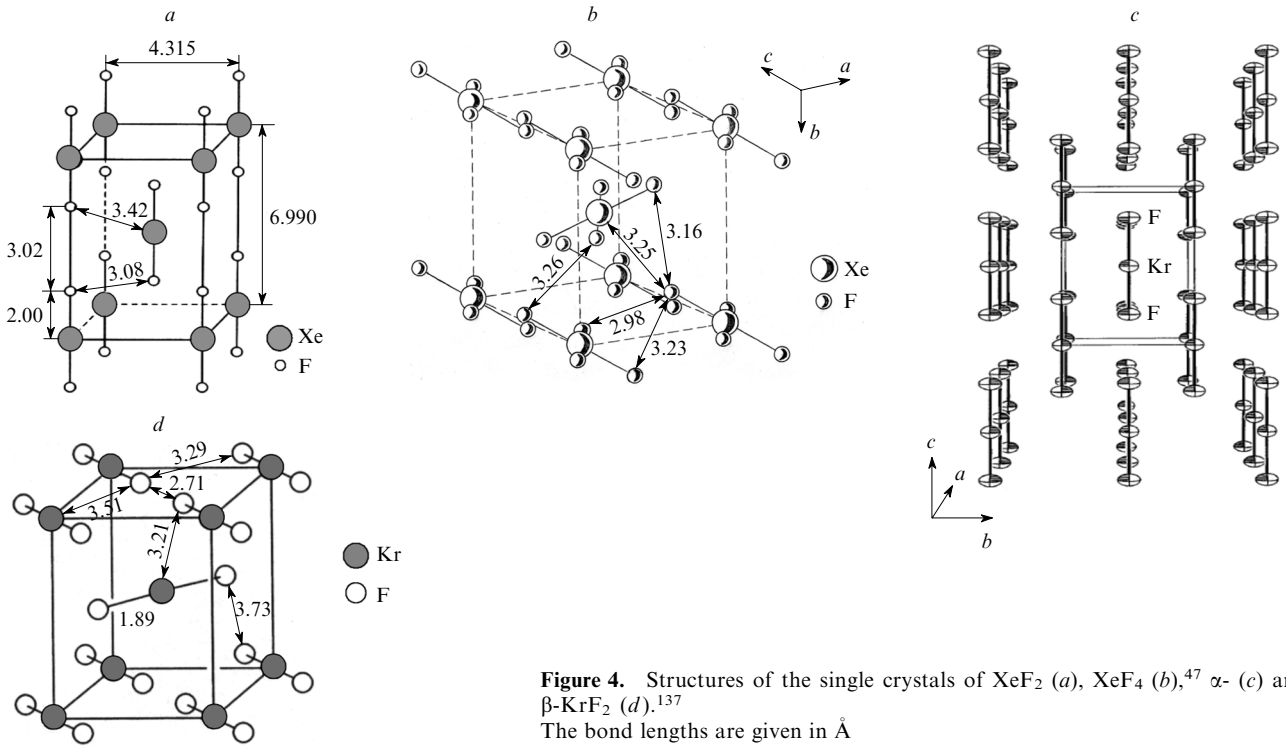


Figure 4. Structures of the single crystals of XeF_2 (*a*), XeF_4 (*b*),[47] α- (*c*) and β-KrF_2 (*d*).[137]
The bond lengths are given in Å

Kim *et al.*[138] were able to detect the formation of new crystallographic modifications of XeF_2 under extreme conditions. They used the method of diamond anvils,[139] which is suitable for investigation of crystallographic and spectroscopic properties of materials and the material conductivity at superhigh pressures (up to million atmospheres) and temperatures (up to 3000 K) in small-size devices. In experiments dealing with the pressure effect on the properties of materials, the authors placed an XeF_2 sample into a high-pressure diamond anvil cell. As pressure increased, the substance structure changed from molecular to atomic. The structural parameters of xenon difluoride in the pressure range from 2 to 98 GPa are presented in Table 5. The initial crystalline XeF_2 phase (tetragonal system, space group $I4/mmm$, $P < 3$ GPa) in the pressure range of 5–40 GPa is transformed into monoclinic (successively, $Immm$ and $Pnn\bar{m}1$). At 50 GPa, a layered graphite-like structure is formed (space group $Pnn\bar{m}2$), while at 98 GPa, a fluorite-like three-dimensional structure arises (space group $Fmmm$) (Fig. 5 *a*,*b*).

The structural changes of XeF_2 are accompanied by transformation of the Raman spectra (see Fig. 5 *c*). Specifically, at relatively low pressures (3–13 GPa), the Raman spectrum displays two active modes, A_g and E_g, at 510 and 160 cm^{-1}, corresponding to the stretching $\nu_1(\Sigma_g^+)$ and intermolecular vibrations of the XeF_2 molecule, respec-

Table 5. Structural parameters of xenon difluoride in the pressure range of 2–98 GPa.[138]

Pressure /GPa	Space group	ρ /g cm^{-3}	Bond length /Å			Unit cell parameters			
			Xe–F(1)	Xe···F(2)	F···F(1)	*a*/Å	*b*/Å	*c*/Å	*V*/Å^3
2	$I4/mmm$	4.883	2.067(1)	3.203(5)	2.774(2)	4.083(2)	4.083(2)	6.909(2)	57.590
4	$I4/mmm$	5.018	1.457(2)	3.475(7)	3.962(3)	4.037(4)	4.037(3)	6.875(3)	56.022
8	$Immm$	5.751	1.792(9)	3.125(5)	3.206(3)	3.812(4)	3.777(4)	6.790(5)	48.880
9	$Immm$	5.996	1.583(3)	3.186(4)	3.580(4)	3.747(5)	3.710(4)	6.747(4)	46.896
11	$Immm$	6.156	1.728(7)	3.077(4)	3.278(5)	3.701(4)	3.666(1)	6.735(1)	45.690
21	$Pnn\bar{m}1$	6.915	1.922(7)	2.842(4)	2.809(4)	3.512(3)	3.479(3)	6.655(2)	40.656
25	$Pnn\bar{m}2$	7.375	1.215(2)	2.330(2)	2.758(3)	3.432(2)	3.406(2)	6.605(2)	38.604
33	$Pnn\bar{m}2$	7.503	1.377(4)	2.023(3)	3.050(3)	3.373(2)	3.372(2)	6.590(2)	37.476
39	$Pnn\bar{m}2$	7.646	1.467(3)	2.236(4)	1.976(3)	3.377(1)	3.366(2)	6.590(2)	37.454
48	$Pnn\bar{m}2$	7.927	1.719(3)	2.081(3)	1.448(2)	3.350(1)	3.334(1)	6.585(2)	36.774
51	$Pnn\bar{m}2$	7.926	1.808(2)	2.040(3)	1.315(3)	3.294(1)	3.280(1)	6.567(1)	35.475
64	$Fmmm$	8.432	2.277(8)	2.277(8)	2.270(6)	4.554(4)	4.540(2)	6.451(3)	33.343
78	$Fmmm$	8.608	2.264(5)	2.264(5)	2.257(7)	4.514(2)	4.499(3)	6.433(2)	32.661
85	$Fmmm$	8.778	2.255(3)	2.255(3)	2.233(1)	4.495(2)	4.456(2)	6.416(1)	32.127
98	$Fmmm$	8.790	2.248(1)	2.248(1)	2.247(2)	4.493(3)	4.455(5)	6.340(6)	31.725

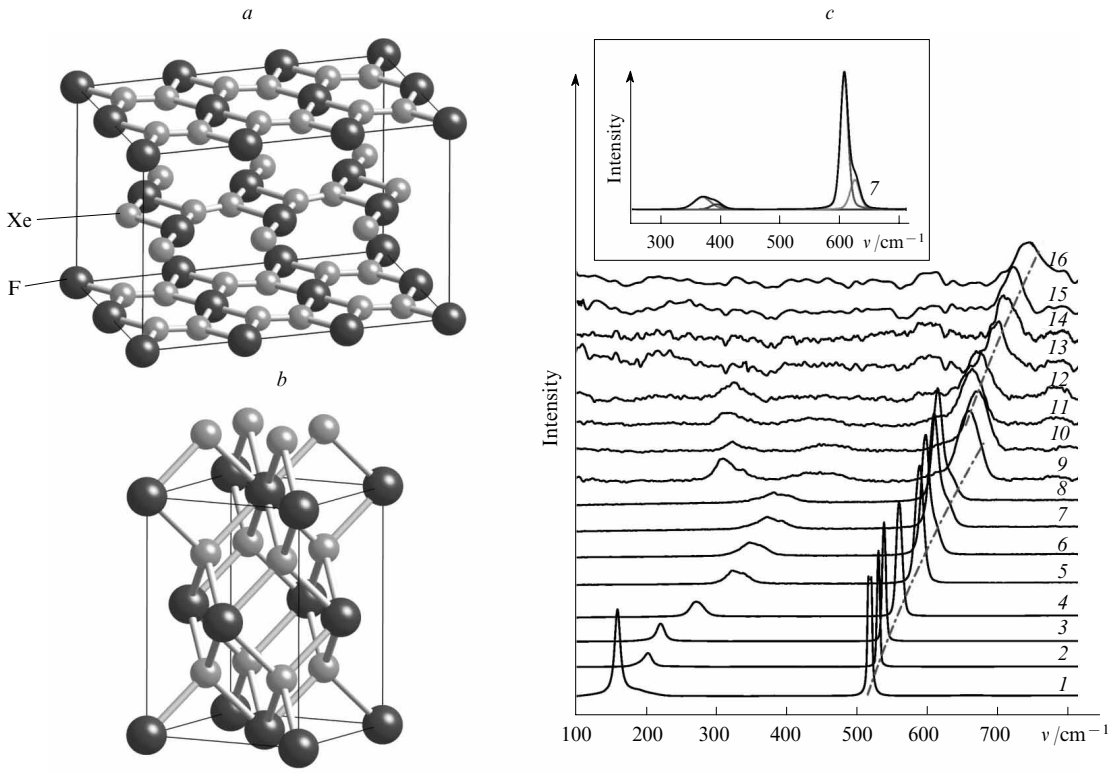


Figure 5. Graphite-like (P = 52 GPa) (*a*) and fluorite-like (P = 98 GPa) (*b*) structures of XeF_2 and the Raman spectra of XeF_2 at different pressures (*c*).[138]
P/GPa: (*1*) 3, (*2*) 7, (*3*) 10, (*4*) 15, (*5*) 25, (*6*) 35, (*7*) 45, (*8*) 50, (*9*) 57, (*10*) 63, (*11*) 67, (*12*) 71, (*13*) 80, (*14*) 87, (*15*) 96, (*16*) 116.

tively. At > 50 GPa, the intensity of the E_g mode tends to zero, while in the range of 50–67 GPa, a line near 300 cm^{-1} appears and on further pressure build-up, it disappears. The $\nu_1(\Sigma_g^+)$ line in the 3–116 GPa range markedly ($\sim$110 cm^{-1}) shifts to higher frequency, its contour being substantially distorted. Note that this type of changes of the Raman spectra typically occurs on phase transitions in some solids.[140]

The structural changes in XeF_2 are also accompanied by the colour gradation

colourless → yellow → red → black

and the conductivity gradation

dielectric → semiconductor → metal¶

The electron redistribution in the atomic shells under the action of superhigh pressure and closer approach of the XeF_2 molecules in the crystal gives rise to new strong chemical bonds. Actually, according to the assumption of Kim *et al.*,[138] the mechanical pressure energy was converted in this experiment into high-density chemical energy. Further development of research along this line may result in elaboration of new classes of energetic materials and fuels, unusual energy storage devices, superoxidants for destruction of chemical and biological agents, design of new high-temperature superconductors and so on.

¶ A compound with metallic properties (XeF_8). The lattice of this compound is composed of complex polyhedra forming rigid three-dimensional bonds.

A more recent publication[141] reports quantum chemical calculations of the structural evolution of XeF_2 in the pressure range of 105–200 GPa. Unlike experimental results,[138] the crystalline phase of XeF_2 (space group $I4/mmm$) was found to remain stable at room temperature up to 105 GPa. According to calculations,[141] at a pressure above 105 GPa, the structure with space group $I4/mmm$ transforms into a structure with space group *Pnma*. In the latter case, the F–Xe–F molecules are bent and the Xe–F distances become unequal (1.98 and 2.09 Å). Further pressure increase (up to 200 GPa) gives rise to ionized modifications of xenon difluoride ($[XeF]^+F^-$).

Xenon tetrafluoride XeF_4 crystallizes in the monoclinic system (space group $P2_1/n$).[47] As in the gas phase, in the single crystal, XeF_4 has a square planar configuration with the distances: Xe–F = 1.953 Å and F–F = 2.69 or 2.71 Å. The shortest distance between two neighbouring XeF_4 molecules is 3.02 Å (see Fig. 4).

According to X-ray diffraction data, KrF_2 single crystals (T = 193 K) have a tetragonal lattice. It was noted[137] that KrF_2 is not isostructural to XeF_2. The researchers cited demonstrated[137] that as the temperature is lowered to 148 K, KrF_2 undergoes a $\beta \rightarrow \alpha$ phase transition, which crucially changes the KrF_2 lattice structure, and α-KrF_2 that has formed is isostructural to XeF_2 (see Fig. 4). All KrF_2 molecules in the α-phase are arranged parallel to one another and to the *c* axis, eight molecules being located at the vertices of the unit cell and one molecule being at the centre of the unit cell. The $\beta \rightarrow \alpha$ phase transition is not accompanied by a loss of crystallinity and occurs *via* rotation of the corner KrF_2 molecules by 45° to be arranged along the *a* axis of the β-phase and rotation of the central

Table 6. Crystal modifications of XeF_6.[47]

System	Space group	Structural unit	T/K	Unit cell parameters				ρ/g cm^{-3}
				a/Å	b/Å	c/Å	Z	
Monoclinic	$P2_1/m$ or $P2_1$	2 tetrameric rings of XeF_5^+ and F^- groups	291.65–322.48	9.33	10.96	8.95	2	3.56
Orthorhombic	*Pnma*	4 tetrameric rings of XeF_5^+ and F^- groups	253.65–291.65	17.01	12.04	8.57	16	3.71
Monoclinic	$P2_1/b$	16 tetrameric rings of XeF_5^+ and F^- groups	< 253.65	16.80	23.93	16.95	64	3.82
Cubic	*Pm*3*c*	24 tetrameric and 8 hexameric rings of XeF_5^+ and F^- groups	93–322.48	25.06	–	–	144	3.73

molecule by 45° in the opposite direction, so that it also becomes parallel to the *a* axis of the α-phase. As a result, the unit cell axes of the β-phase are transformed into the α-phase axes: $a \rightarrow c$ and b, $c \rightarrow a$, b or b, a.

The Kr–F bond length in α-KrF_2 (1.894 Å, 148 K) virtually does not differ from the corresponding lengths in β-KrF_2 (1.892 Å, 193 K) and in gas-phase KrF_2 molecules (1.889 Å, 233 K). In both phases, the KrF_2 molecule has a linear structure ($D_{\infty h}$ symmetry). During the $\beta \rightarrow \alpha$ transition, the F...F distance between the collinear KrF_2 molecules remains unchanged (2.71 Å).

Crystal structure studies showed polymorphism of XeF_6, which exists in four crystal modifications (Table 6). The cubic phase of XeF_6 single crystal at 93 K has been studied in detail; the key structural units are XeF_5^+ tetragonal pyramids with fluorine atoms at the vertices. The pyramids are connected by bridging F^- ions to form tetrameric and hexameric complexes occurring in the structure in dextro- and levorotatory forms. For hexameric rings,

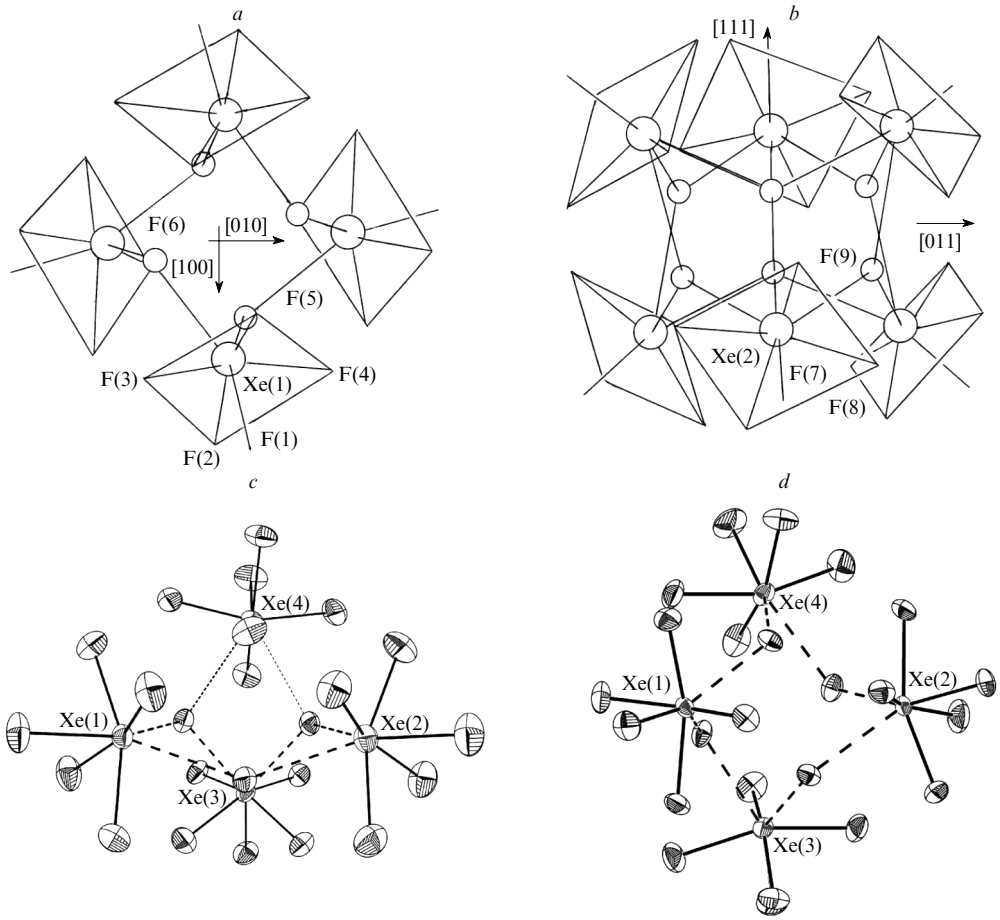


Figure 6. Structure of tetrameric (*a*) and hexameric (*b*) rings in the crystal lattice of XeF_6 (see Ref. 47) and xenon hexafluoride modifications: *mP*32 (*c*), *mP*16 (*d*).[142]

Table 7. Unit cell parameters in XeF_6 modifications.[142]

Modification	a/Å	b/Å	c/Å	α/deg	β/deg	γ/deg	Z
*mP*32	14.340(3)	12.800(3)	18.529(4)	90	90.017(5)	90	32
*mC*32	22.983(7)	12.994(4)	14.125(4)	90	126.156(6)	90	32
*mP*16	14.520(10)	8.452(8)	14.636(15)	90	110.996(4)	90	16

Note. All presented modifications crystallize in the monoclinic system with space group $P2_1/c$.

ordered alternation of the entantiomorphs is observed, while for tetrameric complexes, the alternation is disordered; the rings are three-dimensional and almost spherical.

The tetramer (Fig. 6 *a*) is an eight-membered ring consisting of four XeF_5^+ cations and four F^- anions. The interatomic distances in the XeF_5^+ cation are as follows (F_a stands for vertex F atoms, F_b are F atoms at the basal plane): Xe–F_a = 1.83, Xe–F_b (mean) = 1.84, F_a–F_b (mean) = 2.29, and F_b–F_b (mean) = 2.54 Å. The mean values for the F_a–Xe–F_b and F_b–Xe–F_b angles are 77.2 and 87.2°, respectively. The bridging F^- ion is separated by 2.23 Å from one xenon atom and by 2.60 Å from the other xenon atom; the angle in the bridge is 120.7°.

The hexamer (see Fig. 6 *b*) is a 12-membered ring consisting of six XeF_5^+ cations and six F^- anions. In the XeF_5^+ cation, the interatomic distances are as follows: Xe–F_a = 1.75, Xe–F_b = 1.88, F_a–F_b = 2.33, F_b–F_b = 2.62 Å, and the F_a–Xe–F_b and F_b–Xe–F_b angles are 80.0 and 88.3°, respectively. The bridging F^- ion is located at a 2.56 Å distance from each of the xenon atoms; the angle in the bridge is 118.8°.

A detailed investigation of the crystal structure of XeF_6 revealed[142] three new structural modifications of xenon hexafluoride (*mP*32, *mC*32, *mP*16)† (Table 7). It was found that at 303 K, slow sublimation (for several days) gives two similar XeF_6 structures, *mP*32 and *mC*32, consisting of XeF_6 trimers and monomers, which can be treated as $(XeF_5^+F^-)_3 - XeF_6$. The $(XeF_5^+F^-)_3$ trimer consists of square pyramidal XeF_5^+ fragments and bridging fluorine atoms; the lengths of bridges are 2.289(3), 2.454(3), 2.349(3) and 2.355(3) Å (see Fig. 6 *c*). In the monomer structure (C_{2v} symmetry), there are two short [1.838(3), 1.842(3) Å], two medium [1,867(4), 1.873(3) Å] and two long [1.968(3), 2.065(3) Å] bonds. It is connected with the trimer by 2.618(3) and 2.687(3) Å long F bridges. The XeF_6 modification (*mP*16) representing the $(XeF_5^+F^-)_4$ tetramer was obtained by recrystallization of XeF_6 from inert solutions in n-C_6F_{14}, n-C_4F_9–SO_2F or CF_2Cl_2 at 199–233 K. The square pyramidal environment of the XeF_5^+ cation is identical for all four xenon atoms, and four Xe···F···Xe bridges are almost symmetrical [2.267(2)–2.403(2) Å]; the angles of four bridges are also similar (118.31–121.01°) (see Fig. 6 *d*).

A neutron diffraction study of single crystalline XeO_2F_2 demonstrated[143] that this compound has a rhombohedral structure (space group *Cmcm*) with the unit cell parameters a = 6.443, b = 6.288, c = 8.312 Å, Z = 4, ρ = 4.10 g cm^{-3}. The structure is composed of 2D layers of XeO_2F_2 molecules linked by weak 2.808(4) Å long Xe···O bridges, the O–Xe···O angle being 168.5(2)°.

Xenon trioxide crystallizes in the orthorhombic system (space group $P2_12_12_1$) with the following unit cell parameters:[102] $a = 6.163 \pm 0.008$, $b = 8.115 \pm 0.010$, $c = 5.234 \pm 0.008$ Å, Z = 4, ρ = 4.55 g cm^{-3}. The Xe–O bond lengths are 1.74 ± 0.03, 1.76 ± 0.03 and 1.77 ± 0.03 Å; the O–Xe–O angles are 108 ± 2, 100 ± 2 and 101 ± 2°. The shortest distance between the oxygen atoms in XeO_3 is 2.91 Å; for other atoms, this distance is 3.02 Å.

Zhu *et al.*[144, 145] carried out quantum chemical calculations for the stability and crystal structures of the XeO, XeO_2 and XeO_3 molecules in the pressure range of 5–220 GPa. The most stable XeO structure at 100 GPa was found to have space group *Pbcm* and eight atoms in the unit cell. The xenon atoms are linearly coordinated and the Xe–O bonds form chains (Fig. 7 *a*) in which the O–Xe–O and

† Classification of Hoyer *et al.*:[142] *mP*32 is monoclinic, primitive, Z = 32; *mC*32 is monoclinic, centred, Z = 32; and *mP*16 is monoclinic, primitive, Z = 16.

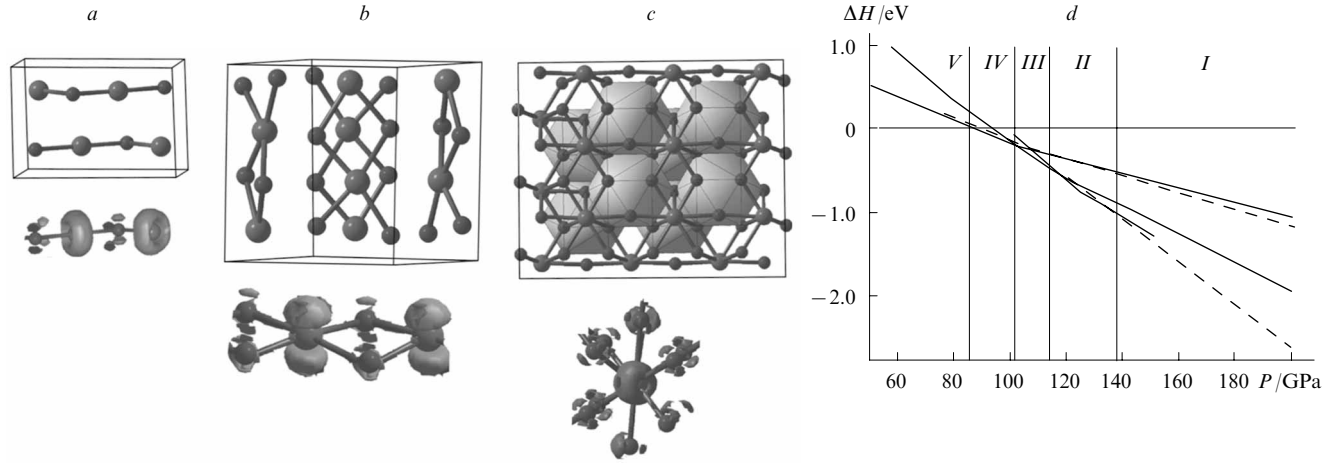


Figure 7. Structures and chemical bonding for XeO (*Pbcm*) at 100 GPa (*a*), XeO_2 ($P2_1/c$) at 120 GPa (*b*), XeO_3 (*Pmmn*) at 200 GPa (*c*) and stability regions of xenon oxides at different pressures (*d*).[144]
ΔH is the enthalpy of formation (continuous lines) and decomposition (dashed lines) of xenon oxides. (*I*) XeO_2 ($P2_1/m$), XeO_2 ($P2_1/c$), XeO_3 ($C2/c$); (*II*) XeO (*Pbcm*), XeO_2 ($P2_1/c$), XeO_3 ($P4_2/mnm$); (*III*) XeO (*Pbcm*), XeO_2 ($P2_1/c$); (*IV*) XeO (*Pbcm*); (*V*) the oxides do not exist.

Xe–O–Xe angles are 175.6 and 112.6°, respectively; the Xe–O bond lengths are 2.0 and 2.1 Å. At a pressure of >145 GPa, phase transition occurs in XeO to give a structure with space group $P2_1/m$. Two different types of environment of xenon atoms [Xe(1) and Xe(2)] are encountered in the structure. The Xe(1) atoms are bonded to four oxygen atoms and have square coordination, thus forming chains identical to the chains in XeO_2 [with the assumption that Xe(1) atoms are tetravalent]. Meanwhile, Xe(2) is neutral and is not bonded to other atoms. In the opinion of the researchers cited, the presence of neutral non-bonded xenon atoms in this structure is energetically favourable, because this increases the packing density.

The XeO_2 structure stable above 102 GPa belongs to space group $P2_1/c$ and has 24 atoms in the unit cell. The coordination of xenon is square and somewhat non-planar; the ribbon-like structure is composed of one-dimensional XeO_4 squares sharing sides, having four Xe–O bonds and two lone electron pairs, which form an octahedron (see Fig. 7 *b*). At a pressure of >198 GPa, XeO_2 (space group $P2_1/c$) is transformed into another XeO_2 structure (*Cmcm*). This non-trivial structure can be represented as having parallel zigzag chains of xenon (the Xe–Xe distance is 2.62 Å) in which each xenon atom is bonded to two adjacent oxygen atoms within bent XeO_2 molecules (Xe–O distance is 1.95 Å and the O–Xe–O angle is 160.7°).

The structure of xenon trioxide at 114 GPa belongs to space group $P4_2/mnm$ and has 16 atoms in the unit cell. This compound is stable against decomposition to Xe and O_2 or to XeO, XeO_2 and O_2; its structure is formed by two sublattices composed of square chains of XeO_2 (the presence of Xe^{4+} state is assumed) and linear chains of O_2. At pressures above 145 GPa, a new phase is formed in which the molecules in the $-O_2-O_2-$ linear chains partly dissociate, giving rise to an $-O_2-O-$ chain in the $C2/c$ phase having 48 atoms in the unit cell. Above 198 GPa, the structure is transformed into the *Pmmn* phase having eight atoms in the unit cell. In this unusual structure, the oxygen atoms form an anticubooctahedral environment around xenon atoms (see Fig. 7 *c*). The distribution of the electron localization function around the xenon atoms in the *Pmmn* phase is spherical, which attests to the Xe^{6+} valence state with the spherically symmetrical $5s^2$ valence shell and confirms the tendency towards increase in the oxidation number upon pressure growth. The crystallographic parameters of xenon oxides at different pressures are summarized in Table 8.

Thus, Zhu *et al.*[144, 145] predicted the stability of xenon oxides at high pressure, which, in their opinion, can be verified experimentally. As pressure grows, the oxidation state of xenon increases, resulting first in XeO (>83 GPa), then in XeO_2 (>102 GPa) and finally in XeO_3 (>114 GPa) (see Fig. 7 *d*). It was found that at higher pressure, xenon loses the chemical inertness and charge transfer from xenon to oxygen starts to play the crucial role in the formation of chemical bonds in oxides; stability of oxides is largely determined by the difference between the electronegativities of the constituent elements. Moreover, elevated pressure is likely to stabilize the increasing oxidation states of the xenon atoms ($Xe^0 \rightarrow Xe^{2+} \rightarrow Xe^{4+} \rightarrow Xe^{6+}$) and to enhance the charge transfer.

Table 8. Crystallographic parameters of xenon oxides as functions of pressure.[145]

Oxide	*P* /GPa	Space group	Unit cell parameters			
			a /Å	*b* /Å	*c* /Å	*β* /deg
XeO	100	*Pbcm*	2.944	6.925	4.781	
	200	$P2_1/m$	4.505	3.308	5.525	101.83
XeO_2	150	$P2_1/c$	6.452	6.536	4.948	92.20
	200	*Cmcm*	5.943	4.424	3.642	
XeO_3	130	$P4_2/mnm$	6.040	3.465		
	150	$C2/c$	9.167	5.835	6.825	98.34
	200	*Pmmn*	3.443	4.440	3.613	

III. Molecular and crystal structures of compounds with Xe–O, Xe–N and Xe–C bonds

III.1. Compounds with the Xe–O bond

During the first years after the discovery of the ability of noble gases to form chemical compounds, a series of relatively stable derivatives of xenon in the oxidation state +2 with polyatomic oxygen-containing ligands have been obtained, namely, $FXeSO_3F$, $Xe(SO_3F)_2$, $FXeClO_4$, $Xe(ClO_4)_2$,[146, 147] $FXeOSO_2F$, $Xe(OSO_2F)_2$,[148] $FXeOXF_5$, $Xe(OXF_5)_2$ (X = Te, Se).[149–151] Subsequently compounds of the FXeL and XeL_2 types have been prepared [L = $P(O)F_2$, $OClO_3$, ONO_2, $OC(O)CH_3$, $OC(O)CF_3$, OSO_2CH_3, OSO_2CF_3, OIOF4].[8, 152] There are noticeably fewer compounds with xenon oxidation states of +4 and +6; among these, note $Xe(OTeF_5)_4$,[153] $Xe(OTeF_5)_6$,[152] $O_2Xe(OTeF_5)_2$ (see Ref. 154) and $O{=}XeF(OTeF_5)_4$.[155]

The structure of $FXeSO_3F$ consists of separate $FXeOSO_2F$ molecules in which the xenon atom is linearly coordinated to the fluorine and oxygen atoms of the distorted tetrahedral fluorosulfonic group.[148] The length of the terminal Xe–F bond in $FXeOSO_2F$ [1.940(8) Å] is close to the corresponding length in XeF_2 [2.00(1) Å] and $Xe_2F_3^+$ (1.908 Å), while the Xe–O bond length is 2.155(8) Å. The crystals of $FXeSO_3F$ have an orthorhombic lattice with $a = 9.88$, $b = 10.00$, $c = 10.13$ Å, $Z = 8$, $\rho = 3.30$ g cm^{-3}, space group *Pbca*, while the $Xe(SO_3F)_2$, the lattice is monoclinic with $a = 7.94$, $b = 13.7$, $c = 6.84$ Å, $\beta = 96°$ (see Ref. 147).

The compound $Xe(OTeF_5)_2$ crystallizes in the monoclinic system (space group $P2_1/c$) with the unit cell parameters $a = 10.289(2)$, $b = 9.605(2)$, $c = 10.478(2)$ Å, $\beta = 106.599(4)°$, $Z = 4$, $V = 992.3(3)$ Å^3, $\rho = 4.073$ g cm^{-3} (see Ref. 156). Note that in an earlier study,[149] this compound was described as having an orthorhombic structure (space group *Cmca*) with the lattice parameters $a = 9.83$, $b = 10.00$, $c = 10.13$ Å, $Z = 8$, $\rho = 3.64$ g cm^{-3}.

Unlike $Xe(OTeF_5)_2$, the compound $Xe(OSeF_5)_2$ crystallizes in the triclinic system ($R\bar{3}$), the unit cell parameters being $a = b = 8.3859(6)$, $c = 13.0355(13)$ Å, $\beta = 90°$, $Z = 3$, $V = 732.98(11)$ Å^3, $\rho = 3.474$ g cm^{-3} (see Ref. 156). The Xe–O bond lengths in $Xe(OTeF_5)_2$ and $Xe(OSeF_5)_2$ are 2.119(11) and 2.09(3) Å, respectively, and the angles Xe–O–Te(Se) are 122.3(5) and 121.2(6)°, respectively. All of the F–Te–F and F–Te–O angles in the ordered $Xe(OTeF_5)_2$ structure are 90° to within the experimental error, while the substantial deviation of the F–Se–F and F–Se–O angles from 90° was attributed[156] to disorder of the $Xe(OSeF_5)_2$ structure. However, although the Se–O [1.58(3) Å)] and Se–F [1.65(3)–1.81(2) Å] bond lengths

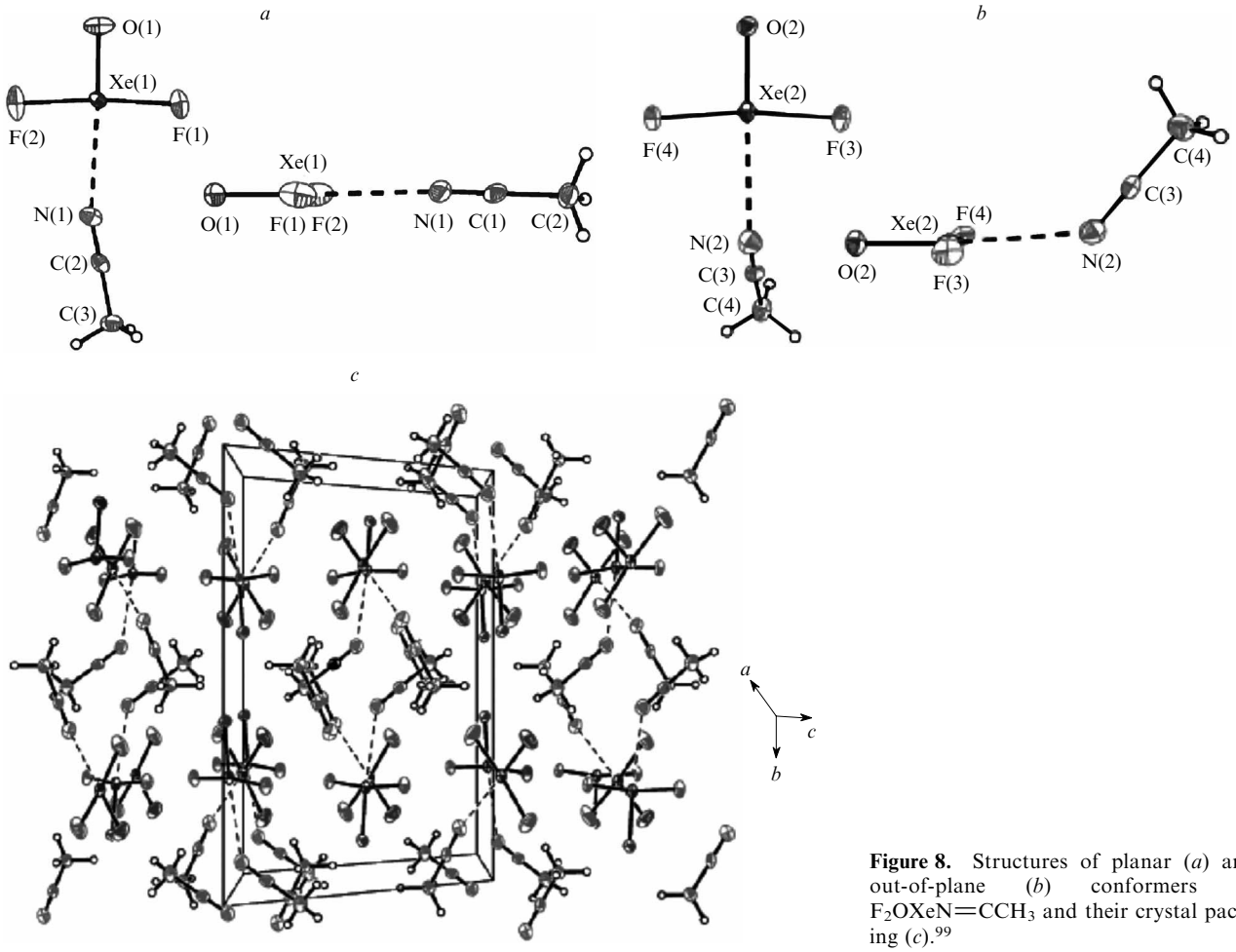


Figure 8. Structures of planar (*a*) and out-of-plane (*b*) conformers of $F_2OXeN{=}CCH_3$ and their crystal packing (*c*).[99]

should depend to a substantial extent on the ordering of the $Xe(OSeF_5)_2$ structure; these values as well as the Te–O [1.843(11) Å] and Te–F [1.823(9)–1.855(11) Å] bond lengths in the ordered $Xe(OTeF_5)_2$ structure are in good agreement with the corresponding values for $OSeF_5$ and $OTeF_5$.[157, 158]

The compound $F_2OXeN{=}CCH_3$ prepared by Brock *et al.*[99] crystallizes in the monoclinic system ($P2_1/c$) with the lattice parameters $a = 8.7819(4)$, $b = 13.9862(6)$, $c = 11.0182(6)$ Å, $\beta = 128.476(2)^\circ$, $Z = 8$, $V = 1059.47(1)$ Å^3, $\rho = 2.838$ g cm^{-3}. The compound $F_2OXeN{=}CCH_3$ was shown to have two crystallographically independent conformations; the unit cell of each conformer comprises four molecules. Both conformers are bent, one of them lying in the $XeOF_2$ plane (Fig. 8 *a*) while the other being located out of the plane (see Fig. 8 *b*). Two lone electron pairs of the planar T-shaped $XeOF_2$ group reside in the equatorial plane, two fluorine atoms being in the *trans*-positions. The Xe–O bond lengths in both conformers are equal, amounting to 1.778(4) and 1.782(4) Å to within $\pm 3\sigma$, which somewhat exceeds the bond lengths in the oxides and oxyfluorides of hexa- and octavalent xenon.

Compound	$XeOF_4$	XeO_2F_2	XeO_2F_2	XeO_3	XeO_4
Bond length /Å	1.713(3)	1.714(4)	1.734(9)	1.74(3) –1.77(3)	1.736(2)
Ref.	159	143	160	102	106

The Xe–F bond lengths in $F_2OXeN{=}CCH_3$ are generally comparable with the bond lengths in XeF_4 [1.953(2) Å]; they are somewhat longer for the out-of-plane conformer [1.975(3), 1.981(3) Å] than for the planar conformer [1.952(3), 1.958(3) Å]; the equatorial F–Xe–F angles for the out-of-plane and planar conformers are 171.9(1) and 174.2(2)°, respectively. The Xe–N bond lengths and especially the Xe–N–C angles in the conformers are substantially dissimilar being 2.808(5) Å and 164.9(4)° for the planar conformer and 2.752(5) Å and 134.6(4)° for the out-of-plane conformer. In our opinion, these differences may be attributable to the noticeable interaction between the $XeOF_2$ and CH_3CN molecules giving rise to a relatively short Xe···N contact in the crystal packing of $F_2OXeN{=}CCH_3$ (see Fig. 8 *c*).

III.2. Compounds with the Xe–N bond

Several xenon compounds with the Xe–N bond are known.[19, 161] The first of these compounds, $FXeN(SO_2F)_2$, was prepared by LeBlond and DesMarteau[162] by the reaction of $HN(SO_2F)_2$ with XeF_2 in a CF_2Cl_2 solution at 273 K. In the molecule of this compound, the F–Xe–N angle is 178.1(1)°, and the Xe–N and Xe–F bond lengths are 2.200(3) and 1.967(3) Å, respectively; nitrogen has a trigonal planar coordination.[163] Compounds with the N–Xe–N bonds are also known, for example, $Xe[N(SO_2F)_2]_2$ (Ref. 164) and $Xe[N(SO_2CF_3)_2]_2$ (Ref. 165).

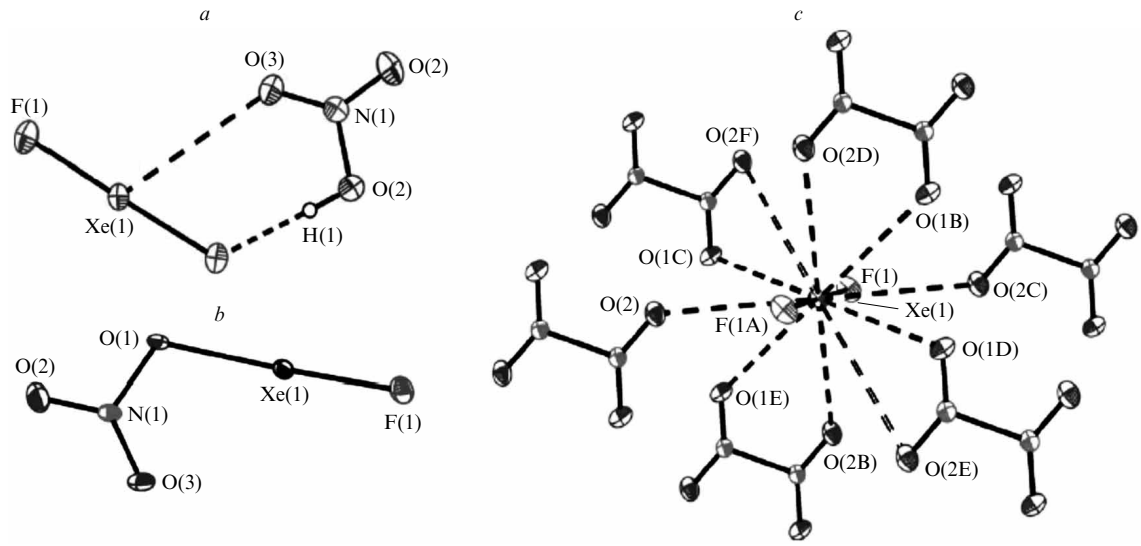


Figure 9. Crystal structure of $XeF_2 \cdot HNO_3$ (*a*), $FXeONO_2$ (*b*) and local spatial environment of XeF_2 in the crystal structure of $XeF_2 \cdot N_2O_4$ (*c*).[166]

Moran *et al.*[166] synthesized $XeF_2 \cdot HNO_3$, $FXeONO_2$ and $XeF_2 \cdot N_2O_4$. The crystal structure of $XeF_2 \cdot HNO_3$ (Fig. 9 *a*) was found to include a hydrogen bond between HNO_3 and the fluorine atom [1.86(2) Å] and a contact between the oxygen and xenon atoms [3.317(1) Å], which gives rise to a crystal lattice comprised of layered sheets. The crystal structure of $FXeONO_2$ (Fig. 9 *b*) attests to the absence of considerable intermolecular contacts; the structure parameters are in good agreement with those for the gas phase determined by quantum chemical calculations.[166] The Xe–O and Xe–F bond lengths and the O–Xe–F angles in the $FXeONO_2$ and $FXeOSO_2F$ molecules do not differ markedly.[148]

Xe–O /Å	Xe–F /Å	O–Xe–F angle /deg
Values for $FXeONO_2$		
2.126(4)	1.992(4)	177.6(2)
Values for $FXeOSO_2F$		
2.155(8)	1.940(8)	177.4(3)

Moran *et al.*[166] noted that a specific feature of the N–O bonds in the ONO_2 groups of the $XONO_2$ molecule (X = Cl,[167] Br [168]) is that in halogen nitrates, the $N-O_{cis}$ bond is shorter than the $N-O_{trans}$ bond, but in $FXeONO_2$, the relation is opposite.

When XeF_2 was dissolved in liquid N_2O_4 at 308 K, a low equilibrium concentration of $FXeONO_2$ was attained but the product $XeF_2\,N_2O_4$, which crystallized in the temperature range of 270–273 K, predominated.[166] X-Ray crystallographic analysis of the crystal structure of $XeF_2 \cdot N_2O_4$ (see Fig. 9 *c*) revealed weak interactions between the xenon and oxygen atoms [3.435(4)–4.180(4) Å]. The Xe–F [1.985(3) Å], N–O [1.194(6), 1.182(6) Å] and N–N [1.378(8) Å] bond lengths in the $XeF_2 \cdot N_2O_4$ molecule are close to those for free XeF_2 and N_2O_4 to within $\pm 3\sigma$. Furthermore, in the vibrational spectra, the frequencies of XeF_2 and N_2O_4 as parts of $XeF_2 \cdot N_2O_4$ almost coincide with the frequencies for free XeF_2 and N_2O_4. This fact, together with X-ray crystal structure analysis of $XeF_2 \cdot N_2O_4$ allowed the authors cited [166] to classify this compound as a molecular adduct.

III.3. Compounds with the Xe–C bond

There exist a number of compounds with Xe–C bonds and rather thoroughly studied structures. The vast majority of these compounds are complexes containing the RXe^+ cation (R is fluorophenyl, alkynyl, *etc.*).[169, 170] The compounds $C_6F_5Xe^+B(C_6F_5)_3F^-$, $F_2C{=}C(F)Xe^+BF_4^-$, $(CH_3)_3CC{\equiv}CXe^+BF_4^-$, $(CH_3)_3SiC{\equiv}CXe^+BF_4^-$ (Ref. 171) and $(C_6F_5)XeF_2^-BF_4^-$ (Ref. 172) can be put into this class. According to crystal structure studies of the complex $CH_3C{\equiv}NXeC_6F_5^+(C_6F_5)_2BF_2^-$,[173] the xenon atom is bonded rather weakly to nitrogen, the Xe–N bond length being 2.681(8) Å, while the Xe–C bond length is 2.092(8) Å.

Neutral compounds with Xe–C bonds that have been synthesized and characterized by ^{13}C, ^{19}F and ^{129}Xe NMR spectroscopy include $(C_6F_5)XeF$,[174] $Xe(C_6F_5)_2$ [175] and $(C_6F_5)XeCl$.[176] According to publications,[177, 178] in the last but one compound, the lengths of two Xe–C bonds in the crystal are 2.35(1) and 2.39(9) Å (Fig. 10 *a*).

As regards structural details of xenon-containing complex organic compounds, of considerable interest is *p*-$C_6F_5XeOC(O)C_6F_4C(O)OXeC_6F_5 \cdot 4(CF_3)_2CHOH$, which has both Xe–C and Xe–O bonds in the molecule.[179] Considering the crystallographic data they obtained, Bilir *et al.*[179] showed that each molecule *p*-$C_6F_5XeOC(O)C_6F_4C(O)OXeC_6F_5$ is hydrogen-bridged to four alcohol molecules and four oxygen atoms of the $C_6F_4(C(O)O)_2$ group (see Fig. 10 *b*). The Xe–C [2.101(4), 2.105(5) Å] and Xe–O [2.495(3), 2.511(4) Å] bond lengths attest that the bonds are essentially covalent, the Xe–C bond lengths being comparable with the corresponding bond lengths in $C_6F_5XeOC(O)C_6F_5$ [2.122(4) Å] and in the $C_6F_5Xe^+$ cation in the $[C_6F_5Xe][AsF_6]$ complex [the mean value is 2.081(6) Å (Ref. 180)]. The xenon atoms are bonded fairly strongly by additional bonds to the second oxygen atom [3.156(5), 3.120(5) Å]. Apparently, greater Xe–O bond length is due to hydrogen bonding of four

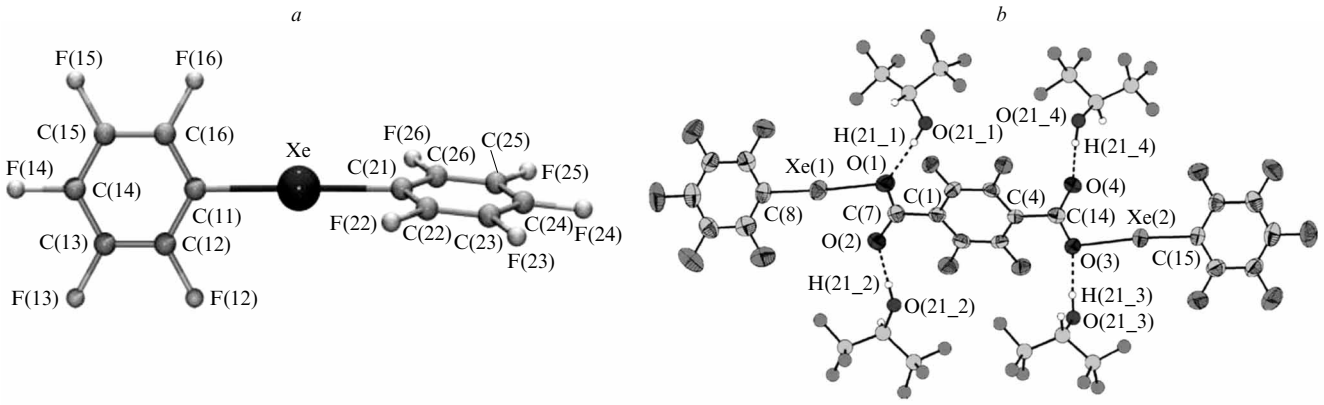


Figure 10. Crystal structures of $Xe(C_6F_5)_2$ (Ref. 175) and p-$C_6F_5XeOC(O)C_6F_4C(O)OXeC_6F_5 \cdot 4(CF_3)_2CHOH$.[179] (*b*): pairs of oxygen and hydrogen atoms involved in the H-bonding of p-$C_6F_5XeOC(O)C_6F_4C(O)OXeC_6F_5$ to four $(CF_3)_2CHOH$ molecules designated by O(21_*n*) and H(21_*n*), $n = 1-4$.

$(CF_3)_2CHOH$ molecules to each oxygen atom in $C_6F_4(C(O)O)_2$, which decreases the oxygen nucleophilicity. The mean angle between the carboxylate groups is 15°, while the angles between the aromatic rings are 42 and 58°.

The chemistry of compounds with carbon–xenon bonds has been considered rather comprehensively in the literature.[20, 21, 56, 181]

IV. Structure of complex xenon and krypton fluorides

Xenon and krypton fluorides behave as Lewis bases and act as fluoride ion donors in the formation of complexes with some fluorides (fluorine ion acceptors) as shown below:[9, 47]

$$KrF_2 \longrightarrow KrF^+, Kr_2F_3^+$$

$$XeF_2 \longrightarrow XeF^+, Xe_2F_3^+ \quad / \quad XeF_3^-$$

$$XeF_4 \longrightarrow XeF_3^+ \quad / \quad XeF_5^-$$

$$XeF_6 \longrightarrow XeF_5^+, Xe_2F_{11}^+ \quad / \quad XeF_7^-, XeF_8^{2-}$$

Unlike lower noble gas fluorides, the compounds XeF_4 and XeF_6 can behave not only as Lewis bases but also as acids.[9, 47, 55, 182] For example, similarly to fluorides of some metals, these compounds accept fluoride ions to give complexes [9, 32, 47, 128]

$$XeF_4 + CsF \longrightarrow Cs[XeF_5]^-$$

$$XeF_6 + CsF \longrightarrow Cs[XeF_7]^-$$

$$XeF_6 + 2\,CsF \longrightarrow Cs_2[XeF_8]^{2-}$$

The complexes of xenon and krypton fluorides were studied by ^{19}F NMR spectroscopy, Mössbauer spectroscopy, X-ray diffraction analysis and vibrational spectroscopy (see the series of publications [5–7, 137, 183, 184] and references cited therein); the two last-mentioned methods were recognized to be the methods of choice for identification of noble gas fluorides.

From the data of examination of X-ray, NMR and vibrational spectra of complexes of noble gas fluorides, it was concluded that their structure can be described in terms of the ionic model.[7, 9, 12–14, 31, 32]

IV.1. Complex compounds of xenon and krypton difluorides

IV.1.a. The XeF^+ and KrF^+ cations

The structure of XeF_2 and KrF_2 complex compounds with Lewis acids MF_4, MF_5, $2MF_5$, MOF_4, MOF_5 (M = As, Sb, Bi, Nb, Ta, Ru, Os, Ir, Pt, Au, Mo, W, U) is the subject of a series of publications (see the papers [9, 47, 51, 136, 183, 185] and references cited therein). As an example, Table 9 presents the crystallographic characteristics of XeF_2 and KrF_2 complexes with arsenic, antimony and bismuth pentafluorides. The structures of the XeF^+ and KrF^+ cations incorporated in these compounds are presented in Fig. 11. The Xe–F(1) bond lengths in $XeF^+AsF_6^-$, $XeF^+SbF_6^-$ and $XeF^+Sb_2F_{11}^-$ differ insignificantly to within $\pm 3\sigma$, and they are somewhat shorter than the corresponding bond lengths in $XeF^+BiF_6^-$ (see Fig. 11 *a*) and $XeF^+Bi_2F_{11}^-$.[47, 136 183] The Xe–F bond lengths in these compounds are shorter than in the crystalline and gaseous XeF_2, which is typical of virtually all $XeF^+MF_6^-$ and $XeF^+M_2F_{11}^-$.

Compound	Xe–F/Å	Compound	Xe–F/Å
$XeF^+AsF_6^-$	1.888(3)	$XeF^+Bi_2F_{11}-$	1.909
$XeF^+SbF_6^-$	1.885(2)	XeF_2 (gas)	1.979
$XeF^+Sb_2F_{11}^-$	1.888	XeF_2 (crystal)	2.00(1)
$XeF^+BiF_6^-$	1.913(7)		

A similar trend is observed for Kr–F bonds in the gaseous and crystalline KrF_2, in $KrF^+MF_6^-$ (M = As, Sb, Bi) [137, 183] (see Fig. 11 *b*) and in $KrF^+AuF_6^-$ (see Ref. 185). Theoretical calculations [186] of the Kr–F bond lengths for the KrF^+ cation give similar values.

Compound	Kr–F/Å	Compound	Kr–F/Å
$KrF^+AsF_6^-$	1.765(2)	KrF_2 (gas)	1.889
$KrF^+SbF_6^-$	1.765(3)	KrF_2 (crystal)	1.894
$KrF^+BiF_6^-$	1.774(6)	KrF^+	1.789
$KrF^+AuF_6^-$	1.783		

Table 9. Unit cell parameters for the complex compounds $XeF^+MF_6^-$ and $KrF^+ MF_6^-$ (M = As, Sb, Bi).

Compound	Unit cell parameters						ρ /g cm^{-3}	T/K	Ref.
	a/Å	b/Å	c/Å	V/Å^3	β/deg	Z			
$XeF^+AsF_6^-$	6.211(1)	6.169(1)	15.793(3)	595.8(2)	100.03	4	3.782	100	136
$XeF^+SbF_6^-$	5.356(3)	10.898(5)	10.926(5)	636.20(5)	94.055(7)	4	4.030	100	136
$XeF^+BiF_6^-$	5.235(2)	9.946(4)	12.333(6)	642.01(5)	91.251(6)	4	4.896	100	136
β-$KrF^+AsF_6^-$	5.1753(2)	10.202(1)	10.576(2)	556.02(6)	95.298(2)	4	3.485	153	137
$KrF^+SbF_6^-$	5.2922(6)	10.444(1)	10.796(1)	594.731(1)	94.693(4)	4	3.781	160	137
$KrF^+BiF_6^-$	5.336(1)	10.513(2)	11.046(2)	617.6(2)	94.79(3)	4	4.579	143	183

Note. All presented compounds crystallize in the monoclinic system with space group $P2_1/n$ for $XeF^+AsF_6^-$ and $P2_1/c$ for other compounds.

This trend is in line with the assumption that the chemical bonds in XeF_2 and KrF_2 are formed by three-centre orbitals for four valence electrons,[65, 66] which makes it possible to consider the linear KrF_2 and XeF_2 molecules as resonance hybrids of the contributing ionic structures with valence bonds

$$F-X^+F^- \leftrightarrow F^-X^+-F$$

The $Xe-F_{bridge}$ bonds (F_{bridge} is the bridging F atom) and $M-F_{bridge}$ bonds in $XeF^+MF_6^-$ and $XeF^+M_2F_{11}^-$ are somewhat longer than the Xe–F bonds in XeF_2 and the M–F bonds in the corresponding anions.[47, 136, 137, 183] The $Xe-F_{bridge}$ bonds have fairly similar lengths in $XeF^+AsF_6^-$ (2.208 Å), $XeF^+BiF_6^-$ (2.204 Å) and $XeF^+RuF_6^-$ (2.182 Å), but they are somewhat longer in $XeF^+SbF_6^-$ (2.278 Å). The $M-F_{bridge}$ bonds also have similar lengths in the compounds $XeF^+AsF_6^-$ (1.838 Å), $XeF^+SbF_6^-$ (1.971 Å) and $XeF^+Sb_2F_{11}^-$ (1.930 Å) and greater lengths in $XeF^+BiF_6^-$ (2.108 Å) and $XeF^+Bi_2F_{11}^-$ (2.075 Å); they are substantially longer than the M–F bonds in the corresponding MF_6^- anions (1.697, 1.863, 1.855, 1.960 and 1.952 Å). The $F-Xe-F_{bridge}$ angles in $XeF^+SbF_6^-$ (177.94°), $XeF^+AsF_6^-$ (179.1°), $XeF^+BiF_6^-$ (178.4°), $XeF^+Sb_2F_{11}^-$ (179.3°) and $XeF^+Bi_2F_{11}^-$ (178.9°) deviate only slightly from 180°, *i.e.*, the structures are linear.

The $Kr-F_{bridge}$ bond lengths in $KrF^+MF_6^-$ are also longer than the Kr–F bonds in KrF_2 (1.884 Å)[47, 137, 183, 185]

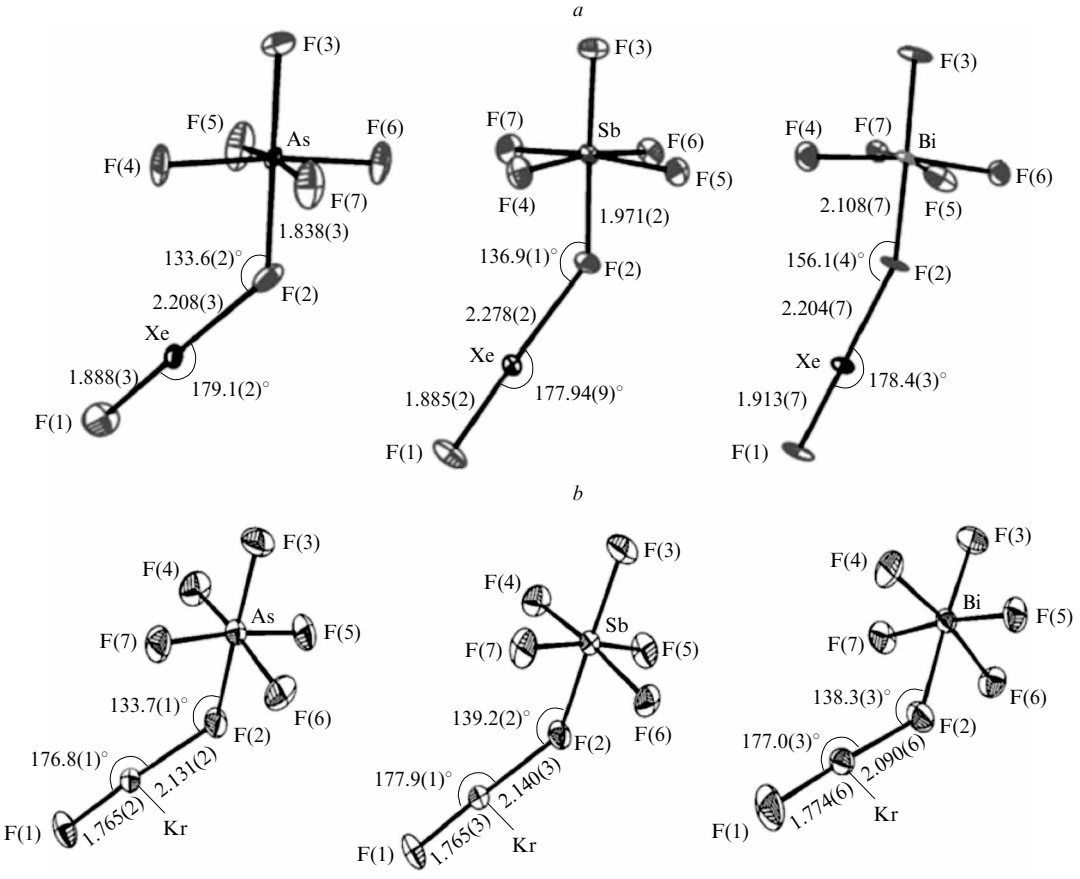


Figure 11. Crystal structures of $XeF^+MF_6^-$ (*a*)[136] and $KrF^+MF_6^-$ (*b*)[185] (M = As, Sb, Bi). The bond lengths are given in Å.

and do not differ substantially for $KrF^+AsF_6^-$ (2.131 Å), $KrF^+SbF_6^-$ (2.140 Å) and $KrF^+BiF_6^-$ (2.089 Å). A similar deviation of the $F-Kr-F_{bridge}$ angles from 180° in $KrF^+MF_6^-$ noted in several papers [137, 183, 185] is apparently caused by mutual repulsion between the lone pairs of valence electrons of the bridging fluorine and krypton atoms.

The $X-F_{bridge}-M$ angles in $XeF^+AsF_6^-$ (133.6°), $XeF^+SbF_6^-$ (136.9°), $XeF^+RuF_6^-$ (137.2°), $KrF^+AsF_6^-$ (133.7°), $KrF^+SbF_6^-$ (139.2°) and $KrF^+BiF_6^-$ (138.3°) are similar to one another. The noticeable difference between the $X-F_{bridge}-M$ angles in the listed compounds and the corresponding angles in $XeF^+BiF_6^-$ (156.1°) and $KrF^+AuF_6^-$ (125.3°) is, in our opinion, due to the fact that BiF_5 is a relatively weak, while AuF_5 is an abnormally strong Lewis acid.[187] The decrease in the value of the $Kr-F_{bridge}-M$ angle is due to the overall influence of cation–anion interactions and the Jahn–Teller effect in the crystal lattice field, resulting in a distortion of the octahedral structure of the AuF_6^- anion.[185, 188, 189]

The vibrational spectra of the XeF^+ and KrF^+ cations incorporated in $NgF^+MF_6^-$ or $NgF^+M_2F_{11}^-$ (Ng = Xe, Kr; M = As, Sb, Nb, Ta, Pt, Au) have been recorded.[185, 188–191] The NgF^+ cations in the spectra of these compounds were characterized by $Ng-F$ and $Ng-F_{bridge}$ stretching vibrations and $F-Ng-F_{bridge}$ bending vibrations. The frequencies of these vibrations for XeF^+ and KrF^+ in the spectra of $NgF^+MF_6^-$ and $NgF^+M_2F_{11}^-$ are similar, being about 600, 300 and 150 cm^{-1}, respectively. It is notable that the $Xe-F$ stretching frequency in the XeF_2 complexes with Lewis acids such as MF_5 depends on their acidic properties; as the acidic properties of MF_5 (M = Nb, Ta, Sb) are weakened, the band shifts to higher frequency.

IV.1.b. $Xe_2F_3^+$ and $Kr_2F_3^+$ cations

The $Ng_2F_3^+$ (Ng = Xe, Kr) cations are formed in reactions of XeF_2 and KrF_2 with the Lewis acids MF_5 (M = As, Sb, Bi, Ta, Ru, Os, Ir, Au) in 2 : 1 ratio.[9, 47, 187, 192, 193] As an example, Table 10 presents the crystallographic parameters of $Xe_2F_3^+MF_6^-$ (M = As, Sb). The $Xe_2F_3^+$ cation has a planar V-shaped configuration with symmetrically arranged terminal and bridging fluorine atoms. The $Xe-F$ bond length in $Xe_2F_3^+AsF_6^-$ (monoclinic phase) is 1.908 Å and the $Xe-F_{bridge}$ bond lengths are 2.142 and 2.148 Å; the $Xe-F_{bridge}-Xe$ angles are 149.5 and 148.6°, while the $F_{bridge}-Xe-F$ angle is in the 177.3–177.7° range.

Fir *et al.*[194] found that the reaction of $XeF^+AsF_6^-$ with $(CH_3)_3CC{\equiv}N$ in a solution of HF affords $Xe_2F_3^+AsF_6^-$, which crystallizes in the trigonal system. Unlike the monoclinic phase, in the trigonal $Xe_2F_3^+AsF_6^-$ phase, the $Xe-F_{bridge}$ bonds are non-symmetrical, their lengths are 2.10 and 2.25 Å, the $Xe-F_{bridge}-Xe$ and $F_{bridge}-Xe-F$ angles are 139.8 and 167.7°, respectively, and the $Xe-F$ bond length is close to the value for the monoclinic phase (1.908 Å). The increase in the $Xe-F_{bridge}-Xe$ and $F_{bridge}-Xe-F$ angles in the cation from 139.8 to 148.6° on going from the trigonal to monoclinic phase of $Xe_2F_3^+AsF_6^-$ is apparently related to crystal packing effects.

The $Kr_2F_3^+$ cation also has a V-shaped configuration; however, unlike monoclinic $Xe_2F_3^+$, the terminal and bridging fluorine atoms in this compound are arranged non-symmetrically.[137, 183, 190] The $Kr-F$ bond lengths in the $Kr_2F_3^+$ cation are shorter than in KrF_2, amounting to 1.78 and 1.81 Å; the $Kr-F_{bridge}$ bond lengths are 2.041 and 2.065 Å and the $Kr-F_{bridge}-Kr$ and $F_{bridge}-Kr-F$ angles are in the ranges of 126.0–127.5 and 177.8–178.7°, respectively.

Considering the X-ray diffraction data for compounds incorporating the $Kr_2F_3^+$ cation and the ^{19}F NMR spectra of HF and BrF_5 in solutions, it was suggested [137, 183, 190, 195] that $Kr_2F_3^+$ should be treated as a combination of three contributing structures, one of them being fully ionic. Within the framework of this approach, it is possible to account for the abnormally high chemical reactivity of $Kr_2F_3^+$ and the noticeable differences between its vibrational spectra and the spectra of $Xe_2F_3^+$ incorporated in compounds with Lewis acids like MF_5.

The vibrational spectra of $Xe_2F_3^+$ in compounds $Xe_2F_3^+MF_6^-$ (M = As, Sb, Bi, Ta, Ru, Os, Ir) have been studied in a number of works.[192–194, 196] In the spectra of these compounds, the $Xe_2F_3^+$ cation, like the NgF^+ cation (Ng = Xe, Kr), gives rise to the Xe_a-F_a and Xe_b-F_b stretching vibrations, the $Xe-F_{bridge}$ vibration and the $F-Xe-F_{bridge}$ bending vibration. The frequencies of these $Xe_2F_3^+$ vibrations in the spectra of $Xe_2F_3^+MF_6^-$ are rather close to one another and are about 600, 580, 410 and 160 cm^{-1}, respectively. The observed minor difference between the $Xe_2F_3^+$ vibrational frequencies in the monoclinic and trigonal phases of $Xe_2F_3^+AsF_6^-$ is related to the above-mentioned differences between their crystal structures.[194]

A study of the vibrational spectra of the $Kr_2F_3^+$ cation incorporated in $Kr_2F_3^+MF_6^-$ (M = As, Sb, P, Ta, Au) revealed [185, 190, 193, 195] the following types of vibrations (unlike the spectra of $Xe_2F_3^+$): stretching vibrations of the Kr_a-F_a and Kr_b-F_c bonds with two terminal fluorine atoms; vibrations of the $Kr_b\cdots F_b$ and $Kr_a\cdots F_b$ bonds with two bridging fluorine atoms and bending vibrations of $F-Kr\cdots F$. The frequencies of $Kr_2F_3^+$ in the complexes $Kr_2F_3^+MF_6^-$ (M = As, Sb, P, Ta, Au) are close to one another and are about 600, 560, 460, 330 and 180 cm^{-1}, respectively. The splitting of bands corresponding to Kr_a-F_a and Kr_b-F_c, $Kr_a\cdots F_b$ and $F-Kr\cdots F$ vibrations, as in the case of the spectra of the XeF^+ and KrF^+ cations incorporated in $NgF^+MF_6^-$ and $NgF^+M_2F_{11}^-$, is attributable to pronounced cation–anion interactions and crystal field effects.

Table 10. Crystallographic parameters of the complexes $Xe_2F_3^+MF_6^-$ (M = As, Sb).[194]

Compound	System	Space group	Unit cell parameters								ρ /g cm^{-3}
			a /Å	b /Å	c /Å	α /deg	β /deg	γ /deg	V /Å^3	Z	
$Xe_2F_3^+AsF_6^-$	monoclinic	$C2/c$	25.756(3)	8.556(1)	15.356(2)	90	126.592(6)	90	2716.9(6)	12	3.730
	trigonal	$P3_221$	8.602(5)	8.602(5)	10.655(9)	90	90	120	683.4(8)	3	3.707
$Xe_2F_3^+SbF_6^-$	monoclinic	C/c	14.575(2)	8.1081(12)	9.9926(14)	90	130.360(3)	90	899.8(2)	4	4.099

IV.1.c. XeF_3^- anion

The attempts to isolate complexes with the XeF_3^- anion, which have been undertaken since the mid-1970,[197] are still continued. This is due to the fact that the mass spectra of gaseous XeF_2 and $XeOF_4$ (Ref. 198) and the products of collision-induced dissociation of XeF_2 (Ref. 199) exhibit negative ions XeF_3^-. In addition, the $XeF_3^{\bullet}$ radical was identified by the IR spectra in an argon matrix [200] and in ^{18}F-based radiochemical experiments on fluoride ion exchange ($\tau_{1/2} = 109.7$ min) in the $XeF_2-CH_2Cl_2$ and XeF_2-CH_3CN systems.[201]

Recently, two groups of researchers [91,202] performed quantum chemical calculations of the structural parameters and vibrational frequencies of the XeF_3^- anion. In addition, ^{19}F and ^{129}Xe NMR spectra of acetonitrile solutions of XeF_2 in the presence of $(CH_3)_4NF$ as fluoride ion donors have been studied.[202] Calculations showed that XeF_3^- has an unusual T-shaped structure typical of only isostructural $HalF_3$ molecules (Hal = Cl, Br).[203–205] Relying on the NMR studies of the $XeF_2-CH_3CN-(CH_3)_4NF$ system, Vasdev *et al.*[202] concluded that the anion in this system can exist as XeF_3^- (C_{2v} symmetry) or F_2Xe-F^- adduct (C_s symmetry).

IV.2. Complex compounds of xenon fluoride

IV.2.a. XeF_3^+ cation

Only a few complex compounds of xenon fluoride containing the XeF_3^+ cation are known: $XeF_3^+MF_6^-$ and $XeF_3^+M_2F_{11}^-$ (M = Sb, Bi). This is due to lower donor ability of XeF_4 compared to XeF_2 or XeF_6.[9,47,81] The XeF_3^+ cation is shaped like a trigonal bipyramid with two lone electron pairs located in the equatorial plane and, like the XeF_3^- anion, has an unusual T-shaped structure (Fig. 12 *a*). Upon crystallization of the compounds $XeF_3^+MF_6^-$ at $T \geqslant 350$ K, the XeF_3^+ cation exists in the α-modification, while at $T = 293$ K, it is the β-modification.[9,47,136,205,206] This is responsible for line splitting for the α-form of the cation in the Raman spectra. The crystallographic parameters of $XeF_3^+MF_6^-$ (M = Sb, Bi) and $XeF_3^+Sb_2F_{11}^-$ are given in Table 11. The Xe–F bond lengths in these compounds are:[9,47,136,206] $Xe-F_{ax} = 1.90$, $Xe-F_{eq} = 1.84$ ($XeF_3^+SbF_6^-$) (see Fig. 12 *b*) and $Xe-F_{ax} = 1.92$, $Xe-F_{ax} = 1.94$, $Xe-F_{eq} = 1.81$ Å ($XeF_3^+BiF_6^-$) (see Fig. 12 *a*). The $F-Xe-F_{bridge}$ angle increases on going from $XeF_3^+SbF_6^-$ (127.5°) to $XeF_3^+Sb_2F_{11}^-$ (171.6°), the $Xe-F_{bridge}$ bond length being 2.71 Å. In $XeF_3^+BiF_6^-$, this bond is markedly shorter (2.25 Å), which can be attributed to the same factors as for $XeF^+BiF_6^-$.

The XeF_3^+ cation, similarly to the $HalF_3$ molecules (Hal = Cl, Br) (C_{2v} symmetry) accounts for six normal vibrations

$$\Gamma_{vib} = 3A_1(IR,R) + 2B_1(IR,R) + B_2(IR,R)$$

The experimental vibrational frequencies of the XeF_3^+ cation incorporated in the compounds $XeF_3^+MF_6^-$ (M = As, Sb, Bi) [192,205,206] are also close to one another: $\nu_1(A_1) \approx 650$, $\nu_4(B_1) \approx 610$, $\nu_2(A_1) \approx 560$, $\nu_5(B_1) \approx 320$, $\nu_6(B_2) \approx 250$ and $\nu_3(A_1) \approx 200$ cm^{-1}.

IV.2.b. XeF_5^- anion

There are several compounds [182] containing the XeF_5^- anion: $M^+XeF_5^-$ (M = K, Na, Rb, Cs), $NO^+XeF_5^-$ and $(CH_3)_4N^+XeF_5^-$. The last-mentioned compound crystallizes in the orthorhombic system with the unit cell parameter: $a = 6.340(2)$, $b = 10.244(3)$, $c = 13.896(4)$ Å, $Z = 4$, space group *Pmcn*, $V = 902.55$ Å^3. The anion has an unusual planar pentagonal structure with D_{5h} symmetry (see

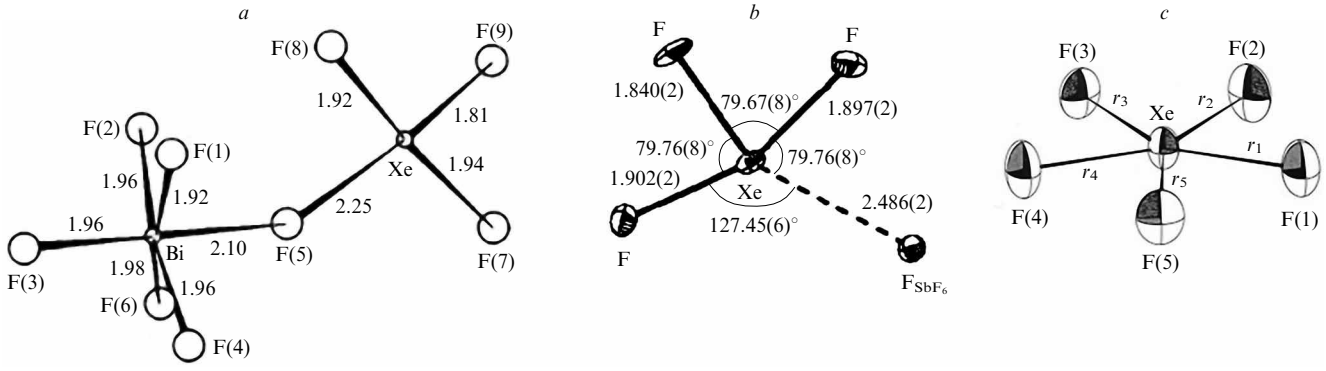


Figure 12. Structure of the XeF_3^+ cation incorporated in $XeF_3^+BiF_6^-$ (*a*),[47] $XeF_3^+SbF_6^-$ (*b*)[206] and the XeF_5^- anion (*c*).[182]

Table 11. Crystallographic parameters of some complexes of XeF_4.

Compound	System	Space group	Unit cell parameters								ρ /g cm^{-3}	Ref.
			a/Å	b/Å	c/Å	α/deg	β/deg	γ/deg	V/Å^3	Z		
$XeF_3^+SbF_6^-$	monoclinic	$P2_1/n$	5.394(1)	15.559(2)	8.782(1)	–	103.10(1)	–	717.84	4	3.92	206
$XeF_3^+BiF_6^-$	triclinic	$P\bar{1}$	5.698(3)	7.811(3)	8.854(4)	99.45(5)	110.09(5)	92.84(3)	362.7	2	4.69	47
$XeF_3^+Sb_2F_{11}^-$	"	$P\bar{1}$	7.929(3)	8.146(3)	9.493(3)	67.676(9)	88.38(2)	66.541(8)	514.8(3)	2	4.134	136

Fig. 12 *c*). The Xe–F bond lengths in the XeF_5^- anion in the complex $(CH_3)_4N^+XeF_5^-$ are as follows: r_1 = 1.979(2), r_2 = 2.001(2), r_3 = 2.030(2), r_4 = 2.018(2), r_5 = 2.034(2) Å, while the bond angles (deg) are as follows: F(2)–Xe–F(1) = 72.3(4), F(3)–Xe–F(2) = 71.7(4), F(4)–Xe–F(3) = 72.2(4), F(5)–Xe–F(1) = 72.3(4), F(5)–Xe–F(4) = 71.5(4).

The structure of the XeF_5^- anion is close to a regular pentagon with an ideal angle of 72°. The mean Xe–F bond length (2.012 Å) in the XeF_5^- anion is somewhat longer than that in the square planar XeF_4 molecule (1.953 Å).[47] The F...F distance between the neighbouring fluorine atoms is in the range of 2.35–2.38 Å, which is considerably shorter than in XeF_4 (2.69–2.71 Å).

The XeF_5^- anion has 12 normal vibrations,[182, 207] of which only six vibrations

$$\Gamma_{vib} = A_1'(R) + A_2''(IR) + 2E_1'(IR) + 2E_2'(R)$$

are IR-active. The experimental vibrational frequencies of the XeF_5^- anion incorporated in $M^+XeF_5^-$ (M = K, Na, Rb, Cs), $NO^+XeF_5^-$, $(CH_3)_4N^+XeF_5^-$ and the assignment of frequencies [182] are summarized in Table 12. It can be seen that the spectra of the XeF_5^- anion existing as a part of the mentioned compounds exhibit some abnormal features. The IR spectra of $M^+XeF_5^-$ (M = K, Rb, Cs) contain lines with A_1' and E_2' symmetry, which should be only Raman-active according to the selection rules. The violation of these rules for D_{5h}-symmetry structures is manifested most vividly in the Raman spectrum of $NO^+XeF_5^-$ in which, apart from the $\nu_1(A_1')$, $\nu_5(E_2')$ and $\nu_6(E_2')$ lines allowed by the selection rules, there are $\nu_2(A_2'')$, $\nu_3(E_1')$ and $\nu_4(E_1')$ lines characteristic of $M^+XeF_5^-$. These abnormal features and splitting of the $\nu_3(E_1')$, $\nu_5(E_2')$ and $\nu_6(E_2')$ lines are probably brought about by the noticeable cation–anion interactions and the crystal lattice field effects. The cation–anion interactions are most pronounced in $NO^+XeF_5^-$; this is typical of most complexes incorporating the NO^+ cation and Lewis acids, in particular, of $NO^+MF_6^-$ (M = P, As, Sb, Au).[116]

In our opinion, the abnormal features observed in the vibrational spectra of the XeF_5^- anion can also be directly related to spectroscopic manifestation of non-rigid intramolecular rearrangements.[87, 88] The foregoing is supported by the fact that, according to theoretical calculations,[207] the XeF_5^- anion can form two more intermediate structures with the activation energies of 77.3, 117.9 and 355.0 kJ mol^{-1}. This fact may attest to the existence of transition states between various minima corresponding to D_{5h}-symmetry structures on the potential energy surface due to noticeable non-rigid intramolecular rearrangements in XeF_5^-.

IV.3. Complex compounds of xenon hexafluoride

IV.3.a. XeF_5^+ cation

A number of complexes of XeF_6 containing the XeF_5^+ cation have been reported.[9, 47, 123–125, 208, 209]

The XeF_5^+ cation should have a perfect tetragonal pyramidal configuration (C_{4v}).[122–125, 184] However, the lone electron pair located on a fourfold axis interacts with bonding electron pairs in different ways, which leads to changes of angles between the bonding pairs and increases the adjacent bond lengths, as the repulsion of the electron pair located in the *cis*-position is stronger than the repulsion of the *trans*-pair.[65, 66] As a result, the axial bond in XeF_5^+ is somewhat stronger than the equatorial bond.[125, 184]

The crystallographic parameters of $XeF_5^+MF_6^-$ (M = As, Pd, Ru, Pt) are summarized in Table 13. The Xe–F bond lengths in these compounds are similar /Å:
for $XeF_5^+RuF_6^-$

$Xe-F_{ax}$ = 1.793, $Xe-F_{eq}$ = 1.841 (two), $Xe-F_{eq}$ = 1.848 (two);
for $XeF_5^+PtF_6^-$

$Xe-F_{ax}$ = 1.81, $Xe-F_{eq}$ = 1.87 (two), $Xe-F_{eq}$ = 1.88 (two);

Table 12. Experimental frequencies (cm^{-1}) in the vibrational spectra of the XeF_5^- anion.[182]

$NO^+XeF_5^-$	$(CH_3)_4N^+XeF_5^-$		$Na^+XeF_5^-$		$K^+XeF_5^-$		$Rb^+XeF_5^-$		$Cs^+XeF_5^-$		Assignment
R	R	IR	R	IR	R	IR	R	IR	R	IR	
503 (100)	502 (100)		519 (100)	523 sh	505 (100) 498 sh		509 (100) 489 sh		504 (100)		ν_1 (A_1'), ν_s (Xe–F)
482 (0+)	–	509 sh 465 vs 420 sh	473 (10)	450 vs 415 s	–	480 vs 410 s	471 (10 453 sh)	470 vw 418 s	–	450 vs 415 s	ν_3 (E_1'), ν_{as} (Xe–F)
440 sh 429 (11)	423 (21)		444 (18) 422 (13)		438 (14) 424 (12)		440 (16) 437 sh		432 (15) 422 (16)		ν_5 (E_2'), ν_{as} (Xe–F)
382 sh 374 (23)	373 (33)		386 (20) 383 sh		388 (24) 381 (19)	379 sh	389 (22) 379 (16)	372 w	380 (22) 369 (23)		ν_6 (E_2'), δ_s (F–Xe–F) in plane
290 (0+)	–	–	293 (0+)	–	290 (0+)	–	299 (0+)	–	312 (0+)	388 sh	ν_4 (E_1'), δ_{as} (F–Xe–F) in plane
240 (2)	–	278 s	–	276 s	–	275 s	278 (0+)	275 s	–	274 s	ν_2 (A_2''), δ_s (F–Xe–F) umbrella out of plane

Table 13. Crystallographic parameters of complex compounds of XeF_6 with Lewis acids MF_5 (M = As, Pd, Ru, Pt).

Compound	System	Space group	Unit cell parameters						ρ /g cm^{-3}	Ref.
			a /Å	b /Å	c /Å	β /deg	V /Å^3	Z		
$XeF_5^+AsF_6^-$	monoclinic	$P2_1/c$	5.886(3)	16.564(10)	8.051(4)	91.57(3)	784.6	4	3.51	9
$XeF_5^+PdF_6^-$	orthorhombic	$Pca2$	9.346(6)	12.786(7)	9.397(6)	–	1122.9	4	3.91	47
$XeF_5^+RuF_6^-$	"	$Pnnma$	16.771(10)	8.206(10)	5.617(10)	–	773.03	4	3.79	208
$XeF_5^+PtF_6^-$	"	$Pnmb$	8.16	16.81	5.73	–	785.4	4	4.52	13

for $XeF_5^+AsF_6^-$

$Xe-F_{ax} = 1.78$, $Xe-F_{eq} = 1.83$;

for $XeF_5^+PdF_6^-$

$Xe-F_{ax} = 1.813$, $Xe-F_{eq} = 1.818$.

The $F_{ax}-Xe-F_{eq}$ angles in the above-listed compounds are equal ($\sim 80^\circ$) and the XeF_5^+ cation occurs in the pseudo-octahedral environment of fluorine atoms and has four bridging bonds of different length: 2.552, 2.601, 2.924, 2.924 Å in $XeF_5^+RuF_6^-$ and 2.52, 2.65, 2.95, 2.95 Å in $XeF_5^+PtF_6^-$. The structure of the XeF_5^+ cation incorporated in $XeF_5^+RuF_6^-$ is shown in Fig. 13 *a*.

Hughes *et al.*[130] conducted the reaction of XeF_6 with $(OsO_3F_2)_\infty$ at 298–323 K, resulting in the synthesis of $[XeF_5][OsO_3F_3]$, $[XeF_5][\mu\text{-}F(OsO_3F_2)_2]$ and $[Xe_2F_{11}][OsO_3F_3]$, and studied the crystal structures of the complexes formed (Table 14). The structure of $[XeF_5][OsO_3F_3]$ is distinguished by the fact that bridging bonds between the XeF_5^+ cation and the $OsO_3F_3^-$ anion are formed by the F(1), F(2) and F(3) fluorine atoms of the anion (see Fig. 13 *b*), which form a tripod under the square base of the XeF_5^+ cation with very similar Xe...F distances [2.514(2), 2.521(2) and 2.468(2) Å, respectively]. The noticeably shorter length of the Xe(1)...F(3) bond is likely to be associated with crystal packing, which also affects the Os–F(3) bond [2.028 (2) Å] and the shorter Os–O(3) bond [1.692(3) Å] located in the *trans*-position with respect to the Os–F(3) bond. The xenon atom is arranged 2.064 Å above the F(1)–F(2)–F(3) plane, which is almost parallel (to within $\pm 5.2^\circ$) to the equatorial F(5)–F(6)–F(7)–F(8) plane of the XeF_5^+ cation. The Xe–F bond lengths in $[XeF_5][OsO_3F_3]$ do not differ markedly, amounting to, Å: Xe(1)–F(4) = 1.819(2), Xe(1)–F(5) = 1.866(2), Xe(1)–F(6) = 1.862(2), Xe(1)–F(7) = 1.866(2) and Xe(1)–F(8) = 1.864(2). It is noteworthy that this type of coordination of a xenon atom was also found in some other complexes, namely $[XeF_5]_2[PdF_6]$,[209] $[XeF_5][AsF_6]$ [210] and $[XeF_5]_2[NiF_6]$,[211] which also contain three long bridging Xe···F bonds within one ion pair.

Higher coordination of the xenon atom in XeF_5^+ incorporated in the compound $[XeF_5][\mu\text{-}F(OsO_3F_2)]$ (see Fig. 13 *b*), unlike that in $[XeF_5][OsO_3F_3]$ (see Fig. 13 *c*), is caused by formation of four short bonds with terminal fluorine atoms in the anion (two atoms from each OsO_3F_2 group); these atoms interact with the xenon atom from

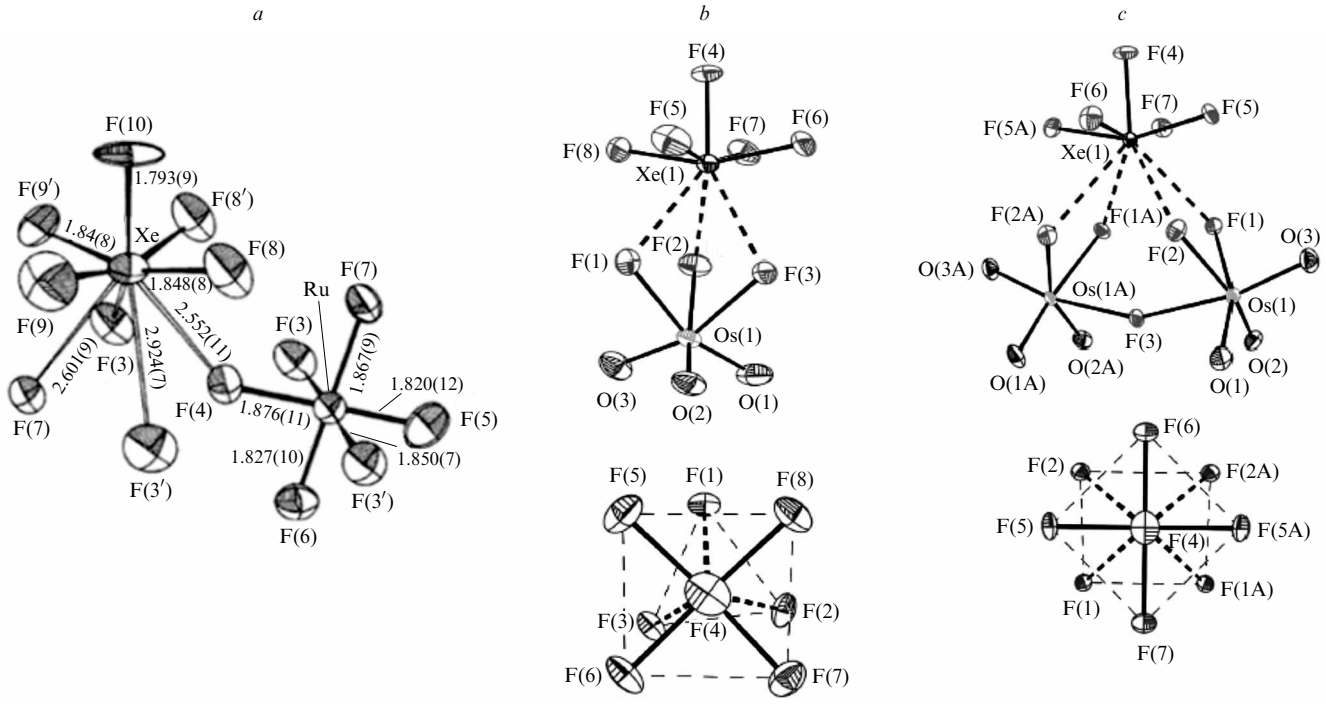


Figure 13. Structures of $XeF_5^+RuF_6^-$ (*a*),[210] $[XeF_5][\mu\text{-}F(OsO_3F_2)_2]$ (*b*) and $[XeF_5][OsO_3F_3]$ (*c*).[130]

Table 14. Crystallographic parameters of $[XeF_5][\mu\text{-}F(OsO_3F_2)_2]$, $[XeF_5][OsO_3F_3]$ and $[Xe_2F_{11}][OsO_3F_3]$.[130]

Compound	Space group	Unit cell parameters					ρ /g cm^{-3}
		a /Å	b /Å	c /Å	V /Å^3	Z	
$[XeF_5][\mu\text{-}F(OsO_3F_2)_2]$	*Pnma*	12.672(1)	11.444(1)	7.5818(7)	1099.6(2)	4	4.819
$[XeF_5][OsO_3F_3]$	$P4_2/n$	16.8876(3)	16.8876(3)	5.3414(2)	1523.3(1)	8	4.548
$[Xe_2F_{11}][OsO_3F_3]$	*Pnma*	9.2479(3)	15.1769(5)	8.1192(2)	1139.46(6)	4	4.470

below the square plane of the cation and do not interact with the lone electron pair. The Xe···F(1) and Xe···F(1A) bond lengths of 2.622(1) Å and the Xe···F(2) and Xe···F(2A) bond lengths of 2.663(1) Å are commensurable, and the xenon atom is located 1.909 Å above the plane confined by the four fluorine atoms involved in the bond formation. This plane is virtually parallel ($\pm 0.1^\circ$) to the equatorial F(5)–F(6)–F(5A)–F(7) plane. The Xe–F bond lengths in the compound $[XeF_5][\mu\text{-}F(OsO_3F_2)]$, as in the case of $[XeF_5][OsO_3F_3]$, are rather close to one another and amount to /Å: Xe(1)–F(4) = 1.822(2), Xe(1)–F(5) = 1.848(1), Xe(1)–F(6) = 1.848(2), Xe(1)–F(7) = 1.852(2) and Xe(1)–F(5A) = 1.848(1).

The vibrational spectrum of the XeF_5^+ cation,[81, 124–126, 184] similarly to the spectra of halogen pentafluorides,[203, 204] comprises nine normal vibrations

$$\Gamma_{vib} = 3\,A_1(IR,R) + 2\,B_1(R) + B_2(R) + 3\,E(IR,R)$$

corresponding to the C_{4v} symmetry of the structure.

Data on the vibrational spectra of XeF_5^+, unlike its isoelectronic analogues IF_5, TeF_5 and SbF_5^{2-},[101] are relatively few in number. The interpretation of the XeF_5^+ vibrations reported by Christe *et al.*[124] is contradictory as regards the assignment of the Xe–F vibration frequencies at about 200–400 cm^{-1}. The assignment of bands in the spectra of XeF_5^+ recorded in a number of studies[123, 208, 210, 211] does not appear quite reliable either, because it was performed almost without invoking polarization measurements for the Raman spectra of solutions of XeF_5^+ in anhydrous HF.

For the proper assignment of frequencies of the XeF_5^+ cation, we carried out precision polarization measurements in the Raman spectra of the compounds $XeF_5^+AuF_6^-$, $XeF_5^+BF_4^-$ and $XeF_5^+PbF_4$ in a solution in anhydrous HF.[184] In addition, published data on the vibrational spectra of solid compounds incorporating the XeF_5^+ cation were analyzed and systematically arranged.

The characteristic features of the IR and Raman spectra of the XeF_5^+ cation incorporated into $XeF_5^+MF_4^-$ (M = B, Ga, Pb, Fe, Co), $XeF_5^+MF_5^-$ (M = Zr, Hf, Mn) and $XeF_5^+MF_6^-$ (M = As, Sb, Au, Pd, Ru, Pt, Nb, Bi, V, U) have been considered in detail.[81, 123–126] The Raman frequencies of the XeF_5^+ cation within some of the listed compounds dissolved in anhydrous HF are summarized in Table 15. It can be seen that the positions and intensities of the Raman lines corresponding to the XeF_5^+ cation in solutions of $XeF_5^+F^-$, $XeF_5^+BF_4^-$, $XeF_5^+PbF_4^-$ and $XeF_5^+AsF_6^-$ virtually coincide. This indicates that the strong axial bond $(Xe-F)_{ax}$ and weaker equatorial bonds $(Xe-F)_{eq}$ have similar lengths. The same conclusion has been drawn from the results of quantum chemical calculations for the structure of $XeF_5^+XF_6^-$ (X = P, As, Sb, Bi, V, Nb, Ta).[212] Furthermore, the data of Table 15 indicate that the $F_{ax}-Xe-F_{eq}$ angles in these compounds are constant. Note that the approximate invariability of the angles between the axial and equatorial bonds, indicating hybridization of the central atomic orbitals, is also observed for isoelectronic analogues of the XeF_5^+ cation.[203]

Isoelectronic analogue	IF_5	TeF_5^-	SbF_5^{2-}
Angle /deg	81.7	78.8	79.4

In solutions of $XeF_5^+AuF_6^-$ in HF, these values for the XeF_5^+ cation (apart from the ν_1 and ν_2 line frequencies and intensities) are somewhat different. As in the case of the XeF_6 molecule and the XeF_5^- anion, the differences are attributable to non-rigid rearrangements in the XeF_5^+ cation located in the strong field of the AuF_6^- anion, which may lead to fast axial–equatorial exchange of the F ligands.[88, 184] Note that a similar intramolecular exchange of F ligands has been observed for the ClF_4^+ cation within the complex ClF_4AuF_6.[88, 187]

Table 15. Frequencies (cm^{-1}) and band assignment in the Raman spectra of the XeF_5^+ cation in solutions in anhydrous HF.

Compound	$\nu_1(A_1)$	$\nu_2(A_1)$	$\nu_3(A_1)$	$\nu_4(B_1)$	$\nu_6(B_1)$	$\nu_7(E)$	$\nu_8(E)$	$\nu_9(E)$	Ref.
$XeF_5^+F^-$	677 (58) p	622 (100) p	361 (3) p	611 sh	300 (3) dp		411 (3) dp	212 (1) dp	125
$XeF_5^+BF_4^-$	679 (54) p	625 (100) p	358 (1) p	610 sh	302 (4) dp		410 (3) dp	218 (1) dp	123
$XeF_5^+BF_4^-$	676 (50) p	621 (100) p	301 (7) p	–	255 (0+) dp		408 (7) dp	216 (2) dp	124
$XeF_5^+BF_4^-$	678 (52) p	622 (100) p	300 (8) p	613 sh	277 (2) dp		408 (4) dp	218 (2) dp	125
$XeF_5^+PbF_4^-$	674 (51) p	623 (100) p	361 (9) p	607 sh	297 (3) dp		410 (5) br,[a] dp	215 ($\leqslant$1) dp	126
$XeF_5^+AsF_6^-$	677 (60) p	625 (100) p	302 (3) p	[625]	255 (0+) dp	[677]	410 (4) dp	216 (1) dp	123
$XeF_5^+AsF_6^-$	679 (63) p	625 (100) p	352 sh	610 sh	299 (10) dp		408 (7) dp	217 (2) dp	124
$XeF_5^+AsF_6^-$	681 (56) p	622 (100) p	349 (3) p	612 sh	301 (6) dp		407 (5) br,[a] dp	–	125
$XeF_5^+AuF_6^-$	680 (59) p	624 (100) p	339 (3) p	579 sh	288 (8) dp	672 sh	420 (9) br,[a] dp	208 (6) dp	184

[a] br is broad.

It has been noted [88, 184] that in high-coordination compounds like EAX_k (k = 4, 5, 6), the non-rigid intramolecular rearrangements occur mainly by mechanisms similar to Berry pseudo-rotation [213] in which the lone electron pair E participates on an equal basis with ligands X. In the electron-excessive compounds EAX_4 (for example, $HalF_4^+$, Hal = Cl, Br), the intramolecular ligand exchange can occur by small and big pseudo-rotation mechanisms [88, 214] (Fig. 14 *a*). In the former mechanism, the C_{2v}-symmetry trigonal bipyramid in which the lone pair occupies an equatorial position is transformed into an equivalent TBP configuration of the same symmetry. The transition proceeds *via* C_{4v}-symmetry square pyramidal configuration in which the lone pair occupies the axial position. In the latter mechanism, the top of the barrier on the potential energy surface corresponds to a TBP configuration with the C_{3v} symmetry with the lone electron pair in the axial position.[88, 214, 215]

For pentacoordinate compounds XF_5 (X = Cl, Br, Xe), the most probable mechanisms of non-rigid intramolecular rearrangements include pseudo-rotation *via* the TBP-configuration (D_{3h} symmetry) and the turnstile exchange of non-equivalent fluorine atoms through rotation of two triangular pyramids [88, 184, 214, 215] in which the sixth ligand site in one of the pyramids is occupied by the lone electron pair (see Fig. 14 *b*). These rearrangements change the axial $[(X-F)_{ax}]$ and equatorial $[(X-F)_{eq}]$ bond lengths and give rise to anomalous relationships of vibration band intensities and unusual values of the principal force constants, coupling constants and so on.[124, 188] In the case of $XeF_5^+AuF_6^-$, these rearrangements may result in distortion of not only the cation structure but also the anion structure by lowering the anion symmetry upon characteristic structural transformations,[43, 189] for example

$$O_h \rightarrow D_{4h}\,,\ O_h \rightarrow C_{4v}$$

One more possible cause for the structural distortion of the XeF_5^+ cation and XF_6^- anions is their non-specific interaction within the compounds $XeF_5^+XF_6^-$. Bobrov and Tsirelson [216] carried out *ab initio* quantum chemical calculations for the complexes $XeF_5^+XF_6^-$ (X = P, As, Sb, Bi) using relativistic pseudopotential for heavy atoms and full-electron basis sets. Chemical bonds were characterized using critical point parameters — electron density, total electron energy and its kinetic and potential constituents. The calculation results showed that the interaction between the XeF_5^+ cation and the XF_6^- anion in the $XeF_5^+XF_6^-$ type

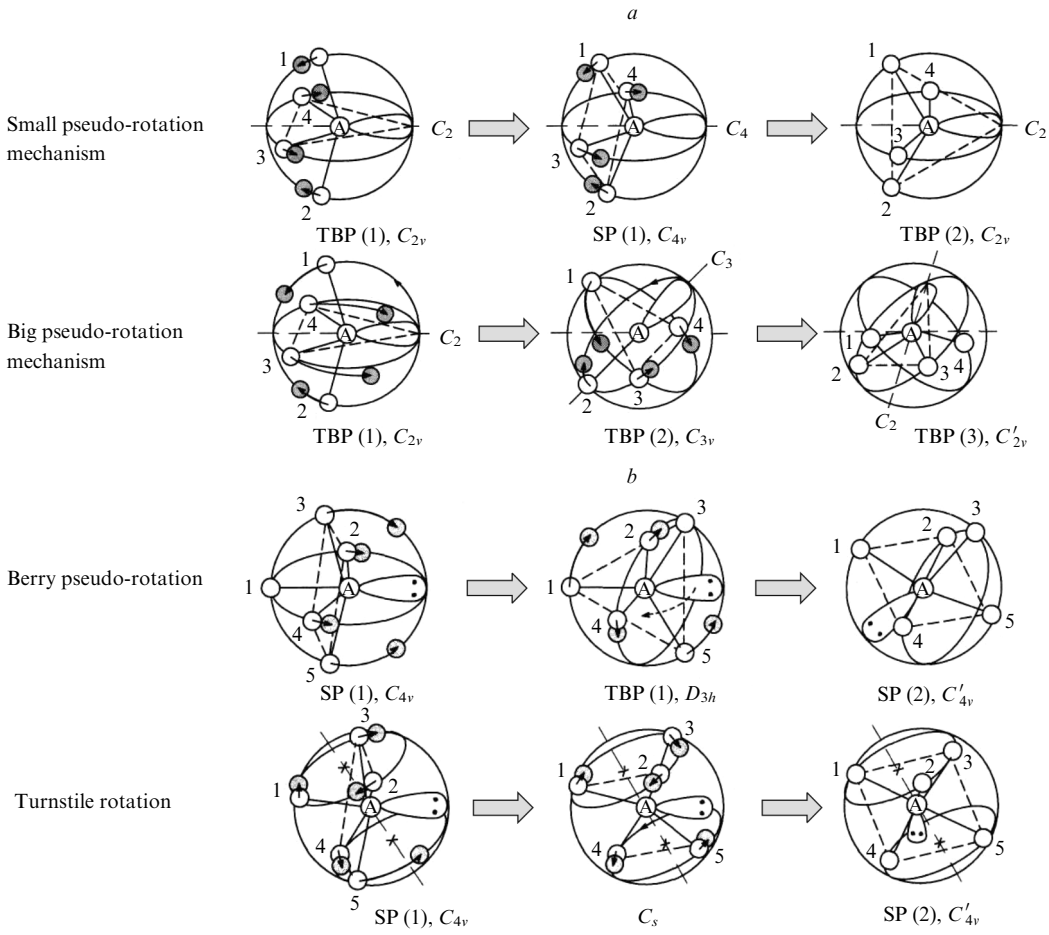


Figure 14. Patterns of axial–equatorial exchange of F ligands in EAX_4 type molecules by small and big pseudo-rotation mechanisms (*a*) [88] and rearrangement mechanisms in EAX_5 type molecules (*b*).[184]
TBP is trigonal bipyramid, SP is square pyramid, the numerals designate non-equivalent fluorine atoms.

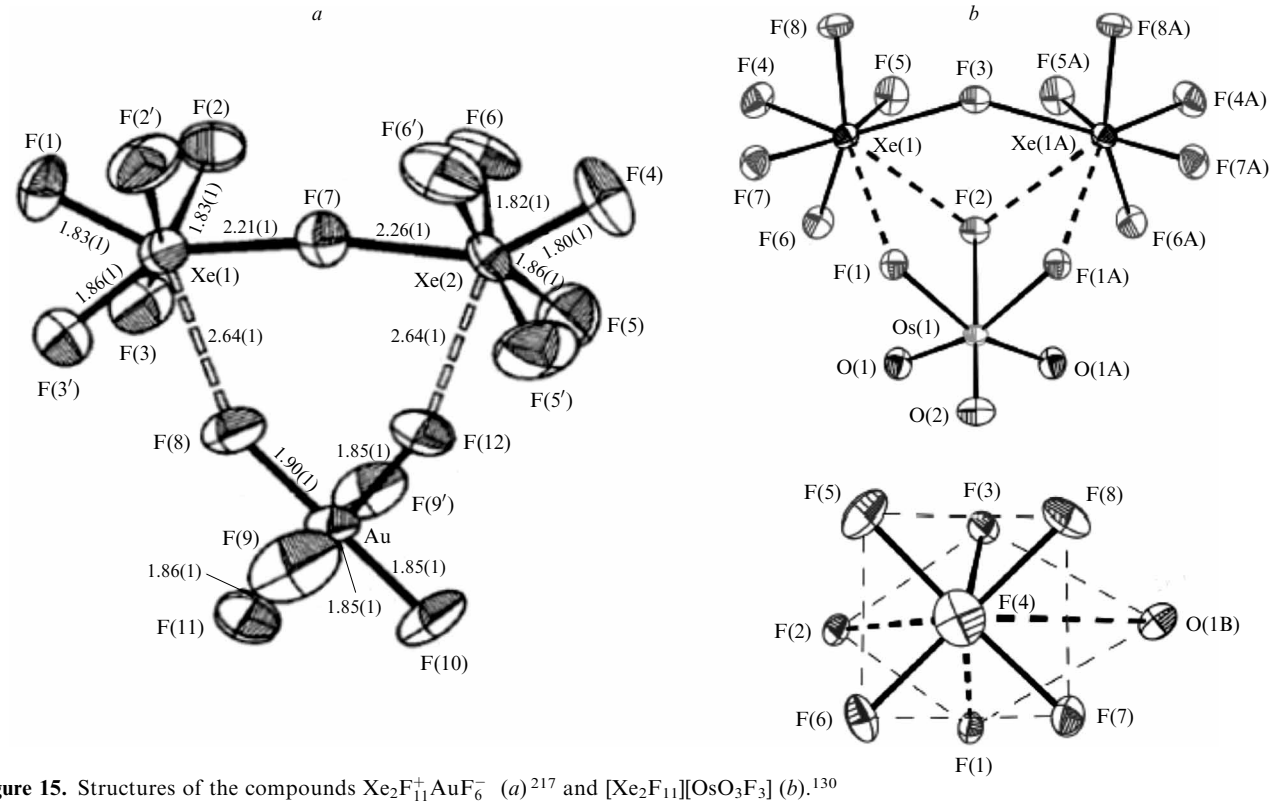


Figure 15. Structures of the compounds $Xe_2F_{11}^+AuF_6^-$ (*a*)[217] and $[Xe_2F_{11}][OsO_3F_3]$ (*b*).[130]

complexes follows the 'key–lock' principle and involves directed interactions $F_{bridge} \rightarrow Xe$, while the structuring role of the lone electron pair of xenon is to counterbalance the destabilizing electrostatic interaction of the Xe and X atoms bearing excessive positive charges.

IV.3.b. $Xe_2F_{11}^+$ cation

The $Xe_2F_{11}^+$ cation incorporated in $Xe_2F_{11}^+MF_6^-$ (M = Ru, Pd, Au)[9,47,209] crystallizes in the orthorhombic system (space group *Pnma*). The above-noted compound $[Xe_2F_{11}][OsO_3F_3]$ crystallizes in the same structure (see Table 14).[130] The unit cell parameters, for example, for $Xe_2F_{11}^+AuF_6^-$ are as follows: $a = 9.115$, $b = 8.542$, c = 15.726 Å, $V = 1224.0$ Å^3, $Z = 4$, $\rho = 4.24$ g cm^{-3} (see Ref. 47, 217). Unlike the listed complexes, the compound $Xe_2F_{11}^+VF_6^-$ (see Ref. 129) crystallizes in the monoclinic system, space group $P21/n$, the unit cell parameters $a = 8.551(1)$, $b = 8.896(1)$, $c = 15.703(1)$ Å, $\beta = 93.31(2)^\circ$, $V = 1192.5(9)$ Å^3, $Z = 4$, $\rho = 3.545$ g cm^{-3}.

The $Xe_2F_{11}^+$ cation in the solid phase of $Xe_2F_{11}^+MF_6^-$ (M = Ru, Pt, Pd, Au) consists of two XeF_5^+ fragments connected by a fluoride bridge (Fig. 15*a*). The structure and molecular parameters of these fragments are comparable with those for the XeF_5^+ cation: the $Xe-F_{bridge}-Xe$ angle is close to 170°, and the $Xe-F_{bridge}$ bond lengths are in the range of 2.20– 2.30 Å.

Study of the crystal structure of $[Xe_2F_{11}][OsO_3F_3]$[130] showed that not all of the bonds involving xenon atoms are confined to the same ion pair $[Xe_2\ F_{11}][OsO_3F_3]$ (Fig. 15*b*). In the case of Xe(1), there are two bonds involving the F(1) and F(2) terminal atoms of the $OsO_3F_3^-$ anion, the bridging Xe(1)···F(3) bond of the $Xe_2F_{11}^+$ cation and the bond with the O(1B) atom [3.353(2)°], which belongs to another $OsO_3F_3^-$ anion in the unit cell. The Xe(1)···F(2) bond [2.800(2) Å] is longer than Xe(1)···F(1) [2.504(2) Å], as F(2) is equally coordinated to both Xe(1) and Xe(1A), whereas F(1) forms only one short bond with Xe(1). The Xe(1) atom is located 1.916 Å above the F(1), F(2), F(3) and O(1B) group of atoms occurring as nearly a parallelogram, which are coplanar to within ±0.0260 Å and are nearly parallel (±2.0°) to the F(5)–F(6)–F(7)–F(8) plane. The Xe–F bond lengths in $[Xe_2F_{11}][OsO_3F_3]$, as in the case of $[XeF_5][\mu\text{-}F(OsO_3\ F_2)]$ and $[XeF_5][OsO_3F_3]$, are quite similar and amount to /Å: Xe(1)–F(4) = 1.830(2), Xe(1)–F(5) = 1.859(2), Xe(1)–F(6) = 1.873(2), Xe(1)–F(7) = 1.873(2) and Xe(1)–F(8) = 1.862(2).

The Raman spectra of the compounds $Xe_2F_{11}^+MF_6^-$ (M = P, As, V, Pd, Sn, Au) in the solid phase have been studied in a number of papers,[123,129,217,218] and the spectra of $Xe_2F_{11}^+MF_6^-$ (M = P, As) dissolved in anhydrous HF have also been reported.[123,129] The experimental vibration frequencies found for the $Xe_2F_{11}^+$ cation are summarized in Table 16.

IV.3.c. XeF_7^- and XeF_8^{2-} anions

Xenon hexafluoride behaves as a Lewis acid in reactions with alkali metal fluorides and with NOF, NO_2F and NF_4HF_2; this affords complexes $M_2^+XeF_8^{2-}$ (M = Na, K, Rb, Cs), $X_2^+XeF_8^{2-}$ (X = NO, NO_2, NF_4), $M^+XeF_7^-$ (M = Rb, Cs) and $X^+XeF_7^-$ (X = NO_2, NF_4).[9,128,131]

An X-ray diffraction study of $(NO^+)_2XeF_8^{2-}$, which is crystallographically identical to $(NO^+)_2WF_8^{2-}$ and $(NO^+)_2ReF_8^{2-}$, showed[219] the presence of NO^+ and XeF_8^{2-} groups in its crystal lattice. The unit cell parameters of this compound were found to be $a = 8.914$, $b = 5.945$, $c = 12.83$ Å, Z = 4, $\rho = 3.354$ g cm^{-3}, space group *Pnma*. The structure of XeF_8^{2-} (square antiprism, D_{4d} symmetry) is shown in Fig. 16*a*. The Xe–F bond lengths in this com-

Table 16. Frequencies (cm^{-1}) and vibration band assignment in the Raman spectra of the $Xe_2F_{11}^+$ cation.

$Xe_2F_{11}^+PF_6^-$ (Ref. 123)	$Xe_2F_{11}^+AsF_6^-$ (Ref. 123)	$Xe_2F_{11}^+PdF_6^{2-}$ (Ref. 123)	$Xe_2F_{11}^+AuF_6^-$ (Ref. 217)	$Xe_2F_{11}^+VF_6^-$ (Ref. 129)	Type of vibration
666 (100) 657 (40)	663 (100) 655 sh	653 s	661 s	671 s	ν (Xe–F_{ax})
651 (58) 640 (3)	644 (44)	634 w	640 w	–	ν (XeF_4)
604 (46) 598 (70)	602 (36) 594 (60)	616 vw 606 w	626 w 600 s	620 s	ν_s (XeF_4)
587 (29)	583 (20)	590 m	595 vs 590 vs	–	ν_{as} (XeF_4)
402 (4)	408 (2)	425 vw	400 w	406 w	δ (F–XeF_4)
360 (6)	358 (6)	396 vw	356 w	359 sh	
299 (4)	298 sh	309 w	290 w	–	δ_s (XeF_4)
–	290 (5)	269 w	–	–	δ_s (XeF_4) in plane
230 (0+)	232 (0+)	245 w	221 m	210 vw	δ_{as} (XeF_4) out of plane
207 (0+)	206 (2)	–	–	183 vw	δ_{as} (XeF_4) in plane

pound are/Å: Xe–F(1) = 2.003(1), Xe–F(2) = 1.938(1), Xe–F(3) = 1.944(9), Xe–F(4) = 2.1519(9) and Xe–F(5) = 203.9(1); the F–Xe–F bond angles are in the range of 73–75°. In the $Cs_2^+XeF_8^{2-}$ fragment incorporated in the $Cs_2^+XeF_8^{2-} \cdot 4BrF_5$ adduct, the crystal structure of the anion is somewhat distorted due to interaction with bromine pentafluoride molecules. The unit cell parameters of this compound are as follows: a = 12.099(1), b = 12.404(1), c = 15.549(2) Å, Z = 4, space group *Pnma*. The Xe–F bond lengths are in the range of 1.954(6)–2.075(4) Å, the F–Xe–F angles are close to the corresponding angles in $(NO^+)_2XeF_8^{2-}$, and the Xe–F···Br distance is 2.74–2.81 Å.

An X-ray diffraction study of $Cs^+XeF_7^-$ indicated[220] that the lone electron pair in the XeF_7^- anion is less stereochemically active than that in the XeF_5^+ cation; as a consequence, the anion exists as a C_{3v}-symmetry monocapped octahedron (Fig. 16 *b*). The structural parameters of $Cs^+XeF_7^-$ at 130 K are a = 8.960(7) Å, Z = 8, V = 605.7(1) Å^3, space group $P2_13$. The Xe–F bond lengths are as follows/Å: Xe–F(1) = 1.932(3), Xe–F(2) = 2.100(6), Xe–F(3) = 1.970(3); the F(2)–Xe–F(1) and F(2)–Xe–F(3) angles are 132.2(1) and 75.91(1)°, respectively. In the compound $NO_2^+Xe_2F_{13}^-$ (see Fig. 16 *c*) obtained by the reaction of NO_2F with an excess of XeF_6,[220] the XeF_7^- anion is an ideal monocapped trigonal prism (C_{2v} symmetry) (see Fig. 16 *d*). Apparently, the existence of this structure is related to pronounced interaction between the lone electron pair of XeF_7^- and the reactive pair of XeF_6 in the $Xe_2F_{13}^-$ anion. According to Ellern and Adam,[219] the unit cell parameters of $NO_2^+Xe_2F_{13}^-$ [a = 15.925(3), b = 7.5435(2), c = 8.649(1) Å, β = 94.77(1)°, Z = 8, V = 1075.8(4) Å^3, space group C_2/m] differ substantially from those for $Cs^+XeF_7^-$. The Xe–F bond lengths (see Fig. 16 *c*,*d*) are as follows/Å: Xe(2)–F(21) = 2.189(2), Xe(2)–F(22) = 1.842(4), Xe(2)–F(23) = 1.901(3) and Xe(2)–F(24) = 1.878(3).

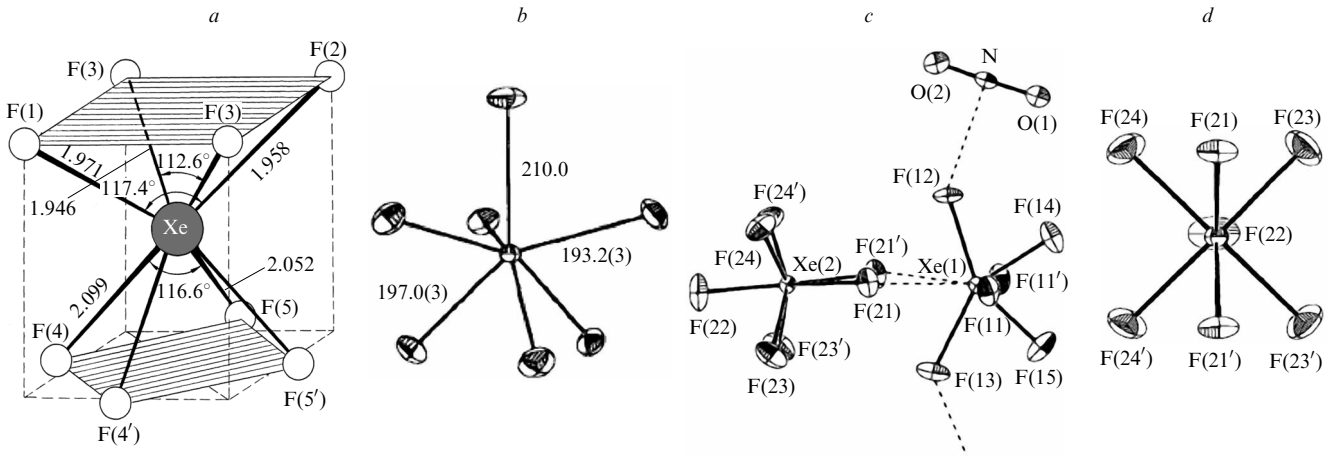


Figure 16. Structures of the anions XeF_8^{2-} (*a*) and XeF_7^- (*b*),[219] the compound $NO_2^+Xe_2F_{13}^-$ (*c*) and view of the structure of XeF_7^- in $Xe_2F_{13}^-$ (*d*).[220]

V. Structures of the complex compounds of xenon oxyfluorides

Xenon oxyfluorides, similarly to xenon fluorides, possess the properties of Lewis acids and bases [9, 205, 221, 222] and can function as fluoride ion donors and acceptors in the formation of complexes

$XeOF_4 \rightarrow XeOF_3^+$, $XeOF_5^-$, $(XeOF_4)_3F^-$

$XeO_2F_2 \rightarrow XeO_2F^+$, $XeO_2F_3^-$

$XeOF_2 \rightarrow XeOF_3^-$

$XeO_3 \rightarrow XeO_3F^-$

The complex compounds of xenon oxyfluorides were studied by ^{19}F NMR spectroscopy, X-ray crystallography and vibrational spectroscopy (see publications [9, 159, 221–227] and the references cited therein). As in the case of complexes of xenon and krypton, these studies provided the conclusion that the structures of xenon oxyfluoride complexes can be described in terms of an ionic model.[9, 12, 31, 32]

V.1. Complex compounds of $XeOF_4$

V.1.a. $XeOF_3^+$ cation

Only two compounds containing the $XeOF_3^+$ cation are known, namely, $XeOF_3^+SbF_6^-$ and $XeOF_3^+Sb_2F_{11}^-$).[205, 206, 222] The structure of the $XeOF_3^+$ cation resembles the structure of the $ClOF_3$ molecule.[204, 215] According to model views of the VSEPR theory,[65, 66] $XeOF_3^+$ has a pseudo-trigonal bipyramid geometry (C_s symmetry) in which two fluorine atoms are axial and the third fluorine atom, the oxygen atom and the lone electron pair occupy the equatorial positions. This structure possesses nine normal vibrations

$$\Gamma_{vib} = 6\,A'(IR,R) + 3\,A''(IR,R)$$

The vibration frequencies [205, 206] of the $XeOF_3^+$ cation incorporated in $XeOF_3^+SbF_6^-$ and $XeOF_3^+Sb_2F_{11}^-$ differ little and amount to /cm^{-1}: $\nu_1(A') \approx 640$, $\nu_2(A') \approx 630$, $\nu_3(A') \approx 340$, $\nu_4(A') \approx 590$, $\nu_5(A') \approx 200$, $\nu_6(A') \approx 190$, $\nu_7(A'') \approx 610$, $\nu_8(A'') \approx 360$ and $\nu_9(A'') \approx 320$.

According to a crystallographic study,[221] $XeOF_3^+SbF_6^-$ crystallizes in the triclinic system (space group $P\bar{1}$) with the unit cell parameters: $a = 8.568(2)$, $b = 9.760(2)$, $c = 10.104(2)$ Å, $\beta = 98.58(2)$, $\gamma = 104.27(2)^\circ$, $V = 763.4$ Å^3, $Z = 4$, $\rho = 3.829$ g cm^{-3}. The Xe–F_{ax} and Xe–F_{eq} bond lengths are 1.879(12) and 1.821(12) Å, respectively, and the Xe–O bond lengths are 1.692(13) Å. Note that the Xe–F bond lengths in $XeOF_3^+$ are similar to those in the XeF_3^+ cation [1.883(13 Å]. The F–Xe–O and F–Xe–F angles are in the ranges of 93–100 and 73–161°, respectively.

V.1.b. $XeOF_5^-$ and $(XeOF_4)_3F^-$ anions

The oxyfluoride $XeOF_4$ reacts with Lewis bases to form the following complexes:[224, 228] $3\,KF \cdot XeOF_4$, $3\,RbF \cdot 2\,XeOF_4$, $CsF \cdot XeOF_4$, $CsF \cdot 3\,XeOF_4$, $NOF \cdot XeOF_4$, $(CH_3)_4N \cdot XeOF_4$, which contain the $XeOF_5^-$ and $(XeOF_4)_3F^-$ anions. The vibrational spectra and structural features of these compounds have been studied.[224, 225, 228] Relying on the data of Raman spectra, the $XeOF_5^-$ anion was interpreted [225, 228] as having a distorted pseudo-octahedral structure with the C_{4v} symmetry characterized by eleven normal vibrations

$$\Gamma_{vib} = 4\,A_1(IR) + 2\,B_1(IR,R) + B_2(IR,R) + 4\,E(IR)$$

In a later study,[224] the conclusion was drawn from analysis of the vibrational spectra of $Cs^+XeOF_5^-$ and $N(CH_3)_4^+XeOF_5^-$ that the geometry of the $XeOF_5^-$ anion is a pseudo-pentagonal bipyramid (C_{5v} symmetry), which in turn possesses nine normal vibrations

$$\Gamma_{vib} = 3\,A_1(IR,R) + 3\,E_1(IR,R) + 3\,E_2(R)$$

Table 17. Vibrational spectra of the $XeOF_5^-$ anion.

$(CH_3)_4N^+XeOF_5^-$ (Ref. 224)		$Cs^+XeOF_5^-$ (Ref. 225)			Assignment	Vibrational mode
IR (T = 303 K)	R (T = 123 K)	R [a] (T = 293 K)	R (^{16}O) (T = 77 K)	R (^{18}O) (T = 77 K)		
878 s	880 (32)	883 (64)	883	839 (66)	ν_1	ν (Xe=O)
516 m	515 (100)	525 (100)	524	524 (100)	ν_2	ν_s (XeF_5)
290 s	296 (7)	290 (7)	293	290 (13)	ν_3	δ_u (XeF_5)
495 vs					ν_4	ν (XeF_5)
370 m	370 sh	368 (20)	410	407 (7)	ν_5	δ_p (Xe=O)
			396	390 (24)		
			384	378 (24)		
			365	352 (15)		
273 w	270 sh	275 (5)	274	267 (8)	ν_6	δ (XeF_5) in plane
	470 (18)	469 (35)	473	473 (34)	ν_7	ν (XeF_5)
	450 (10)	439 (2)	468	468 (29)		
			435	435 (12)		
	397 (54)	397 (47)	420	420 (10)	ν_8	δ_q (XeF_5) in plane
			390	390 (40)		
			361	361 (17)		

Note. The subscripts stand for: p is rocking vibration, q is scissor vibration. [a] Data from Ref. 228.

Table 18. Crystallographic parameters of α-$XeO_2F^+SbF_6^-$ and β-$XeO_2F^+SbF_6^-$, $XeO_2F^+AsF_6^-$, $(FO_2XeFXeO_2F)^+AsF_6^-$ and $XeF_5^+SbF_6^- \cdot XeOF_4$.[159]

Compound	Space group	Unit cell parameters								ρ /g cm^{-3}
		a/Å	b/Å	c/Å	α/deg	β/deg	γ/deg	V/Å^3	Z	
α-$XeO_2F^+SbF_6^-$	$P2_1/c$	10.190(4)	5.719(2)	12.082(4)	90	92.456(4)	90	703.5(4)	4	3.947
β-$XeO_2F^+SbF_6^-$	$R3$	12.9188(9)	12.9188(9)	14.661(2)	90	90	120	2119.1(3)	3	3.931
$XeO_2F^+AsF_6^-$	$P2_12_12_1$	8.658(6)	8.699(6)	8.916(6)	90	90	90	671.5(8)	4	3.672
$(FO_2XeFXeO_2F)^+AsF_6^-$ (see [a])	$P2_1/c$	10.488(4)	5.340(2)	18.346(6)	90	101.168(5)	90	1008.1(6)	4	3.772
$XeF_5^+SbF_6^- \cdot XeOF_4$	$P2_1/m$	5.6586(2)	8.6566(4)	12.4042(2)	90	102.718(2)	90	592.70(4)	2	3.840

[a] Data from Ref. 223.

The vibrational frequencies of the $XeOF_5^-$ anion incorporated in the compounds $Cs^+XeOF_5^-$ and $(CH_3)_4N^+XeOF_5^-$ with the assumption of the C_{5v} symmetry of the anion are given in Table 17. The geometric parameters of the structure of $XeOF_5^-$ calculated by Christe *et al.*[224] are as follows: Xe=O = 1.733 Å, Xe–F = 1.955 Å, the angle F–Xe–F = 72.0° and the angle O=Xe–F = 91.0°.

The $(XeOF_4)_3F^-$ anion was detected [228] in a study of the Raman spectra of $Cs^+(XeOF_4)_3F^-$. According to X-ray diffraction data,[224] there were three $XeOF_4$ groups linked to one another through the central fluoride ion. The compound $Cs^+(XeOF_4)_3F^-$ crystallizes in the cubic system (space group $Pa3$) and the unit cell parameters are as follows: a = 13.933(7) Å, V = 270.8 Å^3, Z = 4, ρ = 4.035 g cm^{-3}.

V.2. Complex compounds of XeO_2F_2

The complexes $XeO_2F^+SbF_6^-$ and $XeO_2F^+Sb_2F_{11}^-$ have been prepared and characterized by Raman spectroscopy and ^{129}Xe and ^{19}F NMR spectroscopy.[205, 222, 229] Subsequently, the compounds $XeO_2F^+AsF_6^-$ and $(FO_2XeFXeO_2F)^+AsF_6^-$ have been obtained and studied by vibrational spectroscopy.[223] According to data [205, 223] derived from the vibrational spectra, the XeO_2F^+ cation incorporated in this compound has a C_s-symmetric structure of a trigonal pyramid and $(FO_2XeFXeO_2F)^+$ has a C_{2v}-symmetry structure with bridging Xe···F···Xe bonds having 21 normal vibrations.

Pointner *et al.*,[159] who prepared $XeO_2F^+SbF_6^-$, found that crystallization of this compound from a hydrogen fluoride solution in the temperature range of 195–228 K yields the tetramer phase β-$XeO_2F^+SbF_6^-$. The crystallographic parameters of α-$XeO_2F^+SbF_6^-$, β-$XeO_2F^+SbF_6^-$, $XeO_2F^+AsF_6^-$, $(FO_2XeFXeO_2F)^+AsF_6^-$ and $XeF_5^+SbF_6^- \cdot XeOF_4$ determined in the studies cited [159, 223] are summarized in Table 18.

The crystal structure of α-$XeO_2F^+SbF_6^-$ consists of discrete XeO_2F^+ cations and SbF_6^- anions linked by F bridges (Fig. 17 *a*). The Xe–F and Xe–O bond lengths are as follows/Å: Xe(1)–F(7) = 1.849(2), Xe(1)–O(1) = 1.740(3), Xe(1)–O(2) = 1.726(3); the O(1)–Xe(1)–O(2), O(1)–Xe(1)–F(7) and O(2)–Xe(1)–F(7) angles are 105.0(2), 95.7(1) and 98.2(1)°, respectively.

The Xe–F bond in the XeO_2F^+ cation is shorter (to within $\pm 3\sigma$) than the same bonds in $XeOF_4$ [1.900(5) Å,[95] 1.901(3)–1.9040(0) Å,[96] 1.895(2) and 1.890(2) Å [159]] or in XeO_2F_2 [1.899(3) Å,[143] 1.892(13) and 1.925(13) Å [160]] but its length is similar to the Xe–F_{ax} [1.879(12) Å] and Xe–F_{eq} [1.821(12) Å] bond lengths in the $XeOF_3^+$ cation.[221] In the researchers' opinion,[159] the shorter and less polar Xe–F bond is engendered by the total positive charge of the XeO_2F^+ cation. The Xe–O bond length in XeO_2F^+ is close to the bond lengths of other xenon(VI) oxyfluorides (Table 19).

The O(1)–Xe(1)–O(2), O(1)–Xe(1)–F(7) and O(2)–Xe(1)–F(7) angles in the structure of the XeO_2F^+ cation markedly differ from the ideal angle in the trigonal pyramid, apparently, due to stronger repulsion from the lone electron pair of xenon. A comparison of the O–Xe–O angle in the XeO_2F^+ cation with the corresponding angles in its isoelectronic analogues IO_2F and TeO_2F^- (Ref. 230 and 231) attests to a decrease in the O–X–O angle (X = Xe, I, Te) in the series

$$XeO_2F^+ > IO_2F > TeO_2F^-$$

In our opinion, this is associated with weakening of the X–O bonds and enhanced interaction of the lone electron pair of element X with the valence shells of the surrounding atoms, in particular, oxygen.

The unit cell of β-$XeO_2F^+SbF_6^-$ consists of three tetrameric units; in each of them, the xenon and antimony atoms alternate in cube vertices (see Fig. 17 *b*). The average Xe–O and Xe–F bond lengths in the tetramer are close to the corresponding bond lengths found for α-$XeO_2F^+SbF_6^-$ (1.772 Å). The Xe(1) atom is linked to the SbF_6^- anions by three bridging bonds the lengths of which are, on average, 2.550 Å, which is ~1 Å shorter than the sum of the van der Waals radii of xenon and fluorine. At the Xe(2) atom, there are three analogous bridging bonds with the SbF_6^- anion, the bond being not longer than 2.570 Å.

The structural unit of $(FO_2XeFXeO_2F)^+AsF_6^-$ consists of two clearly separated $(FO_2XeFXeO_2F)^+$ cations and the AsF_6^- anion (see Fig. 17 *c*). The unit cell of $(FO_2XeFXeO_2F)^+AsF_6^-$ has a layered structure: double layers of the $(FO_2XeFXeO_2F)^+$ cations alternate with layers of the AsF_6^- anions. The cations in these layers are oriented in such a way that the lone electron pairs point towards the AsF_6^- anions, and the oxygen atoms connected by a double bond are located opposite to each other. The $(FO_2XeFXeO_2F)^+$ cation consists of two crystallographically independent XeO_2F units, which are linked by a F bridge, giving rise to a bent Xe–F–Xe group. The

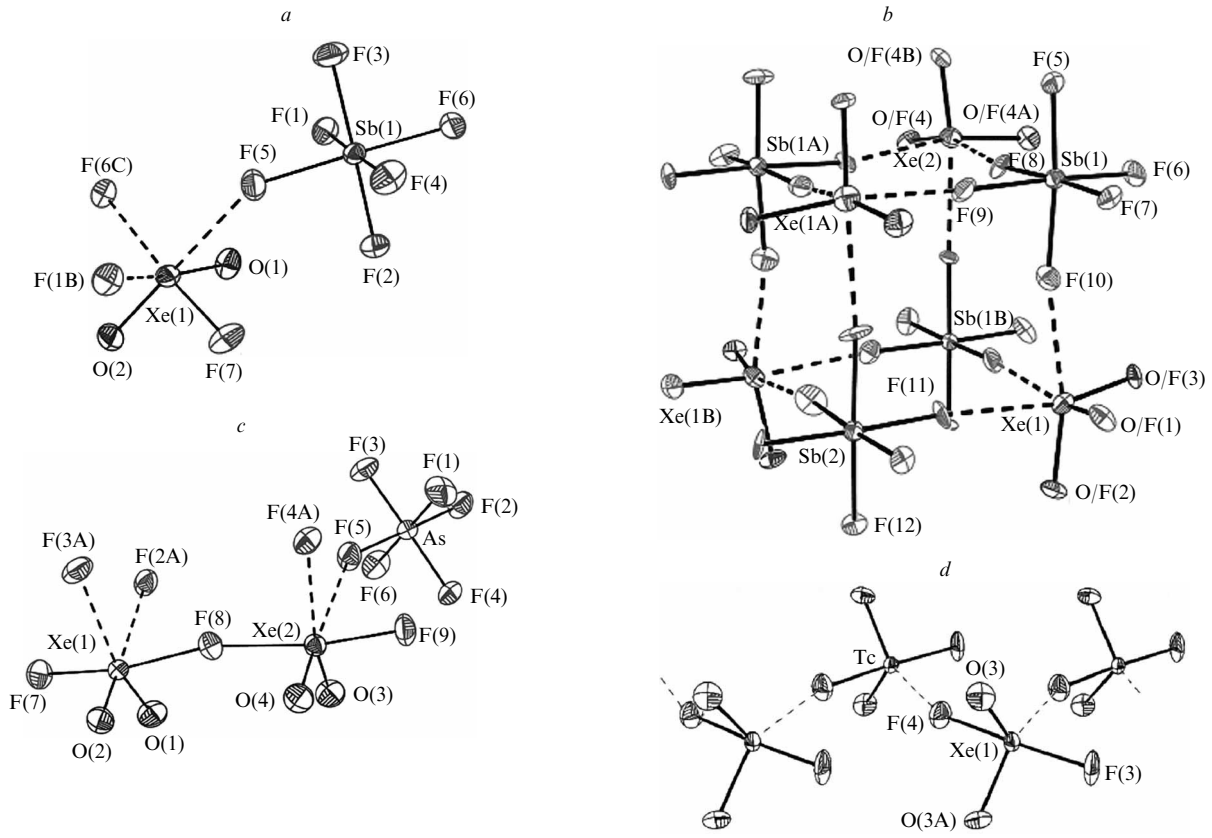


Figure 17. Structures of α-$XeO_2F^+SbF_6^-$ (*a*), β-$XeO_2F^+SbF_6^-$ (*b*),[159] $(FO_2XeFXeO_2F)^+AsF_6^-$ (*c*)[223] and the adduct $TcO_2F_3 \cdot XeO_2F_2$ (*d*).[160]

Table 19. Xe–O bond lengths in xenon(VI) oxyfluorides.

Compound	Bond length /Å	Ref.
$XeOF_4$	1.703	95
	1.7053(9)–1.711(11)	
	1.713(3)	
$XeOF_3$	1.692(13)	221
XeO_2F_2	1.714(4)	143
	1.731(9)	160
XeO_3	1.76(2)	102

Xe–F–Xe angle amounts to 166.4(2)° and the bond lengths are very close to those in the $Xe_2F_{11}^+$ cation incorporated in the complex $Xe_2F_{11}^+AuF_6^-$ [in this case, the Xe···F···Xe angle is 169.2(2)° and the bond lengths are 2.21(1), 2.26(1) Å].[216] However, in the complex $[Xe_2F_{11}]_2[NiF_6]$, the Xe–F–Xe angle is much smaller [140.3°; the bond lengths are 2.35(1), 2.21(1) Å],[208] which, in our opinion, can attest to strong cation–anion interactions in this compound due to higher negative charge on the fluorine atom in the NiF_6^{2-} anion.

Note that $(FO_2XeFXeO_2F)^+$ is one of the four known cations of noble gases with a F bridge [the other three cations are $F(KrF)_2^+$ (Ref. 137), $F(XeF)_2^+$ (Ref. 194) and $F(XeF_5)_2^+$ (Ref. 216)]. Judging by the arrangement of the lone electron pair and four domains with paired bonds, each of the F–XeO_2F functional groups, according to the VSEPR theory,[65,66] corresponds to a bisphenoid structure of the AX_2Y_2E type.

The limiting values for the Xe–F bond lengths in the cation occupy an intermediate position between the bond lengths in the XeO_2F^+ cation in α-$XeO_2F^+SbF_6^-$ and XeO_2F_2, which is consistent with the general trend of the charge on xenon to decrease and the Xe–F bond polarity to increase in the series

$$XeO_2F^+ > FO_2XeFXeO_2F^+ > XeO_2F_2$$

The $FO_2XeFXeO_2F^+$ cation with the Xe(1)···F(8) bond length of 2.161(3) Å and the Xe(2)···F(8) bond length of 2.230(3) Å is located asymmetrically with respect to the F-bridge and the average value for the [O(1/2)–Xe(1)···Xe(2)–O(3/4)] torsion angle is nearly equal to zero, which accounts for the C_s symmetry of the cation.

Apart from the presence of the F bridge, another common feature of the two xenon centres is that each xenon atom in the XeO_2F group forms its own F bridges with the adjacent anions. These bridges are arranged in such a way that they do not interact with the xenon lone electron pair and are located in the *trans*-position with respect to the equatorial oxygen atoms. The bridging fluorine atoms are nearly coplanar with the triangular planes confined by the O(1)–Xe(1)–O(2) and O(3)–Xe(2)–O(4) angles; they protrude beyond these planes by 0.3 Å. The longest bridg-

ing bonds, Xe(1)···F(1A) = 3.484(4) and Xe(2)···F(6A) = 3.226(4) Å, similarly to the short bridges, do not interact with the lone electron pair of xenon.

Schrobilgen *et al.*[160] prepared the stable adduct $TcO_2F_3 \cdot XeO_2F_2$ by the reaction of TcO_2F_3 with XeO_2F_2; the adduct crystallized in the orthorhombic system (space group $Cmc2_1$) with the unit cell parameters $a = 7.895(2)$, $b = 16.204(3)$, $c = 5.198(1)$ Å, $\beta = 90.0°$, $V = 665.0(2)$ Å^3, $Z = 4$, $\rho = 3.878$ g cm^{-3}. The structure of this product consists of infinite TcO_2F_3 chains located parallel to the c axis and linked to the XeO_2F_2 chains by long Tc–F···Xe bridges (see Fig. 17 *d*). In addition, there is one O···O bridging bond between TcO_2F_3 chains [O(1)···O(2) = 2.781 Å] and one O···F bridge between TcO_2F_3 and XeO_2F_2 chains [O(2)···F(3) = 2.799 Å], the length of the bridges being close to the limiting sum of the van der Waals radii of the fluorine and oxygen atoms.

An interesting feature of this structure is that the XeO_2F_2 molecules are linked to xenon *via* a F bridge inside the XeO_2F_2 chains themselves rather than *via* Xe···O as in the XeO_2F_2 structure.[143] The Xe–O distance [1.734(9) Å] is equal (to within $\pm 3\sigma$) to the corresponding distance in XeO_2F_2 [1.714(4) Å] and comparable with the Xe–O bond lengths in $XeOF_4$ [1.706(15) Å,[229] 1.708(2) Å [95]] and XeO_3 [1.76(3) Å].[31] This structure comprises two types of Xe–F bonds, of which one is somewhat longer [1.925(13) Å] than the other [1.892(13) Å] due to the presence of the F bridge with the xenon atom in the neighbouring XeO_2F_2 molecule. The indicated bond lengths are in good agreement with the Xe^{VI}–F bond lengths in XeO_2F_2 [1.899(3) Å][143] and $XeOF_4$ [1.903(5) Å,[229] 1.9024(9) Å [95]].

V.3. Complex compounds of $XeOF_2$ and XeO_3

V.3.a. $XeOF_3^-$ anion

The compounds $Cs^+XeOF_3^-$ and $(CH_3)_4N^+XeOF_3^-$ incorporating the $XeOF_3^-$ anion have been prepared by the reaction of $XeOF_2$ with $[(CH_3)_4N][F](CsF)$ in a CH_3CN solution at ~230 K. The structural features of this anion in the solid phase were studied by low-temperature Raman spectroscopy resorting to quantum chemical calculations.[227]

Table 20. Vibrational frequencies (cm^{-1}) in the Raman spectra of the $Xe^{16}OF_3^-$ and $Xe^{18}OF_3^-$ anions.[227]

Experiment		Calculation		Types of vibrations
$Xe^{16}OF_3^-$	$Xe^{18}OF_3^-$	$Xe^{16}OF_3^-$	$Xe^{18}OF_3^-$	
730.8 (90)	694.0 (100)	731.5 (31)	696.2 (31)	ν (Xe–O)
472 (13)	471.5 (17)	489.5 (~0)	490.8 (~0)	ν_{as} (Xe–F_{2e})
457.5 (27)	457.4 (25)	453.9 (23)	453.8 (23)	ν_s (Xe–F_{2e}+
447.7 (72)	447.6 (66)			+Xe–F_a)
376 sh	376.6 (3)	404.1 (10)	404.1 (10)	ν_s (Xe–F_{2e}–
				–Xe–F_a)
–	–	256.9 (< 1)	253.8 (< 1)	δ_s ($XeOF_3$) out of plane
272 (12)	261.8 (11)	228.2 (4)	220.6 (4)	δ (F_bOXe)
269 (11)	259.6 sh			in plane
194 (2)	192.2 (1)	165.6 (~0)	165.6 (~0)	δ (XeF_{2e}) in plane
159 (4)	153.2 (2)	122.4 (< 1)	121.0 (< 1)	δ ($OXeF_a$)–
				–δ(XeF_b) out of plane
136.5 sh	135.9 (3)	121.4 (< 1)	120.6 (< 1)	δ (F_aXeO) in plane

Analysis of the Raman spectra demonstrated that the $XeOF_3^-$ anion exists as a planar structure with the C_{2v} symmetry characterized by nine normal vibrations

$$\Gamma_{vib} = 4\,A_1(IR,R) + 3\,B_1(IR,R) + 2\,B_2(IR,R)$$

The experimental and calculated vibrational frequencies in the Raman spectra of the $Xe^{16}OF_3^-$ and $Xe^{18}OF_3^-$ anions are summarized in Table 20. The quantum chemical calculations of the geometric parameters of $XeOF_3^-$ gave the following results (Fig. 18): the lengths of the Xe–O and Xe–F_a (in the plane accommodating two lone electron

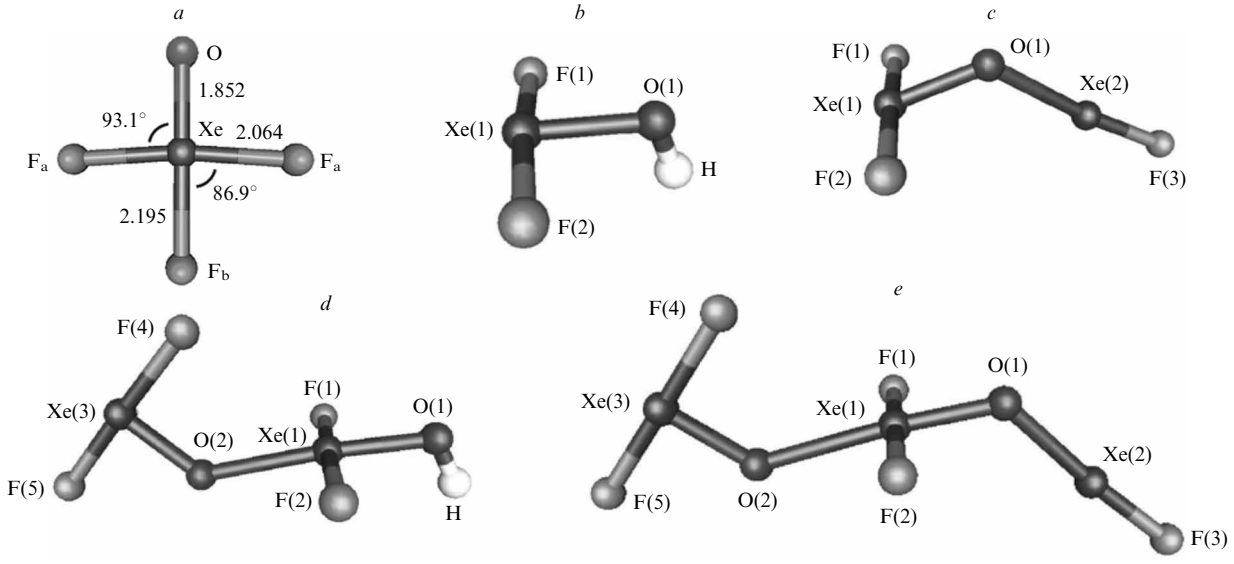


Figure 18. Calculated geometric parameters of $XeOF_3^-$ (*a*),[227] $HOXeF_2^+$ (*b*), $HOXe(F_2)OXeF_2^+$ (*c*), $FXe^{II}OXe^{IV}F_2^+$ (*d*) and $FXe^{II}OXe^{IV}(F)_2OXe^{IV}F_2^+$ (*e*).[232]

Table 21. Crystallographic parameters of $Xe_3OF_3^+XF_6^-$ (X = As, Sb) and $H_3O^+AsF_6^-\cdot 2\,XeF_2$.[234]

Compound	System	Space group	Unit cell parameters						ρ /g cm^{-3}	T/K
			a/Å	b/Å	c/Å	β/deg	V/Å^3	Z		
$Xe_3OF_3^+XF_6^-$	monoclinic	*Pc*	6.711(1)	9.115(2)	8.674(2)	96.85(3)	526.8(2)	2	4.135	157
$Xe_3OF_3^+XF_6^-$	"	$P2_1/c$	6.687(1)	9.306(2)	8.822(2)	96.784(5)	545.1(2)	2	4.281	148
$H_3O^+AsF_6^-\cdot 2\,XeF_2$	tetragonal	*I*4/*mcm*	8.714(4)	8.714(4)	12.988(9)	90	986.4(9)	4	3.680	100

pairs) and Xe–F_b (in the plane normal to the plane accommodating two lone electron pairs) bonds are in the range of 1.821–1.859, 2.032–2.064 and 2.129–2.195 Å, respectively, while the O–Xe–F_a and F_a–Xe–F_a angles are in the 92.8–93.7 and 172.5–174.4° ranges. It is noteworthy that the Xe–F_a and Xe–O bonds in the anion are somewhat longer than in $XeOF_2$, while the F_a–Xe–F_a angle is closer to a straight angle, which may be related to a minor structure distortion caused by the presence of a total negative charge on $XeOF_3^-$.

The reaction of $XeOF_2\cdot n\,HF$ with AsF_5 in a solution in anhydrous HF at 195 K resulted in the formation of $HOXeF_2^+AsF_6^-$, $HOXe(F_2)OXeF_2^+AsF_6^-$, $FXe^{II}OXe^{IV}F_2^+AsF_6^-$ and $FXe^{II}OXe^{IV}(F)_2OXe^{IV}F_2^+AsF_6^-$ (see Ref. 232). As in the case of $XeOF_3^-$, the $HOXeF_2^+$, $HOXe(F_2)OXeF_2^+$, $FXe^{II}OXe^{IV}F_2^+$ and $FXe^{II}OXe^{IV}(F)_2OXe^{IV}F_2^+$ cations were studied by low-temperature Raman spectroscopy and the geometric parameters of the structure were determined using quantum chemical calculations (see Fig. 18).

According to obtained results,[232] the $Xe^{IV}(1)$–O(1) bond in $FXeOXeF_2^+$ (1.837–1.885 Å) is somewhat longer than the Xe–O bond in $XeOF_2$ (1.770–1.821 Å)[27] but is close length to the bond in $HOXeF_2^+$ (1.880–1.929 Å). The $Xe^{II}(2)$–O(1) bond (2.240–2.296 Å) in $FXeOXeF_2^+$ is markedly longer than the $Xe^{IV}(1)$–O(1) bond, which is due to higher electronegativity of tetravaent xenon with respect to divalent xenon. Unlike the $Xe^{IV}(1)$–O(1) bond, the $Xe^{IV}(1)$–F bond lengths, being roughly equal in the $FXeOXeF_2^+$ (1.921–1.946 Å) and $HOXeF_2^+$ (1.903–1.927 Å) cations, are shorter than the Xe–F bond in $XeOF_2$ (1.968–1.997 Å) but longer than the Xe–F_{ax} distance in the XeF_3^+ cation (1.883–1.906 Å). The Xe(1)–O(1)–Xe(2) angle is in the range of 123.8–129.7° and the Xe(1)–O(1)–H angle is 108.1°. The $Xe^{IV}(1)$–O(1), $Xe^{IV}(1)$–F(1) and $Xe^{IV}(1)$–F(2) bonds in $HOXe(F)_2OXeF_2^+$ (1.914–1.945 Å and 1.929–1.958 Å, respectively) and in $FXeOXe(F)_2OXeF_2^+$ (1.863–1.899 and 1.922–1.962 Å, respectively) are somewhat longer than the Xe–O and Xe–F bonds in the cations considered above. The Xe, O(1), O(2), F(4) and F(5) atoms are coplanar in both cations and the ^{IV}Xe(1)–F(1) and ^{IV}Xe(1)–F(2) bonds are perpendicular to this plane.

V.3.b. XeO_3F^- anion

Several alkali metal fluoroxenates ($KXeO_3F$, $RbXeO_3F$ and $CsXeO_3F$) containing the XeO_3F^- anion are known; they possess relatively high thermal stability (up to 500 K).[9, 233]

The vibrational spectra of the XeO_3F^- anion incorporated in these compounds are characterized by six vibration bands[233]

$$\Gamma_{vib} = 3\,A_1(IR,R) + 3\,E(IR,R)$$

corresponding to a C_{3v}-symmetry tetrahedral structure with frequencies $\nu_s(Xe-O) = 781$, $\delta_s(O-Xe-O) = 358$, $\nu_s(Xe-F)_{bridge} = 257$, $\nu_{as}(Xe-O) = 822$, $\delta(O-Xe-O) = 315$, $\delta\,(O-Xe-F) = 222$ cm^{-1}.

The XeO_3F^- anion incorporated in $KXeO_3F$ crystallizes in the orthorhombic system (space group $Pn2_1a$) with the unit cell parameters $a = 7.374(5)$, $b = 6.811(5)$, $c = 8.185(6)$ Å, $V = 411.1$ Å^3, $Z = 4$, $\rho = 3.835$ g cm^{-3}. The geometric structure of the XeO_3F^- anion is similar to the structure of xenon trioxide: the Xe–O bond lengths are 1.75(1), 1.76(1) and 1.79(1) Å, and the O–Xe–O angles are 97.8(7), 100.5 (1) and 101.1(9)°. The lengths of the Xe···F bridging bonds [2.36(1), 2.48(1) Å] are substantially longer than the average value for crystalline binary xenon fluorides (1.9–2.0 Å). Considering the results of examination of the vibrational spectra of $M^+XeO_3F^-$ and the crystallographic data, Bonville *et al.*[233] arrived at the conclusion that $KXeO_3F$ exists as a polymeric chain structure of the general formula $n\,K^+(XeO_3F^-)_n$.

Besides the complex compounds of xenon oxyfluoride considered above, several compounds are known that have been prepared without using simple oxyfluorides as reactants. Vivid examples are the complexes $Xe_3OF_3^+XF_6^-$ (X = As, Sb) synthesized by the reaction of $XeF^+XF_6^-$ (X = As, Sb) with water in an HF solution at 195 K.[234] This reaction also furnished $H_3O^+XF_6^-\cdot 2\,XeF_2$. The obtained products in the solid phase were studied by crystallography and low-temperature Raman spectroscopy (113 K) and by quantum chemical calculations. The crystallographic parameters of the $Xe_3OF_3^+XF_6^-$ and $H_3O^+AsF_6^-\cdot 2\,XeF_2$ structures are summarized in Table 21. In compounds with X = As, the bond lengths are as follows /Å: Xe(1)–F(1) = 1.992(6), Xe(1)–O/F(1) = 2.101(10), Xe(2)–O/ F(1) = 1.919(9), Xe(3)–F/O(2) = 2.104(9), Xe(3)–F(3) = 1.977(6). The presented values are similar to these values in X = Sb: 1.975(6), 2.085(6), 1.908(6), 2.085(6) and 1.975(6) Å, respectively. The same is true for the F(1)–Xe(1)–O/F(1), F(1)–Xe(1)–O/F(2) and Xe(1)–O/F(1)–Xe(2), Xe(1)–O/F(2)–Xe(2) angles, which measure 178 ± 0.6° and 124.0 ± 0.5°, respectively (Fig. 19 *a*). Quantum chemical calculations gave the following results (see Fig. 19 *b*):[234] bond lengths /Å: Xe(1)–F(1) = 1.958, Xe(1)–O(1) = 2.151, O(1)–Xe(2) = 1.952, F(2)–Xe(3) = 2.111, Xe(3)–F(3) = 1.925; bond angles /deg: F(1)–Xe(1)–O(1) = 176.5, Xe(1)–O(1)–Xe(2) = 117.1 and F(2)–Xe(3)–F(3) = 179.9. It can be seen from these data that the lengths of the terminal Xe–F bonds in the $XeOF_3^+$ cation [1.977(6) and 1.992(6) Å, X = As; 1.975(6) Å, X = Sb], which apparently can be regarded as a linear $FXeFXeOXeF^+$ system, are comparable with the lengths of analogous bonds in XeF_2 [2.00(1) Å] (Ref. 136) and are shorter than the lengths of the terminal Xe–F

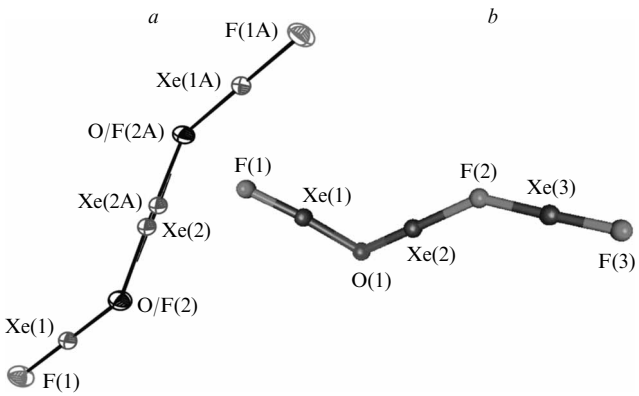


Figure 19. Experimental (*a*) and calculated (*b*) structures of the $Xe_3OF_3^+$ cation.[234]

bonds in the $Xe_2F_3^+$ cation [1.929, 1.908(7) and 1.908(6) Å].[194] The F–Xe–O/F angles [177.4(5)°, 178.2(5)°, X = As; 178.6(3)°, X = Sb] are close to a straight angle. The lengths of the ionic Xe···F bonds in $Xe_3OF_3^+XF_6^-$ are in the range of 3.021–3.114 Å (X = As) and 2.280–3.087 Å (X = Sb), which is noticeably shorter than the sum of the van der Waals radii of xenon and fluorine (3.63 Å).

VI. Complex compounds with the Xe – metal bonds

The synthesis and crystal structure investigations of complex compounds with the Xe–M bond (M = Ag, Au), namely, $XeF_5^+MF_4^-$, were reported for the first time by Žemva and co-workers.[208,235] X-Ray diffraction studies of these compounds have shown [208] that $XeF_5^+AgF_4^-$ and $XeF_5^+AuF_4^-$ are isostructural and crystallize in the tetragonal system (space group *I*4/*m*) with the following unit cell parameters:

for $XeF_5^+AuF_4^-$

$a = 5.735(5)$, $c = 20.007(17)$ Å, V = 658(2) Å^3, $Z = 4$;

for $XeF_5^+AgF_4^-$

$a = 5.593(2)$, $c = 20.379(5)$ Å, $V = 637.5(8)$ Å^3, $Z = 4$.

The structure of $XeF_5^+AgF_4^-$ comprises two XeF_5^+ layers and one AgF_4^- layer, which are parallel to the *ab* plane. The Xe–F_{ax} and Xe–F_{eq} bond lengths are 1.852(19) and 1.826(9) Å, while the Xe···F_{bridge}, Ag–F and Ag···F_{bridge} distances are 2.637(11), 1.902(11) and 2.921(10) Å, respectively. The F_{eq}–Xe–F_{ax}, F_{eq}–Xe–F_{eq} and F_{ax}–Xe···F_{bridge} angles amount to 77.7(3), 87.4(4) and 135.5(2)°, respectively, while the F–Ag–F angles are 91.9(5) and 88.1(5)°, respectively.

Subsequently a number of xenon complexes with gold, interesting from the practical standpoint, have been prepared. In these compounds, xenon acts as a ligand.[236–239] The first complex in this series is $AuXe_4^{2+}(Sb_2F_{11})_2^-$ in which the $AuXe_4^{2+}$ cation has a square planar configuration; it is a rare example of compounds in which gold occurs in the oxidation state +2 and xenon is in the zero oxidation state.[236]

The triclinic crystal structure of $[AuXe_4][Sb_2F_{11}]_2$ (Fig. 20 *a*) consists of the discrete $AuXe_4^{2+}$ cations and the $Sb_2F_{11}^-$ anions. The gold atom is located in the centre of a square plane formed by xenon atoms with Au–Xe distances in the range from 2.728(1) to 2.750(1) Å. The lengths of three bridging Au···F bonds are 2.671(5), 2.949(5) and 3.153(5) Å; together with the square planar $AuXe_4^{2+}$ group, the shortest Au···F(12) bond is responsible for the square pyramidal structure. In the tetragonal phase, these bonds are much weaker [2.927(9) Å)].[236]

Thermally unstable crystals of *cis*-$[AuXe_2][Sb_2F_{11}]_2$ and *trans*-$[AuXe_2][SbF_6]_2$ have been isolated.[236,238] In the *cis*-isomer, the gold atom occurs in a square planar environment consisting of two xenon atoms, which occupy *cis*-positions relative to each other [2.658(1), 2.671(1) Å)] and two bridging fluorine atoms located in the *cis*-positions [2.181(4), 2.238(4) Å] relative to two $Sb_2F_{11}^-$ anions. In the *trans*-isomer, the gold atom is also in the square planar environment of two xenon atoms [2.709(1) Å] located in the *trans*-positions relative to each other and two bridging fluorine atoms [2.159(6) Å] of different SbF_6^- anions.

The obtained crystals of $[Au_2Xe_2F][SbF_6]_3$ proved to be stable up to room temperature. The crystal structure of $[Au_2Xe_2F][SbF_6]_3$ is shown in Fig. 20 *b*. Both gold atoms occur in a square planar environment consisting of one xenon atom and three bridging fluorine atoms. The distances between the bridging atom and the gold atom are substantially shorter [2.045(2) Å] than the Au...F distance in the triclinic structure of $[AuXe_4][Sb_2F_{11}]_2$ [2.671(5) Å].[236]

The only known complex with Au^{3+} is *trans*-$[AuXe_2F][SbF_6][Sb_2F_{11}]$, which has been isolated from a 5 : 1 HF–SbF_5 mixture and proved to be exceptionally stable when the reaction has been performed at 263 K;

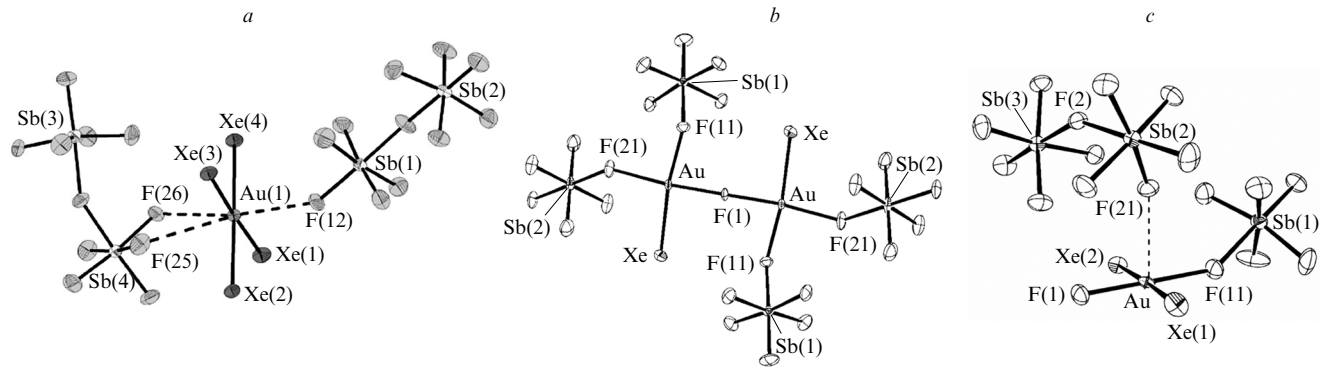


Figure 20. Structures of $[AuXe_4][Sb_2F_{11}]_2$ (*a*),[236] $[Au_2Xe_2F][SbF_6]_3$ (*b*)[237] and $[AuXe_2F][SbF_6][Sb_2F_{11}]$ (*c*).[238]

in this case, the crystals formed at 238 K. In *trans*-$[AuXe_2F][SbF_6][Sb_2F_{11}]$, the gold atom occurs in a square planar environment of two xenon atoms and two fluorine atoms located in the *trans*-positions, one fluorine atom being terminal and the other fluorine atom being involved in the formation of the F(21)···Au bridging bond (see Fig. 20 *c*). The $Au^{III}-Xe$ bonds [2.593(1) and 2.619(1) Å] are shorter than the $Au^{II}-Xe$ bonds in the triclinic and tetragonal structures of $[AuXe_4][Sb_2F_{11}]_2$, *cis*-$[AuXe_2][Sb_2F_{11}]_2$ or *trans*-$[AuXe_2][SbF_6]_2$.[236] Note that the Au–F bond lengths [1.881(4) and 1.983(4) Å] are typical of gold fluorides [for example, the Au–F bond lengths in AuF_3 are 1.91(4) and 2.04(3) Å)].[240]

A xenon cation containing Au^{I} has been synthesized and isolated as a part of $[(F_3As)AuXe][Sb_2F_{11}]$.[237] A key stage of the synthesis of a compound containing the $(F_3As)AuXe^+$ cation was the replacement of the weakly basic SbF_6^- anion in $[(F_3As)Au][SbF_6]$ by the even more weakly basic $Sb_2F_{11}^-$ anion.[239] The reaction was carried out at a $HF:SbF_5$ molar ratio of 5 : 1 in the presence of excess xenon {molar ratio 7 : 1 relative to $[(F_3As)AuXe][Sb_2F_{11}]$}. Crystallization of $[(F_3As)AuXe][Sb_2F_{11}]$ affords colourless needle-like crystals stable at room temperature. The interactions between $(F_3As)AuXe^+$ and $Sb_2F_{11}^-$ are weak, the shortest Au...F distance being 2.84 Å. The As–Au–Xe group is nearly linear and the $Au^{I}-Xe$ bond length [2.6072(6) Å] is comparable with the $Au^{III}-Xe$ bond length in $[AuXe_2F][SbF_6][Sb_2F_{11}]$ and is substantially shorter than the $Au^{II}-Xe$ bond length.[237]

By the reaction of HgF_2 and Xe in a SbF_5 solution at 193 K, the same researchers[237,238] prepared the compound $[HgXe][SbF_6][Sb_2F_{11}]$ containing the $HgXe^+$ cation with the Hg–Xe bond length equal to 2.769(4) Å.

It is noteworthy that a number of recent publications have been devoted to theoretical investigations of the stability, structure and calculation of the vibrational spectra of compounds of the MXe_n^{2-} type (M = Cu, Ag, Au; $n = 1-6$),[241,242] anions of the $XAuNgX^-$ and $HAuNgX^-$ types (X = F, Cl, Br; Ng = Xe, Kr, Ar),[243] compounds NgAuF and $NgAu^+$ (Ng = Ar, Kr, Xe),[244] noble metal clusters M_n (M = Cu, Ag, Au; $n = 2-4$) with krypton, xenon and radon,[245] compounds with the Xe–U bonds, *etc*.[246,247] For example,[242] it was shown that the stability of MXe_n^{2+} varies in the following way in the series of metal atoms

$$Cu < Ag < Au$$

and *n* values

$$6 < 5 < 4 < 1 < 3 < 2$$

In the $HAuNgX^-$ anion, the Au–Ng bond length depends to a larger extent on the electronegativity of the fragment connected to gold than on the electronegativity of the noble gas atom. The conclusion was drawn[245] that stability of the M_n clusters (M = Cu, Ag, Au; $n = 2-4$) with krypton, xenon and radon, as in the case of MXe_n^{2+},[242] decreases in the same series of metal atoms: Cu < Ag < Au.

VII. Compounds of noble gases as ligands

In recent years, new coordination, polymeric, clathrate-like compounds of krypton and xenon fluorides have been synthesized.

Several papers[51,248–255] are devoted to a new class of coordination compounds in which xenon difluoride is coordinated to metal (or non-metal) atoms as a ligand. The first compound of this type to be synthesized was $[Ag(XeF_2)_2]AsF_6$.[248] The compound $[Ag(XeF_2)_2]PF_6$ obtained later[249] proved to be isostructural to $[Ag(XeF_2)_2]AsF_6$. The lattice parameters of $[Ag(XeF_2)_2]PF_6$ were as follows: $a = 8.467(3)$, $b = 12.745(3)$ Å, $V = 913.69(5)$ Å^3, $Z = 4$, space group $I4c2$; the silver atom had a cubic coordination sphere comprising eight fluorine atoms (Fig. 21 *a*). The coordination compounds $[M^{n+}(XeF_2)_m](AF_6)_n$, (M = Ag, Mg, Ca, Sr, Ba, Cd, Pb, lanthanides; A = As, Sb, P) have been prepared; methods used to synthesize them and the nature of chemical bonds have been analyzed; the possibility of preparing polymeric and multilayer structures has been considered.[250–255] The structural features of these compounds have been comprehensively covered in a review.[51] As an example, Fig. 21 *b* shows the magnesium coordination sphere in $[Mg(XeF_2)_2](AsF_6)_2$.[254]

In later publications,[256,257] the complexes $[M_k(XeF_2)_m](PF_6)_n$ were prepared by the reaction of MF_2

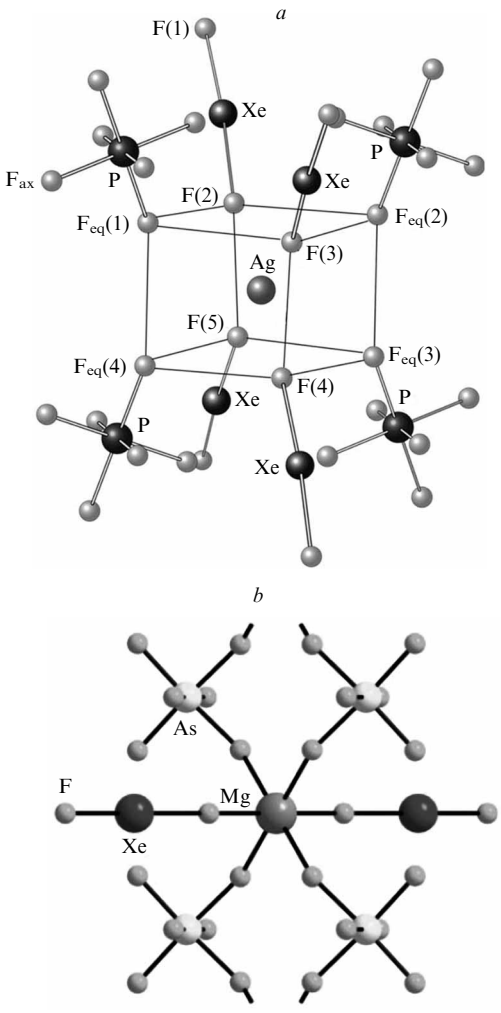


Figure 21. Coordination of the Ag and Mg atoms in the crystal structures of $[Ag(XeF_2)_2]PF_6$ (*a*)[249] and $[Mg(XeF_2)_2](AsF_6)_2$ (*b*).[254]

Table 22. Crystallographic parameters of some coordination compounds of xenon difluoride.

Compound	Space group	Unit cell parameters						ρ /g cm^{-3}	T/K	Ref.
		a/Å	b/Å	c/Å	β/deg	V/Å^3	Z			
$[Cd(XeF_2)_5](PF_6)_2$	$Pna2_1$	14.339(13)	8.366(8)	17.215(6)	–	2065(3)	4	3.784	100 ± 2	256
$[Ca(XeF_2)_5](PF_6)_2$	$Pna2_1$	14.082(2)	17.177(12)	8.4700(15)	–	2048.8(15)	4	4.049	100 ± 2	257
$[Cu(XeF_2)_2](SbF_6)_2$	$P2_1/c$	5.5828(19)	14.741(5)	9.118(3)	90.982(3)	750.2(4)	2	3.867	200	258
$[Cu(XeF_2)_4](SbF_6)_2$	$I4$	11.089(7)	11.089(7)	8.278(6)	–	1017.8(12)	2	–	200	259
$[Li(XeF_2)_3]AsF_6$	$P2_1$	6.901(9)	13.19(2)	6.91(1)	91.84(2)	628(2)	2	3.720	200 ± 1	45
$[Sr_3(XeF_2)_{10}](PF_6)_6$	$C2/c$	11.778(6)	12.497(6)	34.60(2)	95.574(4)	5069(4)	4	3.703	200	256
$[Pd_3(XeF_2)_{11}](PF_6)_6$	$C2/m$	13.01(3)	11.437(4)	18.487(7)	104.374(9)	2665(6)	2	4.180	200	257

(M = Ca, Cd, Pb, Sr) and XeF_2 under a pressure of gaseous PF_5 in anhydrous HF and studied by X-ray crystallography (Table 22). In $[M(XeF_2)_5](PF_6)_2$ (M = Ca, Cd), the calcium and cadmium coordination spheres were found to comprise 9 and 8 fluorine atoms, respectively, of which three (for M = Ca) and two (for M = Cd) belong to the PF_6^- anion and the other six atoms belong to the XeF_2 molecules. The Cd^{2+} cation has a smaller size and is more electronegative

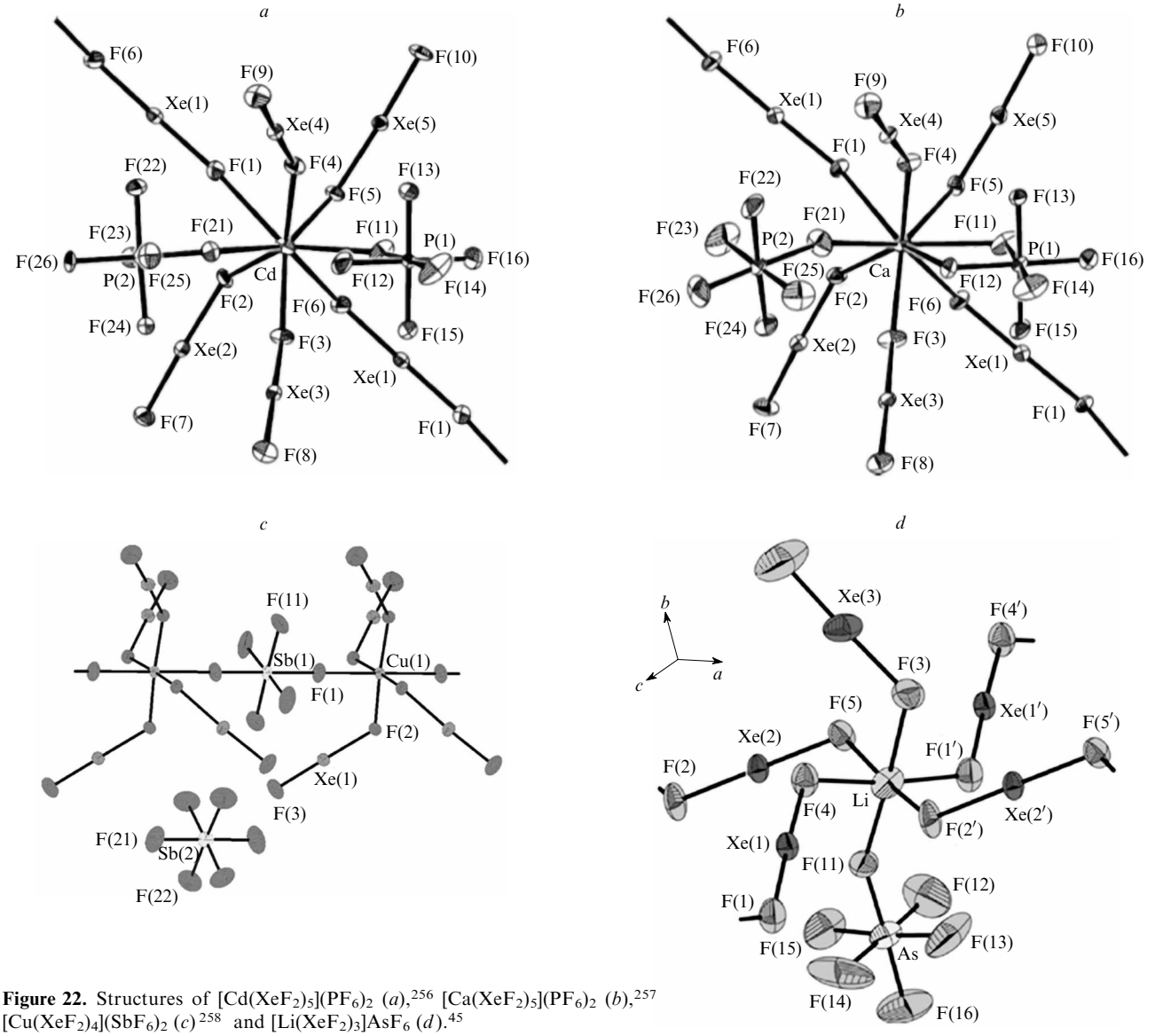


Figure 22. Structures of $[Cd(XeF_2)_5](PF_6)_2$ (*a*),[256] $[Ca(XeF_2)_5](PF_6)_2$ (*b*),[257] $[Cu(XeF_2)_4](SbF_6)_2$ (*c*)[258] and $[Li(XeF_2)_3]AsF_6$ (*d*).[45]

than the Ca^{2+} cation, which accounts for the higher coordination number for the F ligands in the calcium compound. The Ca–F(21) bond in the monodentate $P(2)F_6^-$ anion (2.363 Å) is shorter than the bonds in the bidentate $P(1)F_6^-$ anion [Ca–F(11) = 2.570 Å, Ca–F(12) = 2.759 Å]. The Ca–F(Xe) distance is in the range of 2.270–2.334 Å, the linear geometry of the bound XeF_2 molecules being slightly distorted (Fig. 22 *a*,*b*). The values of angles are the following /deg: F(1)–Xe(1)–F(6) = 178.7, F(7)–Xe(2)–F(2) = 177.2, F(8)–Xe(3)–F(3) = 179.0, F(9)–Xe(4)–F(4) = 178.8 and F(10)–Xe(5)–F(5) = 175.9.

The compounds $[Cu(XeF_2)_2](SbF_6)_2$, $[Cu(XeF_2)_4](SbF_6)_2$ and $[M(XeF_2)_6](SbF_6)_2$ (M = Cu, Zn) have been prepared.[258,259] In the first one, the copper coordination sphere consists of six fluorine atoms, of which four belong to the SbF_6^- anion and two belong to the XeF_2 molecules. The $[Cu(XeF_2)_2]^{2+}$ cation is linked to SbF_6^- by F bridges located in the *cis*-position, thus giving rise to the chain $[Cu(\eta^1\text{-}XeF_2)_2]-(cis\text{-}\eta^2\text{-}SbF_6)_2-[Cu(\eta^1\text{-}XeF_2)_2]$. Due to high electronegativity of Cu^{2+}, the XeF_2 molecules are markedly distorted: Xe–F = 1.906, $Xe-F_{bridge}$ = 2.102 Å, F–Xe–F = 178.3°. In the compound $[Cu(XeF_2)_4](SbF_6)_2$, the copper coordination sphere already incorporates four fluorine atoms that belong to XeF_2 molecules in the equatorial position and the $[Cu(XeF_2)_4]^{2+}$ cation is bonded to the SbF_6^- anion by F bridges in the *trans*-position; this also gives rise to the chain $[Cu(\eta^1\text{-}XeF_2)_4]-(trans\text{-}\eta^2\text{-}SbF_6)_2-[Cu(\eta^1\text{-}XeF_2)_4]$. Owing to the change in the coordination sphere of $[Cu(XeF_2)_4](SbF_6)_2$, the XeF_2 molecules are distorted to a lesser extent: Xe(1)–F(3) = 1.939(4), Xe(1)–F(2) = 2.094(5) Å , F(2)–Xe(1)–F(3) = 177.0(2)° (see Fig. 22 *c*).

In order to prepare the coordination compounds $[M(XeF_2)_n]AF_6$, Tavčar and Žemva[45] investigated the reactions between MAF_6 (M is alkali metal; A = P, As, V, Ru, Ir, Sb, Nb, Ta) and XeF_2 in anhydrous HF. These reactions furnished coordination compounds of the $[Li(XeF_2)_n](AF_6)$ type only for A = P, As, Ru, Ir. The crystal structure of the compounds $[Li(XeF_2)_3]AsF_6$ was studied (see Table 22). The structure of $[Li(XeF_2)_3]AsF_6$ was found to consist of $Li_4(XeF_2)_4$ squares connected by bridges to form layers in which the XeF_2 molecule and the AsF_6^- anion from two neighbouring layers adjoin each of these squares (see Fig. 22 *d*). The coordination sphere of lithium consists of six fluorine atoms, one belonging to the AsF_6^- anion and five belonging to the XeF_2 molecules. There is only one non-bridging XeF_2 molecule linked to lithium by a F ligand, the Li–F(Xe) distance being 2.07(3) Å. In the four bridging XeF_2 molecules the length of the Li–F(Xe) bridge varies from 1.97(2) to 2.03(3) Å. The bridging XeF_2 molecules that are linked to lithium atoms form infinite layers arranged perpendicular to the *b* axis. The layers are shifted diagonally in the *ac* plane; the AsF_6^- anions and non-bridging XeF_2 molecules are located at the centres of the $Li_4(XeF_2)_4$ squares of the neighbouring layers (see Fig. 22 *d*). The layers are connected through electrostatic interactions between the positively charged xenon atoms and negatively charged fluorine atoms in XeF_2 molecules and AsF_6^- anions. The lengths of the bridging Xe···F bonds vary in the following ranges: Xe(1)···F = 3.18(3)–3.60(1), Xe(2)···F = 3.28(1)–3.40(2) and Xe(3)···F = 3.32(1)–3.61(3) Å; the $F_{XeF2}-Li-F_{AsF6}$ angles exceed 90° and amount to 93(1), 94(1) and 98(1)°. The bridging $F_{Li}\cdots Xe$ distances vary in the range of 1.976(8)–2.005(8) Å, which is close to ~2.0 Å — the length of almost any bridging bond in the metal coordination compounds containing AF_6^- anions and bridging XeF_2 ligands.

It was found[260] that the reaction of XeF_2 with *cis*-$(HO)_2TeF_4$ yields the insoluble polymer $(XeO_2TeF_4)_n$ stable up to 350 K. The reaction of *cis*-$(HO)_2TeF_4$ with $Xe_2F_3^+AsF_6^-$ affords $FXeOTeFOXe^+AsF_6^-$. Upon recrystallization from anhydrous HF, this product is converted to the polymer $HF\cdot HOTeF_4OXe^+AsF_6^-$. The unit cell parameters for the polymer were determined to be a = 5.0474, b = 7.5893, c = 1.3873 Å, a = 90.14, β = 95.74, γ = 99.67°, Z = 2, space group $P\bar{1}$; it was concluded that, in this case, the xenon coordination number is ~1, as opposed to other compounds.

Until recently, the XeF^+ adducts of *s*-trifluorothiazine and some perfluoropyridines have been the only examples in which the formally sp^2-hybridized nitrogen atom is bonded to xenon. By crystallization (T = 263 K) from a solution of $[F_3S{\equiv}NXeF][AsF_6]$ in $N{\equiv}SF_3$, Smith and Schrobilgen[261] isolated the compound $[F_4S{=}N-Xe-N{\equiv}SF_3][AsF_6]$ in which the $[F_4S{=}N-Xe\cdots N{\equiv}SF_3]^+$ cation was identified by single crystal X-ray diffraction (T = 100 K). The Xe–N bond (2.079 Å) in the cation is the shortest among such bonds in compounds of noble gases. The $F_4S{=}NXe^+$

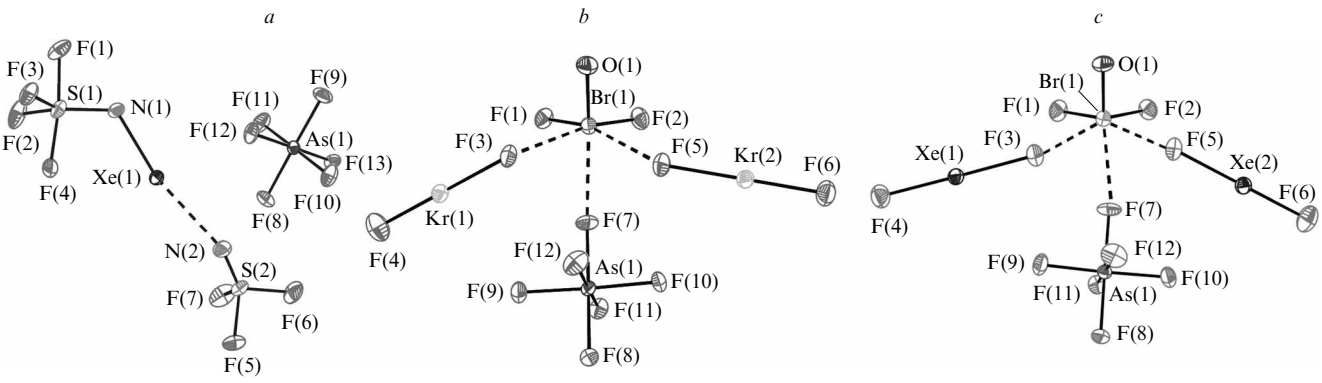


Figure 23. Structures of $[F_4S{=}N-Xe-N{\equiv}SF_3][AsF_6]$ (*a*),[261] $[BrOF_2][AsF_6]\cdot 2KrF_2$ (*b*)[262] and $[BrOF_2][AsF_6]\cdot 2XeF_2$ (*c*).[46]

cation (Fig. 23 *a*) interacts with $N{\equiv}SF_3$ *via* a donor–acceptor Xe···N bond (2.583 Å), which is substantially longer than the primary Xe—N bond (2.079 Å) but is markedly shorter than the sum of the van der Waals radii of xenon and nitrogen atoms (3.71 Å).

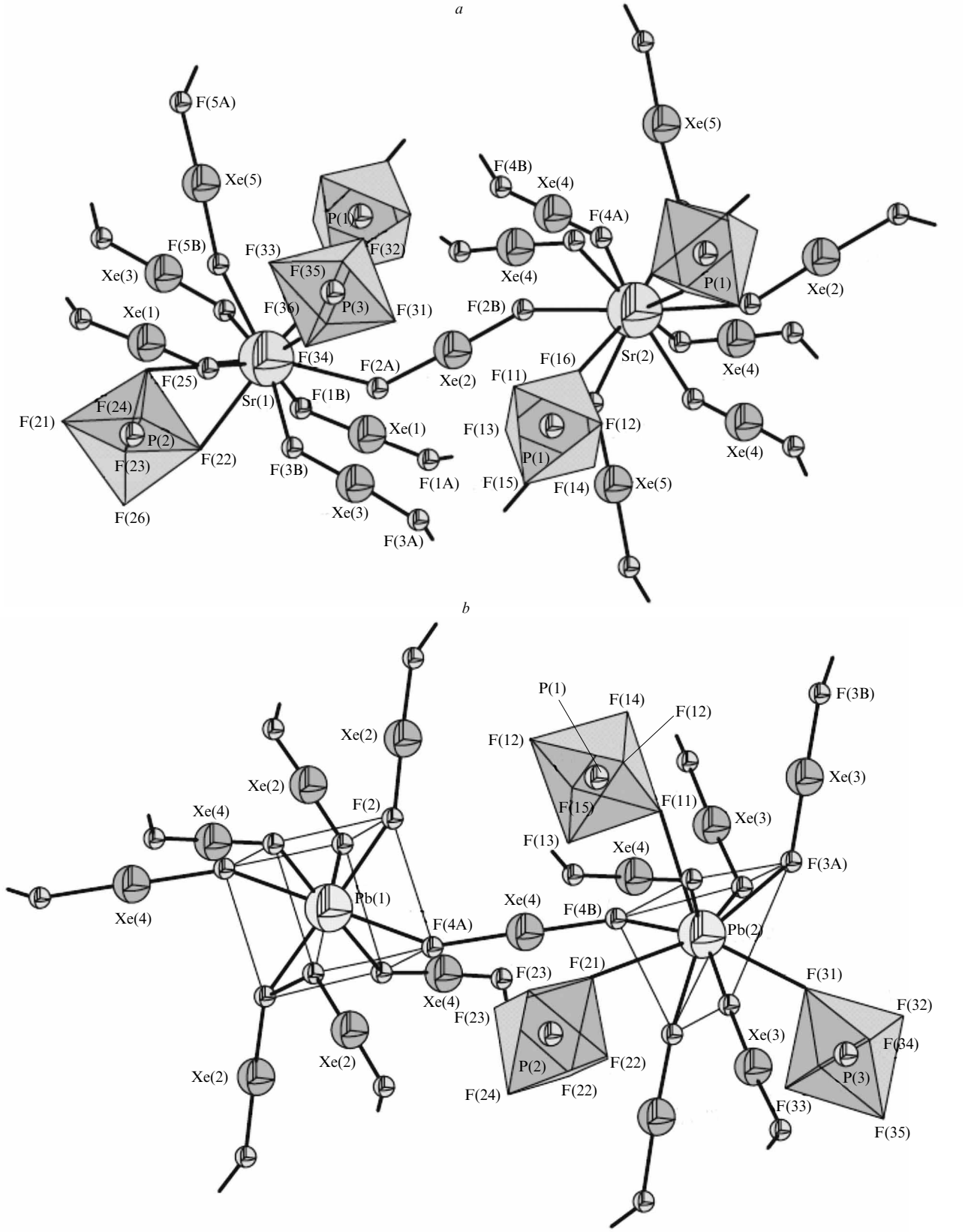


Figure 24. Structures of $[Sr_3(XeF_2)_{10}](PF_6)_6$ (*a*)[256] and $[Pb_3(XeF_2)_{11}](PF_6)_6$ (*b*).[257]

The compounds $[BrOF_2][AsF_6]\cdot 2\,NgF_2$ (Ng = Kr, Xe) have been prepared and investigated by X-ray crystallography (T = 100 K).[46, 262] Both compounds crystallize in the same $P2_1/c$ space group and have similar crystallographic parameters:

for Ng = Kr,

a = 5.7166(6), b = 13.644(2), c = 15.105(2) Å, β = 111.446(4)°, Z = 4, V = 1096.6(2) Å^3, ρ = 3.431 g cm^{-3} (see Ref. 262);

for Ng = Xe,

a = 5.9282(3), b = 13.9789(8), c = 15.3983(9) Å, β = 111.859(2)°, Z = 4, V = 1184.3(1) Å^3, ρ = 3.710 g cm^{-3} (see Ref. 46).

The structure of $[BrOF_2][AsF_6]\cdot 2\,KrF_2$ (see Fig. 23 *b*) consists of isolated molecular units and represents an example of KrF_2 coordination to a main group atom. The Kr–F bond lengths in both KrF_2 molecules are as follows /Å: Kr(1)–F(4) = 1.840 and Kr(2)–F(6) = 1.847; the Kr–F_{bridge} distances are longer: Kr(1)–F(3) = 1.94 and Kr(2)–F(5) = 1.933(4). The latter values are markedly different for compounds incorporating KrF^+ and $Kr_2F_3^+$ ions.[137]

Compound	Kr–F_{bridge} /Å
$KrF^+AsF_6^-$	2.131
$KrF^+SbF_6^-$	2.140
$Kr_2F_3^+AsF_6^-\cdot KrF^+AsF_6^-$	2.061, 2.049, 2.106
$Kr_2F_3^+SbF_6^-\cdot KrF_2$	2.027, 2.046

This is due to the fact that the Kr–F_{bridge} bond in $[BrOF_2][AsF_6]\cdot 2\,KrF_2$ is much more covalent than the bonds in other compounds containing KrF^+ and $Kr_2F_3^+$ cations and the KrF_2 molecules are not fluorine atom donors but ligands. Also, both KrF_2 molecules retain a linear geometry: the F(3)–Kr(1)–F(4) and F(5)–Kr(2)–F(6) angles are 179.9 and 178.7°, respectively. Charge transfer to $BrOF_2$ from two KrF_2 ligands (0.1 e each) and from AsF_6^- (0.05 e) was established. A substantial polarization also takes place within the KrF_2 ligands, which enhances the anionic character of bridging fluorine atoms, *i.e.*, electrostatic interaction occurs between the positively charged bromine atom and the surrounding fluorine atoms.

The compound $[BrOF_2][AsF_6]\cdot 2\,XeF_2$ (see Fig. 23 *c*) is isomorphic to $[BrOF_2][AsF_6]\cdot 2\,KrF_2$ but has a somewhat larger unit volume. Both XeF_2 ligands are almost linear: the F(3)–Xe(1)–F(4) and F(5)–Xe(2)–F(6) angles are 178.4 and 179.8°, respectively. The Xe–F bonds (1.960, 1.956 Å) are shorter than in solid XeF_2 (2.00 Å), while the Xe···F_{bridge} distances (2.052, 2.053 Å) are comparable with analogous distances for $[M_k(XeF_2)_m](PF_6)_n$ (2.026–2.087 Å).[256, 257] The difference between the structures of $[BrOF_2][AsF_6]\cdot 2\,NgF_2$ (Ng = Kr, Xe) is that the Br...F_{bridge} distances are shorter in the compound with Ng = Xe (2.292, 2.306 Å) than in the compound with Ng = Kr (2.318, 2.356 Å), which is attributable to higher polarity of the Xe–F bonds.

It was shown[256, 257] that the XeF_2 molecules can function as bridging ligands $(XeF_2)_{bridge}$, each of them being linked to two metal atoms to form infinite chains (–M–F–Xe–F–M–F–Xe–F–). The authors of the cited works isolated the compounds $[Sr(XeF_2)_3](PF_6)_2$, $[Pb(XeF_2)_3](PF_6)_2$, $[Sr_3(XeF_2)_{10}](PF_6)_6$ and $[Pb_3(XeF_2)_{11}](PF_6)_6$ in the MF_2–PF_5–XeF_2–HF system.

The compound $[Sr_3(XeF_2)_{10}](PF_6)_6$ contains two independent sites formed by strontium atoms with the coordination number of 10 in an unusual coordination sphere shaped like a tetracapped trigonal prism (Fig. 24 *a*). The $(XeF_2)_{bridge}$ and one bridging PF_6^- anion connected to the central atom form three-dimensional structures.

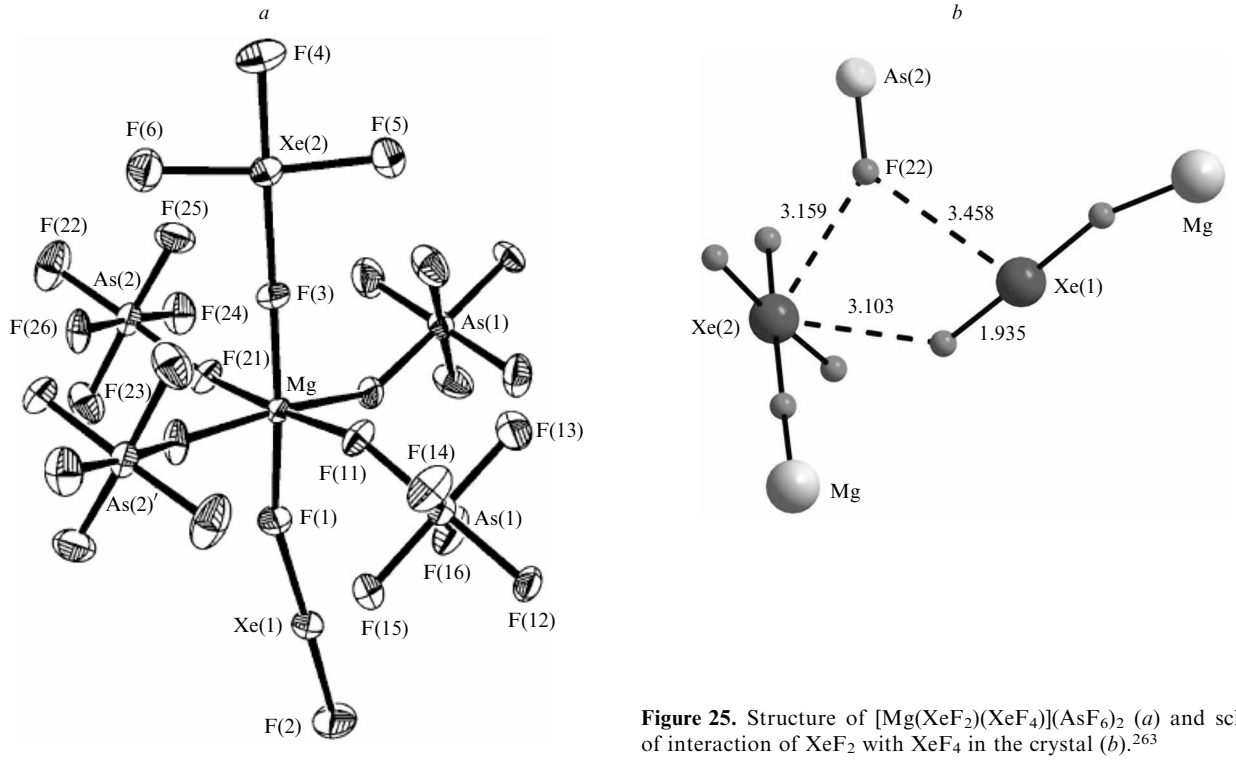


Figure 25. Structure of $[Mg(XeF_2)(XeF_4)](AsF_6)_2$ (*a*) and scheme of interaction of XeF_2 with XeF_4 in the crystal (*b*).[263]

Table 23. Crystallographic parameters of $Hg(OTeF_5)_2$ and $Hg(OTeF_5)_2 \cdot 1.5\,NgF_2$ (Ng = Xe, Kr).[265]

Compound	Space group	Unit cell parameters						ρ /g cm^{-3}
		a/Å	b/Å	c/Å	β/deg	V/Å^3	Z	
$Hg(OTeF_5)_2$	$C2/c$	18.681(1)	8.6489(4)	5.8008(3)	96.215(3)	931.74(1)	4	4.832
$Hg(OTeF_5)_2 \cdot 1.5\,XeF_2$	$P2_1/n$	9.0574(2)	17.8943(3)	9.1285(2)	114.548(1)	1345.78(6)	2	4.599
$Hg(OTeF_5)_2 \cdot 1.5\,KrF_2$	$P2_1/n$	8.7981(4)	17.4153(9)	9.2243(4)	113.788(3)	1293.3(2)	2	4.419

The complex $[Pb_3(XeF_2)_{11}](PF_6)_6$ comprises uncoordinated (free) XeF_2 molecules retained in the crystal lattice by electrostatic forces. It has a three-dimensional network structure, which can be described by the general formula $\{[Pb_3(XeF_2)_{11}](PF_6)_6\}_n$. The structure of this compound comprises two independent Pb units, one having a unique cubic coordination sphere formed by the fluorine atoms belonging to eight XeF_2 molecules. The second lead atom with the coordination number of 9 forms a sphere shaped like a tricapped trigonal prism characteristic of lead compounds (Fig. 24 *b*).

The intricate complex $[Mg(XeF_2)(XeF_4)](AsF_6)_2$ can serve as an example of a compound in which XeF_4 is coordinated to the metal atom.[263] This compound crystallizes in the monoclinic system (space group $P2_1/n$) with the unit cell parameters $a = 12.915(19)$, $b = 8.560(11)$, $c = 13.25(3)$ Å, $\beta = 101.558(15)^\circ$, $V = 1435.0(4)$ Å^3, $Z = 4$, $\rho = 3.604$ g cm^{-3}. A specific feature of the coordination sphere of magnesium in $[Mg(XeF_2)(XeF_4)](AsF_6)_2$ is that it is formed by six fluorine atoms, of which four atoms belong to the AsF_6^- anion and two atoms belong to XeF_2 and XeF_4 molecules (one atom from each of the molecules) (Fig. 25 *a*). Both xenon fluorides are actually unbound ligands, because the surrounding AsF_6^- anions are linked to the magnesium atom through the formation of bonds along the *b* axis. As in the case of $[Li(XeF_2)_3]AsF_6$, the layers are connected through electrostatic interactions between the positively charged xenon atoms of XeF_2 molecules and negatively charged fluorine atoms of XeF_4 molecules and the AsF_6^- anions. In these layers, the bridging bond involving the $As(1)F_6^-$ anion is located in the *trans*-position, whereas a similar bond involving the $As(2)F_6^-$ anion is in the *cis*-position. The shortest XeF_2...XeF_4 distance is 3.103(8) Å (see Fig. 25 *b*), which is substantially shorter than the same distance in the adduct $XeF_2 \cdot XeF_4$ (3.359 Å).[264]

DeBackere *et al.*[265] reported the synthesis of $Hg(OTeF_5)_2$ and $Hg(OTeF_5)_2 \cdot 1.5\,NgF_2$; the first compound was formed upon the reaction of HgF_2 with $HOTeF_5$ taken in 1 : 2.05 ratio ($T = 323$ K), while the other two compounds were prepared by the reaction of $Hg(OTeF_5)_2$ with NgF_2 (Ng = Xe, Kr) taken in 1 : 1.7 ratio ($T = 133$ K) for Ng = Xe and 1 : 1.22 ratio ($T = 195$ K) for Ng = Kr in a SO_2ClF solution. The interest in the coordination compounds of this type is due to the fact that the $OTeF_5$ group can be regarded as a bulky analogue of fluorine atoms with the overall electronegativity of 3.87,[153] comparable with the fluorine electronegativity (3.98). The distribution of the negative charge over the five fluorine atoms and one oxygen atom gives rise to the ligand with low nucleophilicity and fairly high stability to oxidation.[266]

The crystallographic data for the listed compounds are summarized in Table 23. It was found that the Hg^{II} coordination sphere in $Hg(OTeF_5)_2$ is a distorted octahedron, which comprises, along with the Hg–O bonds [2 × 2.016(6) Å], longer bridging Hg···O [2 × 2.641(7) Å]

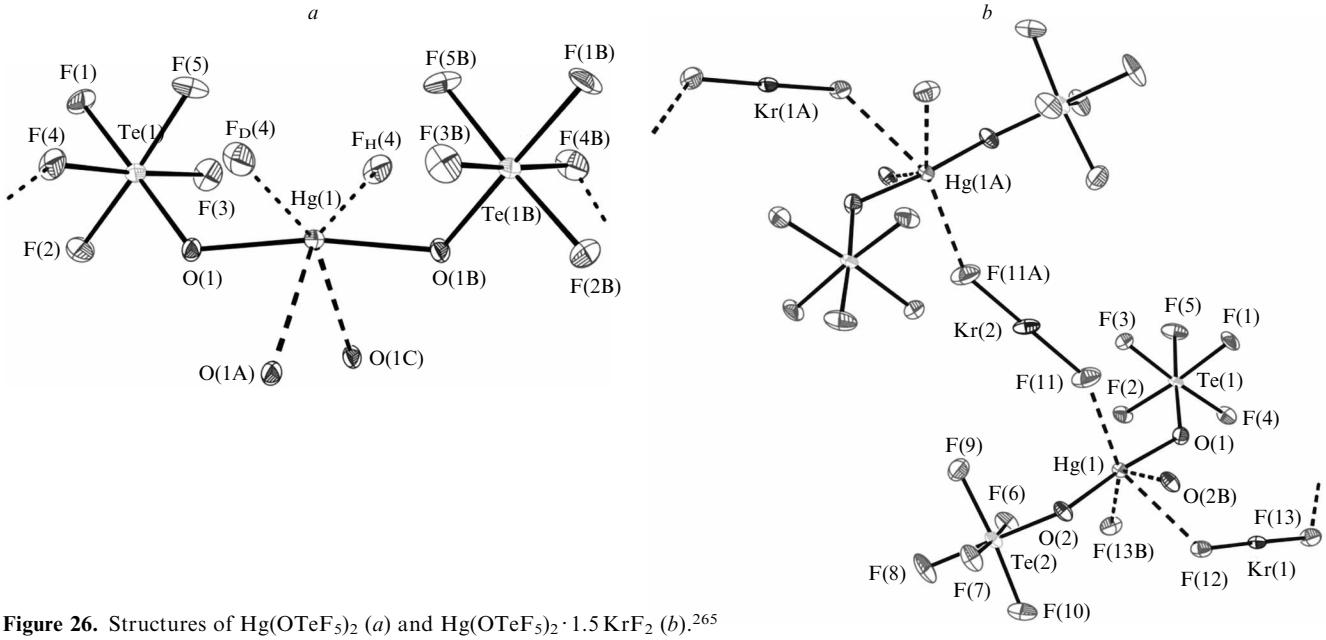


Figure 26. Structures of $Hg(OTeF_5)_2$ (*a*) and $Hg(OTeF_5)_2 \cdot 1.5\,KrF_2$ (*b*).[265]

and Hg···F [2 × 2.810(7) Å] bonds. As a result, $Hg(OTeF_5)_2$ exists as a chain structure (Fig. 26 *a*).

The coordination compounds $Hg(OTeF_5)_2 \cdot 1.5\,NgF_2$ (Ng = Kr, Xe) are isomorphic and crystallize in the same space group $P2_1/n$. The structures of $Hg(OTeF_5)_2 \cdot 1.5\,NgF_2$ are similar and contain $Hg(OTeF_5)_2$ units linked to one another by bridging NgF_2 molecules (see Fig. 26 *b*). As was to be expected, the unit cell of $Hg(OTeF_5)_2 \cdot 1.5\,XeF_2$ has somewhat larger dimensions than the unit cell of $Hg(OTeF_5)_2 \cdot 1.5\,KrF_2$ due to the difference between the covalent radii of xenon (1.40 Å) and krypton (1.16 Å).[267] The coordination spheres of mercury in $Hg(OTeF_5)_2 \cdot 1.5\,NgF_2$ are similar to those in $Hg(OTeF_5)_2$ and consist of highly distorted pseudo-octahedra. The Hg–F bonds [2.606(5) and 2.623(4) Å for Ng = Xe; 2.664(3) and 2.675(3) Å for Ng = Kr], which are located in the *trans*-positions relative to each other, are somewhat shorter than the Hg–F and Hg–O bonds [2.701(5) and 2.749(4) Å for Ng = Xe; 2.741(3) and 2.725(3) Å for Ng = Kr], which are also in the *trans*-positions relative to each other. The Hg–F and Hg–O bond lengths in $Hg(OTeF_5)_2 \cdot 1.5\,NgF_2$ are smaller and larger, respectively, than the corresponding bonds in $Hg(OTeF_5)_2$ [Hg–F = 2.810(7) and Hg–O = 2.641(7) Å]. These bonds, which are similar in the type of interaction to analogous bonds found in the crystal structure of $Hg(OTeF_5)_2$, apparently make a contribution to realization of the *gauche*-conformation established by DeBackere *et al.*[265] for the $Hg(OTeF_5)_2$ moiety. Both structures of $Hg(OTeF_5)_2 \cdot 1.5\,NgF_2$ are similar; however, the lengths of the bridging bonds between the mercury and fluorine atoms of the NgF_2 group are somewhat shorter in $Hg(OTeF_5)_2 \cdot 1.5\,XeF_2$ than in the similar compound $Hg(OTeF_5)_2 \cdot 1.5\,KrF_2$, which can be attributed to higher polarity of the Xe–F bonds.[136] The Xe–F bond lengths are comparable with the bond lengths found for the bridging bonds involving XeF_2 in $Cd(XeF_2)_4(AsF_6)_2$ [Xe–F = 1.995(5) and 2.017(5) Å (see Ref. 255)] and $Cd(XeF_2)_5(PF_6)_2$ [Xe–F = 1.999(6) and 2.016(6) Å].[256] The structure of $Hg(OTeF_5)_2 \cdot 1.5\,KrF_2$ is now probably the only example of KrF_2 coordination to the centred metal atom and the bridging KrF_2 molecule. The compound $[BrOF_2][AsF_6] \cdot 2\,KrF_2$ considered above is the second complex with a similar coordination of KrF_2 to be studied by X-ray diffraction.

A series of studies of physicochemical and spectroscopic properties of the complexes formed by anomalously strong Lewis acid, AuF_5, with group IA and IIA metals have been carried out.[116,268–270] It was found that KrF_2 reacts with gold metal in anhydrous HF in the presence of metal fluorides to give complex hexafluoroaurates of the general formula $M^IAu^VF_6$ (M^I = Li, Na, K, Rb, Cs) and bis(hexafluoroaurates) $M^{II}(Au^VF_6)_2$ (M^{II} = Mg, Ca, Sr, Ba).

The compounds $Mg(AuF_6)_2$ and $Ca(AuF_6)_2$ crystallize in the tetragonal system (space group $P\bar{4}$, unit cell parameters $a = 4.938$, $c = 7.714$ and $a = 5.019$, $c = 8.428$ Å, respectively, $Z = 1$), while $Sr(AuF_6)_2$ and $Ba(AuF_6)_2$ crystallize in the cubic system [space group $P\bar{4}3m$ or $P23$, unit cell parameters $a = 9.535(6)$ and $a = 9.901(3)$ Å, respectively, $Z = 4$]. The subsequent reactions of bis(hexafluoro-

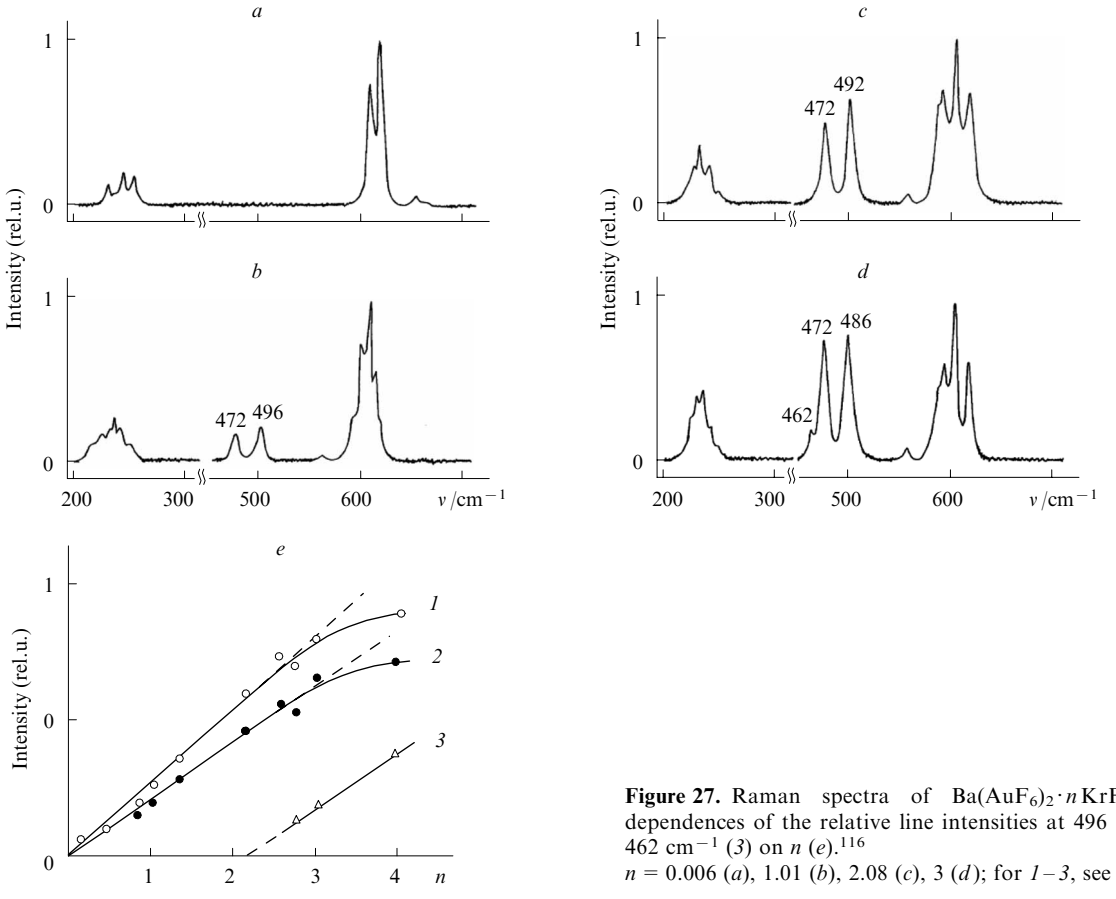


Figure 27. Raman spectra of $Ba(AuF_6)_2 \cdot n\,KrF_2$ (*a*–*d*) and dependences of the relative line intensities at 496 (*1*), 472 (*2*) and 462 cm^{-1} (*3*) on *n* (*e*).[116]
n = 0.006 (*a*), 1.01 (*b*), 2.08 (*c*), 3 (*d*); for *1*–*3*, see the text.

aurates) with KrF_2 yielded new compounds of variable composition (clathrates) $M^{II}(Au^{V}F_6)_2 \cdot n\,KrF_2$ (M^{II} = Ca, Sr, Ba; $n = 0-4$). The Raman spectra of these compounds considerably differ from the spectra of bis(hexafluoroaurates). The spectra of the clathrates, apart from the lines for the AuF_6^- anion, exhibit lines for the $\nu_1(\Sigma_g^+)KrF_2$ stretching mode. The vibration frequency of the Kr–F bonds in the KrF_2 molecules inserted into the crystal lattice of bis(hexafluoroaurates) is shifted by 10–30 cm^{-1} to shorter wavelengths with respect to the $\nu_1(\Sigma_g^+)$ vibrational frequency of non-bonded KrF_2 molecule, which is 462 cm^{-1}. As an example, Fig. 27 shows the spectra of $Ba(AuF_6)_2 \cdot n\,KrF_2$ depending on the number of KrF_2 molecules inserted into its crystal lattice. It can be seen that as n increases, lines at about 472 and 496 cm^{-1} appear, corresponding to Kr–F vibrations in two different crystal modifications of the KrF_2 molecules. The line frequency of 472 cm^{-1} virtually does not depend on n, while the 496 cm^{-1} frequency shifts to longer wavelengths (to 484 cm^{-1}). This indicates that as the number of KrF_2 molecules inserted in the lattice increases, their interaction with bis(hexafluoroaurate) becomes weaker. It was also found that the increase in n gives rise to one more spectral line at 462 cm^{-1}, which was assigned to the $\nu_1(\Sigma_g^+)$ stretching mode of virtually unbound KrF_2 molecules. The dependences of the relative intensities of the 496, 472 and 462 cm^{-1} lines on n are shown in Fig. 27 *e*. It can be seen that up to $n = 2.5$, the plots for intensities of the 496 and 472 cm^{-1} lines are linear. As n further increases, the linearity of the plots is violated. The violation is due to the appearance of weakly bound KrF_2 molecules giving rise to lines (ν = 462 cm^{-1}) the intensity of which varies linearly with increase in n. The intercept on the x axis of line *3* (Fig. 27 *e*) corresponds to the n values at which only bound KrF_2 molecules that interact with $M^{II}(ArF_6)_2$ are present in the bis(hexafluoroaurate) lattice.

VIII. Low-temperature matrix-isolated compounds of noble gases

An interesting area of the noble gas chemistry is the synthesis and study of the physicochemical and spectral properties of compounds generally described as HNgY (Ng is a noble gas atom, Y is an electronegative fragment) isolated in a low-temperature matrix.[271] The stabilization energy of systems of this type is due to a contribution of the ionic electron configuration $(HRg)^+X^-$ (Ref. 272). Note that properties of compounds of this class have been considered fairly comprehensively in reviews [52, 53] and original papers.[271, 272]

The first and yet the only HNgY, where Ng = Ar, is hydrofluoride HArF, which was obtained by UV photolysis of HF (λ = 127–160 nm) in a solid argon matrix ($T \leqslant 27$ K).[273] According to the IR spectra, the HArF molecule has a linear configuration [273] and gives three absorption bands

$$\Gamma_{vib} = 2\Sigma^+(IR,R) + \Pi(IR,R)$$

with frequencies ν(H–Ar) = 1466, δ(H–Ar–F) = 513 and ν(Ar–F) = 435 cm^{-1} corresponding to the $C_{\infty v}$ symmetry of the structure. The matrix annealing was accompanied by a noticeable shift ($\sim$50 cm^{-1}) of the H–Ar stretching band to shorter wavelengths. This shift was attributed [273] to transition of HArF from a less stable to a more stable configuration. Later this conclusion was supported by results of theoretical calculations [274] resorting to the hybrid quantum mechanics/molecular mechanics (QM/MM) approach. The results of further studies of the spectra of HArF in an argon matrix [275] at 30 K attest to the existence of a more thermally stable modification of argon hydrofluoride responsible for vibrational frequencies of 2020.8 and 697.0 cm^{-1}.

The hydrofluoride HKrF, which also has a linear configuration ($C_{\infty v}$ symmetry) has been prepared in a similar way (UV photolysis of HF in a krypton matrix, λ = 127–160 and 193 nm, T = 30 K). [276] The IR spectrum of HKrF, similarly to the spectrum of HArF, has three absorption bands: ν(H–Kr) = 1950, δ(H–Kr–F) = 650 and ν(Kr–F) = 415 cm^{-1}. It was concluded [276] that the krypton hydrofluoride molecule has two relaxed configurations, the H–Kr stretching frequency for one configuration being shifted to shorter wavelengths by $\sim$26 cm^{-1}.

Apart from krypton hydrofluoride, the hydrochloride HKrCl and the compounds described as HKrY (Y = CN, C≡CH, C≡CCN, C≡CC≡CH) are also known. The compounds were synthesized by UV photolysis of HCl,[277] acetylene and diacetylene [278, 279] in a krypton matrix at $\sim$30 K. Their IR spectra were studied and vibrational frequencies were assigned using quantum chemistry techniques. The spectra of HKrC≡CH exhibit a triplet with frequencies of 1241.5, 1249.5 and 1257 cm^{-1}, which were assigned [278] to H–Kr vibrations in three HKrC≡CH modifications differently oriented in space. The bands at about 3290 and 608 cm^{-1} were assigned to the H–C stretching mode and the C≡C–H bending mode, respectively.

Among the HNgY type compounds synthesized to date, xenon compounds are greatest in number. They are prepared, most often, by UV photolysis of appropriate precursors in a xenon matrix. Noteworthy are HXeF,[280] HXeCl,[280, 281] HXeBr,[280] HXeI,[281] HXeOH,[282] HXeSH,[283] HXeH,[280] HXeCN,[284] HXeNCO [285] and HXeC≡CH.[278] The IR spectra of these compounds have been studied and the vibrational frequencies have been assigned. Matrix-isolated H(D)XeY molecules (Y = Cl, Br, I) were found to exist in a linear configuration, which is expected to give rise to three absorption bands in the IR spectra. However, only the H(D)–Xe stretching band was observed in spectroscopic experiments.[286] The vibrational frequency of this band decreases in the series Cl > Br > I:

Compound	HXeCl	DXeCl	HXeBr	DXeBr	HXeI	DXeI
ν /cm^{-1}	1648	1198	1504	1100	1193	893

Compounds with the general formula $CUO(Ar)_{4-n}(Xe)_n$ (n = 1–4) have been obtained in an argon matrix.[287] From analysis of the IR spectra, the researchers drew the conclusion that the observed weakening of the U–O and U–C bonds attests to the presence of bridging bonds of argon and xenon atoms with the uranium atom. Quantum chemical calculations indicate a pseudo-octahedral environment of uranium.

In later publications,[271, 288, 289] the compound HXeOXeH has been prepared by UV photolysis of water in a xenon matrix at 40–45 K; this molecule is the smallest known individual matrix-isolated molecule containing two noble gas atoms. The IR spectra of HXeOXeH have been

studied and the geometric parameters of the molecule have been calculated.

The fluorine-containing compounds HNgCCF and HCCNgF (Ng = Kr, Xe) were obtained by UV photolysis of HCCF in a krypton or xenon matrix.[290] The HNgC≡CF molecule was found to be more stable than HNgC≡CH (Ng = Kr, Xe).[278] The possibility to prepare relatively stable compounds containing no hydrogen — XNgC≡CX and XNgC≡CNgX (Ng = Kr, Ar; X = F, Cl) — has been reported.[291]

Recently three new xenon compounds containing a cyano group have been synthesized:[292] isomeric ClXeCN and ClXeNC and BrXeCN. The synthesis was accomplished by photolysis of the ClCN and BrCN precursors on exposure to an ArF excimer laser (λ = 193 nm) in a solid xenon matrix at 8 K. The obtained xenon compounds were studied by IR spectroscopy, the frequencies were assigned with the help of isotope labelling ($^{13}C/^{12}C$) and quantum chemistry (B3LYP and MP2) methods. On the basis of analysis of the IR spectra, it was shown that the frequencies of the C≡N groups for the ClXeCN and ClXeNC isomers are somewhat different, being 2145 and 2030 cm^{-1}, respectively. The isotope shifts of the $^{12}C{\equiv}N$ vibrational frequency with respect to the $^{13}C{\equiv}N$ vibration frequency in ClXeCN and ClXeNC are 47 and 40 cm^{-1}, respectively, which is in good agreement with calculation results (49 and 43 cm^{-1}). According to Arppe *et al.*,[292] the synthesis of ClXeCN, ClXeNC and BrXeCN is the first step on the way to krypton-containing compound, FKrCN, and YNgY′ type compounds (Y and Y′ are electronegative groups).

Of considerable interest is the ability of noble gas atoms (Ng = Ar, Kr, Xe) to form bonds with protein molecules, which may find use in modern biochemical technologies.[293] However, for understanding of the molecular mechanisms of interaction of Ng atoms with these molecules, investigations of relatively simple model systems are required; therefore, complexes incorporating organic aromatic molecules, for example, phenol, are often used as prototypes of the corresponding biological formulations. Depending on the type of ligand, phenol can form either H-bonded complexes or π-complexes; ligands without a constant dipole or quadrupole moment (for example, noble gas atoms) form mainly π-complexes with phenol.[294, 295]

Cao *et al.*[296] studied the reaction of phenol molecules with xenon (1 : 1) in a neon matrix. Analysis of the IR spectra of the phenol···Xe system [296] and results of quantum chemical calculations by means of MP2 [(aug)-cc-pVTZ basis set], molecular mechanics (MM), molecular dynamics (MD) and QM/MM techniques demonstrated[297] that, unlike the phenol···Ng systems (Ng = Ar, Kr),[295] in this case, several stable conformations are formed: π-complexes and H-bonded complexes of the phenol···Xe_n type (n = 1–4). For the obtained structures, the binding energies and the geometric parameters of various conformers of the phenol···Xe_n system were calculated, the vibrational frequencies were analyzed in the harmonic approximation, and the vibrational frequency shifts induced by the formation of phenol complexes with xenon were estimated. The calculated values were compared with the experimental IR-spectroscopic data. An example is given in Fig. 28, which shows the structures of two stable conformations in the phenol···Xe(1) system, namely, the π-complex (the xenon atom is located above the aromatic ring with a slight shift towards the hydroxyl oxygen atom) and H-bonded complex

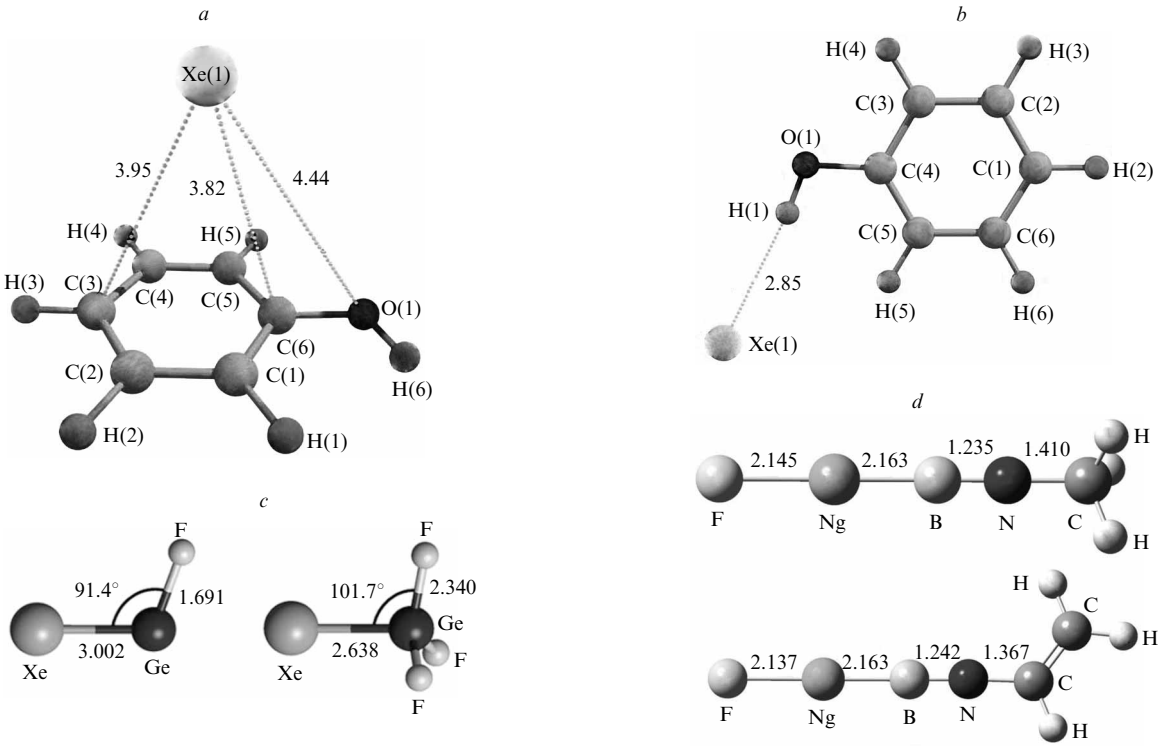


Figure 28. Structures of the π-complex (*a*) and H-bonded complex (*b*) in the phenol···Xe system[296] and geometric parameters of matrix-isolated molecules: $FGe{-}Xe^{+}$, $F_3Ge{-}Xe^{+}$ (*c*) and FNgBNR (Ng = Ar, Kr, Xe; R = CH_3, $CH{=}CH_2$) (*d*).

(the xenon atom is located in the plane of the ring on the line that passes through the O–H bond). The binding energy and the characteristic Xe–H(OH) distance for H-bonded phenol···Xe(1) complex calculated using different functionals of the density functional theory [296, 297] are 6.7 kJ·mol^{-1} and 3.03 Å, respectively, which are somewhat smaller than the corresponding values for the benzene···Xe complex [7.5 kJ mol^{-1} and 3.81 Å (Ref. 298)].

It is noteworthy that immediately after the synthesis of the first matrix-isolated compounds of noble gases,[273, 277, 282–284] several papers have been published dealing with theoretical calculations of the stability, structures, and vibrational spectra of matrix-isolated molecules with various types of bonds for noble gas atoms. Among the latest publications, note studies devoted to the structures of HArC≡CH, HKrC≡CKrH, HKrC≡CXeH,[299] F_2NXe^+, FGe–Xe$^+$, $F_3Ge–Xe^+$, FXeGeF, $FXeGeF_3$ (Refs 300–302) (see Fig. 28 *c*), the clusters $(HXeF)_n$ (n = 2, 3),[303] the vibrational spectra of NgBeS (Ng = Ne, Ar, Kr, Xe),[304] XeO_nS_m (n, m = 0–4; $1 \leqslant n+m \leqslant 4$).[105] Chen *et al.*[305] studied the thermodynamic characteristics and calculated the geometric parameters of the FNgBNR type compounds (Ng = Ar, Kr, Xe; R = H, F, OH, CH_3, C≡CH, CH=CH_2) (see Fig. 28 *d*) and their dissociation energies (F + Ng + BNH). The calculations showed that at low temperatures, the FNgBNR molecules are thermally stable and should have a compact structure with F–Ng and Ng–B bond lengths of 1.9–2.2 and ~1.8 Å, respectively. The researchers cited [305] deem that in the near future, preparation of the compounds FNgBNR both in the cryogenic (matrix) conditions and in the gas phase would be possible. As a matter of fact, a similar opinion has been stated by the vast majority of authors of the above-mentioned publications devoted to theoretical investigations of parameters of some matrix-isolated molecules of noble gas compounds.

IX. Conclusion

A huge amount of information about the physicochemical properties of simple and complex compounds of noble gases has been accumulated to date, including data on the diversity of structural features of these compounds in various physical states.

A wide range of compounds with Ng–F (Ng = Kr, Xe), Xe–O, Xe–N, Xe–C and other bonds (Refs 9, 29, 47, 51–53, 56, 181, 259) and complex compounds with Xe–M bonds (M = Ag, Au and other) [234–239] have been synthesized; aspects concerning the geometric structure and the nature of chemical bonds in other compounds are discussed.[306–308]

The performed crystallographic investigations of the noble gas fluorides, transition metal fluorides and their compounds with Lewis acids and bases attest to pronounced distortions of the theoretically predicted polyhedra.[43, 48, 309] The intermolecular fluoride bridges give rise to intricate crystal packing modes with several crystallographically non-equivalent molecules.[47, 51, 56]

The investigation results of recent years outline new aspects of the chemistry of noble gases. These include targeted synthesis of coordination compounds with unusual structural characteristics in which the binary fluorides XeF_2, XeF_4 and KrF_2 function as bridging ligands.[45–47, 256–259, 262, 263, 310] One more issue is the synthesis of XeF_2-containing coordination compounds with independent sites (mainly metal atoms) [248, 249, 256–259] and compounds containing non-coordinated (free) XeF_2 molecules, which are retained in the crystal lattice due to electrostatic properties.[45, 263] Finally, mention should be made of especially stable chain and network multilayer polymeric compounds of xenon and krypton containing macromolecules, clathrate-like compounds and so on.

Further development of research into the unusual physicochemical properties and crystal structures of xenon compounds, in particular, XeF_2 and XeO_3, under extreme conditions (superhigh pressure or temperature) [138, 144, 145] can give rise to a new class of energetic materials and fuels, unusual energy storage devices, superoxidants for destruction of chemical and biological agents, new high-temperature superconductors and so on. Methods suitable for theoretical prediction of the key crystal structure parameters of compounds at superhigh pressures already exist.[311]

Increasing interest is also being aroused by thermodynamically unstable hydrofluorides of noble gases such as HArF, HKrF,[273, 276] and derivatives of noble gases containing no fluorine atoms [52, 53, 278–281, 285–287] (HXeBr, HKrCl, HXeH, HXeOH, HXeO, HXeCCH, HKrCCH and other). More than 20 such compounds are known to date (according to a publication,[53] there were 27 compounds in 2012); one of the latest synthesized compounds was HXeOXeH.[288] Note that the synthesis of HXeOXeH [288] and also XeO_2 (Ref. 100) may not only serve as the first step towards the preparation of polymeric chain structures $(Xe–O)_n$ and $(XeO_2)_n$ needed to solve some special problems but also shed light on the cosmochemistry of xenon,[312, 313] in particular, this could explain the very low content of xenon in the Earth atmosphere. In addition, much attention is attracted by intermolecular complexes of noble gases, in particular, xenon, with small organic molecules (benzene, phenol and so on).[296, 297, 314] The results of simulation of intermolecular xenon complexes with aromatic compounds [297, 315, 316] and experimental studies of the structures and vibrational spectra of these complexes [296, 314] may give the key to understanding of the mechanisms of xenon interaction with components of protein macromolecules and identification of the protein active sites and channels by which the substrates approach the active sites.

Of special practical interest are the complex compounds of nitrogen fluorides and oxyfluorides (NF_3, N_2F_4, N_2F_2, FNO, FNO_2, NF_3O) with Lewis acids, which are usually synthesized in solutions in anhydrous HF by fluorination with krypton difluoride at $T < 293$ K in the presence of appropriate gaseous reagents.[117, 317, 318] These compounds can be used to prepare homoleptic polynitrogen compounds the possible existence of which was predicted in some quantum chemical investigations.[319–321] According to estimates, polynitrogen compounds may have better characteristics and service properties than many existing rocket fuels [320] and prove to be promising energetic compounds.[321] The synthesis of $XeF_2 \cdot HNO_3$, $FXeONO_2$, $XeF_2 \cdot N_2O_4$, $[XeONO_2][AsF_6]$,[166] complexes containing N_k^+ ($k \geqslant 5$) and N_7O^+ cations [322–324] and also NF_4^+, $N_2F_3^+$, N_2F^+ and NOF_2^+ cations with strong Lewis acids [117, 317, 318] may provide a real possibility to manufacture new energetic materials based on polynitrogen compounds.

Meanwhile, some issues still remain unsolved, in particular, the nature of chemical bonds in these derivatives, transformations of molecular and crystal structures under

various conditions, mechanisms of formation and orientation of XeF_2 and KrF_2 molecules in clathrate-like and polymeric (chain or network) entities.

The answers to some of these questions can be derived from the data of crystallography with the help of other physical methods,[325, 326] in particular, terahertz (THz) spectroscopy,[327, 328] which recently gained popularity in many fields of physics and chemistry. By means of terahertz spectroscopy based on effects of interaction of phase-manipulated pulses with resonant-absorbing molecules and fast transmission,[329, 330] it is possible to gain spectroscopic information over a broad range and to rapidly record (time of single measurement < 10 μs) the spectra of low-frequency vibrations of functional groups not only for the reaction products but also for the products of their decomposition, which is especially important for the study of thermodynamically unstable compounds.

It is also possible to resort to modern theoretical methods, for example, MM, MD and hybrid QM/MM techniques,[331, 332] which have already proved efficient in the analysis of the structure of HArF[274] and various conformers of the phenol$\cdots Xe_n$ system ($n = 1-4$).[296, 297, 315] Combination of these techniques with traditional methods and with other rapidly developing structural methods can enable unambiguous interpretation of structural details of noble gas compounds.

References

1. N Bartlett *Proc. Chem. Soc.* 218 (1962)
2. D F Smith, in *Noble Gas Compounds* (Ed. H H Hyman) (Chicago: University of Chicago Press, 1963) p. 295
3. J G Malm, H Selig, J Jortner, S A Rice *Chem. Rev.* **65** 199 (1965)
4. J H Holloway *Noble Gas Chemistry* (London: Methuen, 1968)
5. V B Sokolov, V N Prusakov *At. Energ.* **31** 990 (1971) [a]
6. N Bartlett, F O Sladky, in *Comprehensive Inorganic Chemistry* (Eds J C Bailor Jr, H J Emeleus, R Nyholm, A F Trotman-Dickenson) (New York: Pergamon Press, 1973) p. 213
7. A B Neiding, V B Sokolov *Russ. Chem. Rev.* **43** 1043 (1974)
8. K Seppelt, D Lentz, in *Progress in Inorganic Chemistry* Vol. 29 (Ed. S J Lippard) (New York: Wiley, 1982) p. 167
9. H Selig, J H Holloway, in *Topics in Current Chemistry* Vol. 124 (Ed. F L Boschke) (Berlin, Heidelberg: Springer, 1984) p. 33
10. D T Hawkins, W E Falconer, N Bartlett *Noble Gas Compounds. A Bibliography: 1962–1976* (New York: Plenum, 1978)
11. *The Oxidation of Oxygen and Related Chemistry: Selected Papers of Neil Bartlett* (Ed. N Bartlett) (Singapore, River Edge, NJ, London: World Scientific Publ., 2001)
12. N Bartlett, in *Fluorine Chemistry at the Millenium. Fascinated by Fluorine* (Ed. R E Banks) (Amsterdam: Elsevier, 2000) p. 29
13. L Graham, O Gaudejus, N K Jha, N Bartlett *Coord. Chem. Rev.* **197** 321 (2000)
14. K O Christe *Chem. Commun.* **49** 4588 (2013)
15. I Hargittai *Struct. Chem.* **20** 953 (2009)
16. P Ball *Elegant Solutions: Ten Beautiful Experiments in Chemistry* (London: Royal Society of Chemistry, 2005)
17. V B Sokolov, S N Spirin, B B Chaivanov, in *Sbornik Nauchnykh Trudov IAE* (Moscow: Institute of Atomic Energy, 1989)
18. G N Makeev, V B Sokolov, B B Chaivanov, in *Khimiya Plazmy* (Plasma Chemistry) No. 2 (Ed. B M Smirnov) (Moscow: Atomizdat, 1975) p. 62
19. *Synthetic Fluorine Chemistry* (Eds G A Olah, R D Chambers, G K S Prakash) (New York: Wiley, 1992)
20. V K Brel, N Sh Pirkuliev, N S Zefirov *Russ. Chem. Rev.* **70** 231 (2001)
21. *Handbook of Reagents for Organic Synthesis: Fluorine-Containing Reagents* (Ed. L A Paquette) (Chichester; Wiley, 2007)
22. G J Schrobilgen, D S Brock *Annu. Rep. Prog. Chem., Sect. A: Inorg. Chem.* **109** 101 (2013)
23. *High Power Laser Handbook* (Eds H Injeyan, G Goodno) (London: McGraw Hill, 2011)
24. P Knauth, H L Tuller *J. Am. Ceram. Soc.* **85** 1654 (2001)
25. V D Klimov, V N Prusakov, V B Sokolov *Dokl. Akad. Nauk SSSR* **217** 1077 (1974) [b]
26. A V Nikolaev, A A Opalovskii, A S Nazarov, G V Tretyakov *Izv. Akad. Nauk, SSSR, Ser. Khim. Nauk* 21 (1972) [c]
27. Sh Sh Nabiev, A V Ryzhkov, V B Sokolov, S N Spirin *J. Fluorine Chem.* **54** 333 (1991)
28. B Žemva, in *Inorganic Chemistry. Encyclopedia of Inorganic Chemistry* Vol. 5 (Ed. R B King) (New York: Wiley, 1994) p. 2660
29. G J Schrobilgen, in *Encyclopedia of Physical Science and Technology* Vol. 10 (Ed. M F Hawthorne) (San Diego, CA: Academic Press, 2002) p. 449
30. *Encyclopedia of Inorganic Chemistry* (Ed. R B King) (Chichester: Wiley, 2006)
31. G J Schrobilgen, D S Brock, H P A Mercier, in *Kirk-Othmer Encyclopedia of Chemical Technology* (Hoboken, NJ: Wiley, 2012) p. 1
32. K O Christe *Angew. Chem., Int. Ed.* **40** 1419 (2001)
33. K Nomura, M Kobayashi *Ionics* **14** 131 (2008)
34. A V Eletskii, I M Iskandarova, A A Knizhnik, D N Krasikov *Phys.-Usp.* **54** 227 (2011) [*Usp. Fiz. Nauk* **181** 233 (2011)]
35. R R Nair, W C Ren, R Jalil, I Riaz, V G Kravets, L Britnell, P Blake, F Schedin, A S Mayorov, S Yuan, M I Katsnelson, H M Cheng, W Strupinski, L G Bulusheva, A V Okotrub, I V Grigorieva, A N Grigorenko, K S Novoselov, A K Geim *Small* **6** 2877 (2010)
36. A Fridman *Plasma Chemistry* (Cambridge: Cambridge University Press, 2007)
37. S Franssila *Introduction to Microfabrication* (New York: Wiley, 2010)
38. Yu M Kiselev, N A Dobrynina *Khimiya Koordinatsionnykh Soedinenii* (The Chemistry of Coordination Compounds) (Moscow: Akademiya, 2007)
39. P E Erilov, V V Titov, V F Serik, V B Sokolov *At. Energ.* **92** 56 (2002) [a]
40. T Bunič, M Tramšek, E Goreshnik, B Žemva *Solid State Sci.* **10** 1511 (2008)
41. P E Erilov, V N Prusakov, V F Serik, V B Sokolov, S V Fedichev *At. Energ.* **107** 142 (2009) [a]
42. H A Bent *Molecules and the Chemical Bond* (Bloomington, IN: Trafford Publ., 2013)
43. V I Minkin, B Ya Simkin, R M Minyaev *Teoriya Stroeniya Molekul* (The Theory of Molecular Structure) (Rostov-on-Don: Feniks, 1997)
44. J Barrett *Structure and Bonding* (Cambridge: Royal Society of Chemistry, 2001)
45. G Tavčar, B Žemva *Inorg. Chem.* **52** 4319 (2013)
46. D S Brock, J J C de Pury, H P A Mercier, G J Schrobilgen, B Silvi *J. Am. Chem. Soc.* **132** 3533 (2010)
47. Sh Sh Nabiev, V B Sokolov, B B Chaivanov *Crystallogr. Rep.* **56** 774 (2011) [*Kristallografiya* **56** 889 (2011)]
48. U Muller *Inorganic Structural Chemistry* (New York: Wiley, 2006)
49. J F Liebman, C A Deakyne *J. Fluorine Chem.* **121** 1 (2003)
50. A K Brisdon *Annu. Rep. Prog. Chem., Sect. A: Inorg. Chem.* **100** 131 (2004)
51. M Tramsek, B Zemva *Acta Chim. Slov.* **53** 105 (2006)
52. W Grochala *Chem. Soc. Rev.* **36** 1632 (2007)

53. W Grochala, L Khriachtchev, M Räsänen, in *Physics and Chemistry at Low Temperatures* (Ed. L Khriachtchev) (New York: CRC Press, 2012) p. 419
54. G J Schrobilgen, D S Brock *Annu. Rep. Prog. Chem., Sect. A: Inorg. Chem.* **107** 135 (2011)
55. G J Schrobilgen, D S Brock *Annu. Rep. Prog. Chem., Sect. A: Inorg. Chem.* **108** 138 (2012)
56. E Hope *Coord. Chem. Rev.* **257** 902 (2013)
57. J L Huston *Inorg. Nucl. Chem. Lett.* **4** 29 (1968)
58. J L Huston *J. Am. Chem. Soc.* **93** 5255 (1973)
59. D E McKee, C J Adams, A Zalkin, N Bartlett *J. Chem. Soc., Chem. Commun.* 26 (1973)
60. V V Avrorin, R N Krasikova, V D Nefedov, M A Toropova *Russ. Chem. Rev.* **51** 12 (1982)
61. L Stein *Radiochim. Acta* **32** 163 (1983)
62. I J Vasilescu *Rev. Roum. Chim.* **12** 835 (1967)
63. M-S Liao, Q-E Zhang *J. Phys. Chem. A* **102** 10647 (1998)
64. R S Catton, K A R Mitchell *Can. J. Chem.* **48** 2695 (1970)
65. R J Gillespie *Coord. Chem. Rev.* **252** 1315 (2008)
66. R J Gillespie, I Hargittai *The VSEPR Model of Molecular Geometry* (London: Dover, 2012)
67. G A Collins, D Cruickshank, A Breeze *J. Chem. Soc., Faraday Trans. 2* **70** 393 (1974)
68. S Reichman, F Schreiner *J. Chem. Phys.* **51** 2355 (1969)
69. R M Gavin, L S Bartell *J. Chem. Phys.* **48** 2460 (1968)
70. P Tsao, G Cobb, H Claassen *J. Chem. Phys.* **54** 5247 (1971)
71. N J Brassington, H G M Edwards *J. Mol. Struct.* **162** 69 (1987)
72. Sh Sh Nabiev, V D Klimov, B S Khodzhiev *Zh. Fiz. Khim.* **65** 2125 (1991) [d]
73. Sh Sh Nabiev, B S Khodzhiev *Vysokoch. Veshch.* (5) 111 (1993)
74. J H Holloway, E G Hope *Adv. Inorg. Chem.* **46** 51 (1999)
75. W E Falconer, M J Vasile, F A Stevie *J. Chem. Phys.* **66** 5335 (1977)
76. *Molecules and Models: the Molecular Structures of Main Group Element Compounds* (Ed. A Haaland) (Oxford: Oxford University Press, 2008)
77. K Fang, X Wu, C Du, Y Dai, S Chu, L Hu, J Deng, Y Feng *Int. J. Mod. Phys. C* **22** 155 (2011)
78. H Bürger, R Kuna, S Ma, J Breidung, W Thiel *J. Chem. Phys.* **101** 1 (1994)
79. W Harshbarger, R K Bonn, S H Bauer *J. Am. Chem. Soc.* **89** 6466 (1967)
80. H H Claassen, G L Goodman, J G Malm, F Schreiner *J. Chem. Phys.* **42** 1229 (1965)
81. Sh Sh Nabiev *Russ. Chem. Bull. (Engl. Transl.)* **47** 535 (1998) [*Izv. Akad. Nauk, Ser. Khim.* 560 (1998)]
82. R M Gavin, L S Bartell *J. Chem. Phys.* **48** 2466 (1968)
83. C Trindle, S Datta, T Bouman *Int. J. Quant. Chem.* **11** 627 (1977)
84. M Klobukowski, S Husinaga, L Sejio, Z Barandiaran *Theor. Chim. Acta* **71** 237 (1987)
85. Sh Sh Nabiev, V D Klimov *Proc. SPIE (Washington)* **1811** 248 (1991)
86. T D Crawford, K W Springer, H F Schaefer III *J. Chem. Phys.* **102** 3302 (1995)
87. Sh Sh Nabiev, L P Sukhanov *Proc. SPIE (Washington)* **4063** 56 (2000)
88. Sh Sh Nabiev, L P Sukhanov *Russ. Chem. Bull. (Engl. Transl.)* **48** 1397 (1999) [*Izv. Akad. Nauk, Ser. Khim.* 1415 (1999)]
89. K Seppelt, D Lentz *Prog. Inorg. Chem.* **29** 167 (1982)
90. D A Dixon, W A de Jong, K A Peterson, K O Christe, G J Schrobilgen *J. Am. Chem. Soc.* **127** 8627 (2005)
91. D J Grant, T-H Wang, D A Dixon, K O Christe *Inorg. Chem.* **49** 261 (2010)
92. K A Peterson, D A Dixon, H Stoll *J. Phys. Chem. A* **116** 9777 (2012)
93. T B Adler, G Knizia, H-J Werner *J. Chem. Phys.* **127** 221106 (2007)
94. G Knizia, T B Adler, H-J Werner *J. Chem. Phys.* **130** 054104 (2009)
95. J F Martins, E B Wilson *J. Mol. Spectrosc.* **26** 410 (1968)
96. E J Jacob H B Thompson, L S Bartell *J. Mol. Struct.* **8** 383 (1971)
97. H H Claassen, E L Gasner, H Kim, J L Huston *J. Chem. Phys.* **49** 253 (1968)
98. R D Willett, P LaBonville, J R Ferraro *J. Chem. Phys.* **63** 1474 (1975)
99. D S Brock, V Bilir, H P A Mercier, G J Schrobilgen *J. Am. Chem. Soc.* **129** 3598 (2007)
100. D S Brock, G J Schrobilgen *J. Am. Chem. Soc.* **133** 6265 (2011)
101. K Nakamoto *Infrared and Raman Spectra of Inorganic and Coordination Compounds Part A: Theory and Applications in Inorganic Chemistry* (6th Ed.) (Hoboken, NJ: Wiley, 2009)
102. D H Templeton, A Zalkin, J D Forrester, S M Williamson *J. Am. Chem. Soc.* **85** 817 (1963)
103. H H Claassen, G Knapp *J. Am. Chem. Soc.* **86** 2341 (1964)
104. P Pyykkö, T Tamm *J. Phys. Chem. A* **104** 3826 (2000)
105. A Papakondylis *Comput. Theor. Chem.* **1015** 15 (2013)
106. G Gundersen, K Hedberg, J L Huston *J. Chem. Phys.* **52** 812 (1970)
107. R S McDowell, L B Asprey *J. Chem. Phys.* **57** 3062 (1972)
108. *Spectroscopic Properties of Inorganic and Organometallic Compounds* (Ed. G Davidson) (Cambridge: Royal Society of Chemistry, 2002)
109. *Advanced Inorganic Fluorides: Synthesis, Characterization, and Applications* (Eds T Nakajima, B Žemva, A Tressaud) (New York: Elsevier, 2000)
110. H H Hyman, L A Quarterman, in *Noble Gas Compounds* (Ed. H H Hyman) (Chicago: University of Chicago Press, 1963) p. 275
111. V N Prusakov, V B Sokolov *Zh. Fiz. Khim.* **45** 2950 (1971) [d]
112. J Chipperfield *Non-Aqueous Solvents* (Oxford: Oxford University Press, 1999)
113. V B Sokolov, Yu V Drobyshevskii, V N Prusakov *Dokl. Akad. Nauk SSSR* **225** 641 (1976) [b]
114. I V Nikitin *Khimiya Kislorodnykh Soedinenii Galogenov* (The Chemistry of Oxygen Compounds of Halogens) (Moscow: Nauka, 1986)
115. I V Nikitin *Russ. Chem. Rev.* **71** 85 (2002)
116. Sh Sh Nabiev, V B Sokolov, S N Spirin, B B Chaivanov *Russ. J. Phys. Chem. A* **85** 1931 (2011) [*Zh. Fiz. Khim.* **85** 2071 (2011)]
117. Sh Sh Nabiev, V B Sokolov, B B Chaivanov *Russ. Chem. Bull. Int. Ed.* **61** 497 (2012) [*Izv. Akad. Nauk, Ser. Khim.* 497 (2012)]
118. Sh Sh Nabiev, I I Ostroukhova *Spectrochim. Acta, Part A* **49** 1537 (1993)
119. Sh Sh Nabiev, I I Ostroukhova *Spectrochim. Acta, Part A* **49** 1527 (1993)
120. Sh Sh Nabiev, I I Ostroukhova, L A Palkina *Spectrochim. Acta, Part A* **55** 2529 (1999)
121. W Rothschild *Dynamics of Molecular Liquids* (New York: Wiley, 1984)
122. Sh Sh Nabiev *Spectrochim. Acta, Part A* **56** 1589 (2000)
123. C J Adams, N Bartlett *Israel J. Chem.* **17** 114 (1978)
124. K O Christe, E G Curtis, R D Wilson, in *J. Inorg. Nucl. Chem. (Suppl. H H Hyman Memorial Volume)* (Oxford: Pergamon Press, 1976) p. 159
125. Sh Sh Nabiev *Russ. J. Inorg. Chem.* **40** 1936 (1995) [*Zh. Neorg. Khim.* **40** 2016 (1995)]
126. Sh Sh Nabiev *Proc. SPIE (Washington)* **4063** 166 (2000)
127. M A Zapol'skaya, N G Zenkevich, E G Komarova *Fiziko-khimicheskie Svoistva Ftoristogo Vodoroda* (Physico-chemical Properties of Hydrogen Fluoride) (Moscow: Nauka, 1977)
128. K O Christe, W W Wilson *Inorg. Chem.* **21** 4113 (1982)

129. P Benkic, L Golic, J Koller *Acta Chim. Slov.* **46** 239 (1999)
130. M J Hughes, H P A Mercier, G J Schrobilgen *Inorg. Chem.* **49** 3501 (2010)
131. J H Holloway, H Selig, U El-Gad *J. Inorg. Nucl. Chem.* **35** 3624 (1973)
132. H A Levy, P A Agron *J. Am. Chem. Soc.* **85** 241 (1963)
133. S Siegel, E Gebert *J. Am. Chem. Soc.* **86** 3896 (1964)
134. W-K Li, G Zhou, T C W Mak *Advanced Structural Inorganic Chemistry* (Oxford: Oxford University Press, 2008)
135. D W H Rankin, N Mitzel, C Morrison *Structural Methods in Molecular Inorganic Chemistry* (Chichester: Wiley, 2013)
136. H A Elliott, J F Lehmann, H P A Mercier, H D B Jenkins, G J Schrobilgen *Inorg. Chem.* **49** 8504 (2010)
137. J F Lehmann, D A Dixon, G J Schrobilgen *Inorg. Chem* **40** 3002 (2001)
138. M Kim, M Debessai, C S Yoo *Nat. Chem.* **2** 784 (2010)
139. W A Bassett *High Pres. Res.* **29** 163 (2009)
140. R L McCreery *Raman Spectroscopy for Chemical Analysis* (New York: Wiley, 2000)
141. D Kurzydłowski, P Zaleski-Ejgierd, W Grochala, R Hoffmann *Inorg. Chem.* **50** 3832 (2011)
142. S Hoyer, T Emmler, K Seppelt *J. Fluorine Chem.* **127** 1415 (2006)
143. S W Peterson, R D Willett, J L Huston *J. Chem. Phys.* **59** 453 (1973)
144. Q Zhu, D Y Jung, A R Oganov, C W Glass, C Gatti, A O Lyakhov *Nat. Chem.* **5** 61 (2013)
145. Q Zhu, D Y Jung, A R Oganov, C W Glass, C Gatti, A O Lyakhov *Nat. Chem.* (Suppl. Inform.); DOI: 10.1038/NCHEM.1497 (2013)
146. N Bartlett, M Wechsberg, F Sladky, P A Bulliner, G R Jones, R D Burbank *J. Chem. Soc., Chem. Commun.* 703 (1969)
147. M Wechsberg, P Bulliner, F Sladky, R Mews, N Bartlett *Inorg. Chem.* **11** 3063 (1972)
148. N Bartlett, M Wechsberg, G R Jones, R D Burbank *Inorg. Chem.* **11** 1124 (1972)
149. F O Sladky *Monatsh. Chem.* **101** 1571 (1970)
150. K Seppelt *Angew. Chem.* **84** 715 (1972)
151. K Seppelt, D Nothe *Inorg. Chem.* **12** 2727 (1973)
152. R G Syvret, G J Schrobilgen *Inorg. Chem.* **28** 1564 (1989)
153. T Birchall, R D Myers, H de Waard, G J Schrobilgen *Inorg. Chem.* **21** 1068 (1982)
154. G A Schumacher, G J Schrobilgen *Inorg. Chem.* **23** 2923 (1984)
155. D Lentz, K Seppelt *Angew. Chem., Int. Ed. Engl.* **18** 66 (1979)
156. B A Fir, H P A Mercier, J C P Sanders, D A Dixon, G J Schrobilgen *J. Fluorine Chem.* **110** 89 (2001)
157. H P A Mercier, J C P Sanders, G J Schrobilgen *Inorg. Chem.* **34** 5261 (1995)
158. W J Casteel Jr, D M MacLeod, H P A Mercier, G J Schrobilgen *Inorg. Chem.* **35** 7279 (1996)
159. B E Pointner, R J Suontamo, G J Schrobilgen *Inorg. Chem.* **45** 1517 (2006)
160. G J Schrobilgen, N LeBlond, D A Dixon *Inorg. Chem* **39** 2473 (2000)
161. G L Smith, H P A Mercier, G J Schrobilgen *Inorg. Chem.* **50** 12359 (2011)
162. R D LeBlond, D D DesMarteau *J. Chem. Soc., Chem. Commun.* 555 (1974)
163. J F Sawyer, G J Schrobilgen, S J Sutherland *Inorg. Chem.* **21** 4064 (1982)
164. G A Schumacher, G J Schrobilgen *Inorg. Chem.* **22** 2178 (1983)
165. J Foropoulos Jr, D D DesMarteau *J. Am. Chem. Soc.* **104** 4260 (1982).
166. M D Moran, D S Brock, H P A Mercier, G J Schrobilgen *J. Am. Chem. Soc.* **132** 13823 (2010)
167. A Obermeyer, H Borrmann, A Simon *J. Am. Chem. Soc.* **117** 7887 (1995)
168. R Minkwitz, T Hertel *Z. Naturforsch.* **526** 1307 (1997)
169. H-J Frohn, S Jakobs, C Rossbach *Eur. J. Solid State Inorg. Chem.* **29** 729 (1992)
170. H-J Frohn, A Klose *J. Fluorine Chem.* **64** 201 (1993)
171. V V Zhdankin, P J Stang, N S Zefiov *J. Chem. Soc., Chem. Commun.* 578 (1992)
172. H-J Frohn, N LeBlond, K Lutar, B Zemva *Angew. Chem., Int. Ed.* **39** 391 (2000)
173. H-J Frohn, S Jakobs, G Henkel *Angew. Chem., Int. Ed. Engl.* **28** 1506 (1989)
174. H-J Frohn, M Theiyen *Angew. Chem., Int. Ed.* **39** 4591 (2000)
175. N Maggiarosa, D Naumann, W Tyrra *Angew. Chem., Int. Ed.* **39** 4588 (2000)
176. H-J Frohn, T Schroer, G Henkel *Angew. Chem., Int. Ed.* **38** 2554 (1999)
177. V Bilir, H-J Frohn *Acta Chim. Slov.* **60** 505 (2013)
178. H Bock, D Hinz-Hubner, U Ruschewitz, D Naumann *Angew. Chem., Int. Ed.* **41** 448 (2002)
179. V Bilir, D Bälser, R Boese, H-J Frohn *J. Fluorine Chem.* **130** 824 (2009)
180. H-J Frohn, A Klose, T Schroer, G Henkel, V Buss, D Opitz, R Vahrenhorst *Inorg. Chem.* **37** 4884 (1998)
181. H-J Frohn, V V Bardin *Organometallics* **20** 4750 (2001)
182. K O Christe, E C Curtis, D A Dixon, H P A Mercier, J C P Sanders, J G Schrobilgen *J. Am. Chem. Soc.* **113** 3351 (1991)
183. J F Lehmann, H P A Mercier, G J Schrobilgen *Coord. Chem. Rev.* **233–234** 1 (2002)
184. Sh Sh Nabiev, V B Sokolov *Khim. Fiz.* **32** 15 (2013) [e]
185. J F Lehmann, G J Schrobilgen *J. Fluorine Chem.* **119** 109 (2003)
186. D A Dixon, T-H Wang, D J Grant, K A Peterson, K O Christe, G J Schrobilgen *Inorg. Chem.* **46** 10016 (2007)
187. Sh Sh Nabiev *Russ. Chem. Bull. (Engl. Transl.)* **48** 711 (1999) [*Izv. Akad. Nauk, Ser. Khim.* 715 (1999)]
188. Sh Sh Nabiev, in *Tezisy Dokladov 23-go S"ezda po Spektroskopii* (Abstracts of Reports of the 23rd Congress on Spectroscopy) (Zvenigorod: FIAN Moscow, 2005) p. 147
189. K Seppelt *Acc. Chem. Res.* **36** 147 (2003)
190. R J Gillespie, G J Schrobilgen *Inorg. Chem.* **15** 22 (1976)
191. J H Holloway, G J Schrobilgen *J. Chem. Soc., Chem. Commun.* 623 (1975)
192. R J Gillespie, D Martin, G J Schrobilgen *J. Chem. Soc., Dalton Trans.* 1898 (1980)
193. B Frlec, J H Holloway *Inorg. Chem.* **15** 1263 (1976)
194. B A Fir, M Gerken, B E Pointner, H P A Mercier, D A Dixon, G J Schrobilgen *J. Fluorine Chem.* **105** 159 (2000)
195. S M Yeh, Ph.D. Thesis Lawrence Berkeley Laboratory and Department of Chemistry, University of California, Berkeley, CA, 1984
196. F O Sladky, P A Bulliner, N Bartlett *J. Chem. Soc. A* 2179 (1969)
197. I L Wilson *J. Fluorine Chem.* **5** 13 (1975)
198. G M Begun, R N Compton *Int. J. Mass Spectrom. Ion Phys.* **30** 379 (1979)
199. I H Krouse, C Hao, C E Check, K C Lobring, L S Sunderlin, P G Wenthold *J. Am. Chem. Soc.* **129** 846 (2007)
200. E Y Misochko, A V Akimov, V A Belov, D A Tyurin *Inorg. Chem.* **48** 8723 (2009)
201. N Vasdev, B E Pointner, R Chirakal, G J Schrobilgen *J. Am. Chem. Soc.* **124** 12863 (2002)
202. N Vasdev, M D Moran, H M Tuononen, R Chirakal, R J Suontamo, A D Bain, G J Schrobilgen *Inorg. Chem.* **49** 8997 (2010)
203. Sh Sh Nabiev *Athmos. Ocean Opt.* **13** 109 (2000) [*Opt. Atmosf. Okeana* **13** 123 (2000)]

204. I V Nikitin *Ftoridy i Oksiftoridy Galogenov* (Halogen Fluorides and Oxyfluorides) (Moscow: Nauka, 1989)
205. R I Gillespie, B Landa, G J Schrobilgen *Inorg. Chem.* **15** 1256 (1976)
206. D E McKee, C J Adams, N Bartlett *Inorg. Chem.* **12** 1722 (1973).
207. E Baran *J. Mol. Struct.* **271** 327 (1992)
208. K Lutar, A Jesih, B Žemva, N Bartlett *Inorg. Chem.* **28** 3467 (1989)
209. K Leary, D H Templeton, A Zalkin, N Bartlett *Inorg. Chem.* **12** 1726 (1973)
210. N Bartlett, B G DeBoer, F J Hollander, F O Sladky, D H Templeton, A Zalkin *Inorg. Chem.* **13** 780 (1974)
211. A Jesih, K Lutar, I Leban, B Zemva *Eur. J. Solid State Inorg. Chem.* **28** 829 (1991)
212. A V Tsvetkov, M F Bobrov, V G Tsirelson *J. Mol. Struct. (THEOCHEM)* **624** 145 (2003)
213. R S Berry *J. Chem. Phys.* **32** 933 (1960)
214. V L Pershin, A I Boldyrev *J. Mol. Struct. (THEOCHEM)* **150** 171 (1987)
215. Sh Sh Nabiev, I I Ostroukhova, N A Revina, L P Sukhanov *Russ. Chem. Bull. (Engl. Transl.)* **47** 417 (1998) [*Izv. Akad. Nauk, Ser. Khim.* 432 (1998)]
216. M F Bobrov, V G Tsirelson *Russ. J. Coord. Chem.* **31** 708 (2005) [*Koord. Khim.* **31** 746 (2005)]
217. K Leary, A Zalkin, N Bartlett *Inorg. Chem.* **13** 775 (1974)
218. A Jesih, B Žemva, J Slivnik *J. Fluorine Chem.* **19** 221 (1982)
219. A Ellern, S Adam, K Seppelt *Chem. – Eur. J.* **2** 398 (1996)
220. A Ellern, A-R Mahjoub, K Seppelt *Angew. Chem., Int. Ed. Engl.* **35** 1123 (1996)
221. H P A Mercier, J C P Sanders, G J Schrobilgen, S S Tsai *Inorg. Chem.* **32** 386 (1993)
222. R J Gillespie, G J Schrobilgen *Inorg. Chem.* **13** 2370 (1974)
223. K O Christe, W W Wilson *Inorg. Chem.* **27** 2714 (1988)
224. K O Christe, D A Dixon, J C P Sanders, G J Schrobilgen, S S Tsai, W W Wilson *Inorg. Chem.* **34** 1868 (1995)
225. J H Holloway, V Kaučcič, D Martin-Rovet, D R Russel, G J Schrobilgen, H Selig *Inorg. Chem.* **24** 678 (1985)
226. K O Christe, W W Wilson *Inorg. Chem.* **27** 3763 (1988)
227. D S Brock, H P Mercier, G J Schrobilgen *J. Am. Chem. Soc.* **132** 10935 (2010)
228. G J Schrobilgen, D Martin-Rovet, P Charpin, M Lance *J. Chem. Soc. Chem. Commun.* 894 (1980)
229. G J Schrobilgen, J H Holloway, P Granger, C Brevard *Inorg. Chem.* **17** 980 (1978)
230. R Minkwitz, M Berkei, R Ludwig *Inorg. Chem.* **40** 6493 (2001)
231. U Kessler, M Jansen *Eur. J. Inorg. Chem.* 1767 (2000)
232. D S Brock, H P Mercier, G J Schrobilgen *J. Am. Chem. Soc.* **135** 5089 (2013)
233. P La Bonville, J R Ferraro, T M Spittler *J. Chem. Phys.* **55** 631 (1971)
234. M Gerken, B E Pointner, M Moran, G J Schrobilgen, H P A Mercier, J A Boatz, B Hoge, K O Christe *J. Am. Chem. Soc.* **131** 13474 (2009)
235. B Žemva, R Hagiwara, W J Casteel Jr, K Lutar, A Jesih, N Bartlett *J. Am. Chem. Soc.* **112** 4816 (1990).
236. T Drews, S Seidel, K Seppelt *Angew. Chem., Int. Ed.* **41** 454 (2002)
237. I C Hwang, S Seidel, K Seppelt *Angew. Chem., Int. Ed.* **42** 4392 (2003)
238. K Seppelt *Z. Anorg. Allg. Chem.* **629** 2427 (2003)
239. R Kuster, K Seppelt *Z. Anorg. Allg. Chem.* **626** 236 (2000)
240. F W B Einstein, P R Rao, J Trotter, N Bartlett *J. Chem. Soc. A* 478 (1967)
241. X-Y Li, X Cao *Phys. Rev. A* **77** 022508 (2008)
242. X-Y Li *J. Chem. Phys.* **137** 124301 (2012)
243. G Liu, Y Zhang, X Bai, F He, X Zhang, Z Wang, W Zhang *Struct. Chem.* **23** 1693 (2012)
244. L Belpassi, I Infante, F Tarantelli, L Visscher *J. Am. Chem. Soc.* **130** 1048 (2008)
245. Z Jamshidi, M F Far, A Maghari *J. Phys. Chem. A* **116** 12510 (2012)
246. L Dąbrowski, M Szuta *Nukleonika* **58** 453 (2013)
247. A E Thompson, B Meredig, C Wolverton *J. Phys.: Condens. Matter* **26** 105501 (2014)
248. R Hagiwara, F Hollander, C Maines, N Bartlett *Eur. J. Solid State Inorg. Chem.* **128** 855 (1991)
249. K Matsumoto, R Hagiwara, Y Ito, O Tamada *Solid State Sci.* **4** 1465 (2002)
250. K Lutar, H Borrman, Z Mazej, M Tramšek, P Benkič, B Žemva *J. Fluorine Chem.* **101** 161 (2000)
251. M Tramšek, P Benkič, A Turičnik, G Tavčar, B Žemva *J. Fluorine Chem.* **114** 143 (2002)
252. M Tramšek, P Benkič, B Žemva *Solid State Sci.* **4** 9 (2002)
253. G Tavčar, M Tramšek, T Bunič, P Bunič, B Žemva *J. Fluorine Chem.* **125** 1579 (2004)
254. M Tramšek, P Benkič, B Žemva *Inorg. Chem.* **43** 699 (2004)
255. G Tavčar, P Benkič, B Žemva *Inorg. Chem.* **43** 1452 (2004)
256. T Bunič, M Tramšek, G Tavčar, B Žemva *Inorg. Chem.* **45** 1038 (2006)
257. T Bunič, M Tramšek, G Tavčar, B Žemva *Inorg. Chem.* **46** 5276 (2007)
258. G Tavčar, E Goreshnik, Z Mazej *J. Fluorine Chem.* **127** 1368 (2006)
259. Z Mazej, E Goreshnik *Inorg. Chem.* **47** 4209 (2008)
260. L Turowsky, K Seppelt *Inorg. Chem.* **29** 3226 (1990)
261. G L Smith, G J Schrobilgen *Inorg. Chem.* **48** 7714 (2009)
262. D S Brock, J J C de Pury, H P A Mercier, G J Schrobilgen, B Silvi *Inorg. Chem.* **49** 6673 (2010)
263. G Tavčar, B Žemva *Angew. Chem., Int. Ed.* **48** 1432 (2009)
264. K Lutar, I Leban, T Ogrin, B Žemva *Eur. J. Solid State Inorg. Chem.* **29** 713 (1992)
265. J R DeBackere, H P A Mercier, G J Schrobilgen *J. Am. Chem. Soc.* **136** 3888 (2014)
266. S Riedel, M Kaupp *Coord. Chem. Rev.* **253** 606 (2009)
267. B Cordero, V Gómez, A E Platero-Prats, M Revés, J Echeverría, E Cremades, F Barragán, S Alvarez *Dalton Trans.* 2832 (2008)
268. Yu M Kiselev, A I Popov, A V Goryunov, N A Chumaevskii, L N Savinova, V B Sokolov, S N Spirin *Zh. Neorg. Khim.* **35** 611 (1990) [f]
269. A I Popov, M D Val'kovskii, Yu M Kiselev, P A Chumaevskii, V B Sokolov, S N Spirin *Zh. Neorg. Khim.* **35** 1970 (1990) [f]
270. B B Chaivanov, Sh Sh Nabiev, V B Sokolov, S N Spirin *J. Fluorine Chem.* **54** 12 (1991).
271. Khriachtchev, M Räsänen, R B Gerber *Acc. Chem. Res.* **42** 183 (2009)
272. R B Gerber *Annu. Rev. Phys. Chem.* **55** 55 (2004)
273. L Khriachtchev, M Pettersson, N Runeberg, J Lundell, M Räsänen *Nature (London)* **406** 874 (2000)
274. A V Bochenkova, V E Bochenkov, L Khriachtchev *J. Phys. Chem. A* **113** 7654 (2009)
275. L Khriachtchev, M Pettersson, A Lignell, M Räsänen *J. Am. Chem. Soc.* **123** 8610 (2001)
276. L M Pettersson, L Khriachtchev, A Lignell, M Räsänen, Z Bihary, R B Gerber *J. Chem. Phys.* **116** 2508 (2002)
277. M Pettersson, J Lundell, M Räsänen *J. Chem. Phys.* **102** 6423 (1995)
278. L Khriachtchev H Tanskanen, A Cohen, R B Gerber, J Lundell, M Pettersson, H Kiljunen, M Räsänen *J. Am. Chem. Soc.* **125** 6876 (2003)
279. H Tanskanen, L Khriachtchev, J Lundell, M Räsänen *J. Am. Chem. Soc.* **125** 16361 (2003)
280. M Lorenz, M Räsänen, V E Bondybey *J. Phys. Chem. A* **104** 3770 (2000)

281. Z Bihary, G M Chaban, R B Gerber *J. Chem. Phys.* **116** 5521 (2002)
282. M Pettersson, J Lundell, L Khriachtchev, M Räsänen *J. Am. Chem. Soc.* **121** 11904 (1999)
283. M Pettersson, J Lundell, L Khriachtchev, E Isoniemi, M Räsänen *J. Am. Chem. Soc.* **20** 7979 (1998)
284. M Pettersson, J Lundell, L Khriachtchev, M Räsänen *J. Chem. Phys.* **109** 618 (1998)
285. M Pettersson, J Lundell, L Khriachtchev, S Jolkkonen, M Räsänen *J. Phys. Chem. A* **104** 3579 (2000)
286. J Lundell, L Khriachtchev, M Pettersson, M Räsänen *Low Temp. Phys.* **26** 680 (2000)
287. B Liang, L Andrews, J Li, B E Bursten *J. Am. Chem. Soc.* **124** 9016 (2002)
288. L Khriachtchev, K Isokoski, A Cohen, M Räsänen, R Gerber *J. Am. Chem. Soc.* **130** 6114 (2008)
289. E Tsivion, R B Gerber *Chem. Phys. Lett.* **482** 30 (2009)
290. L Khriachtchev, A Domanskaya, J Lundell, A Akimov, M Räsänen, E Misochko *J. Phys. Chem. A* **114** 4181 (2010)
291. S Yockel, E Gawlik, A K Wilson *J. Phys. Chem. A* **111** 11261 (2007).
292. T Arppe, L Khriachtchev, A Lignell, A V Domanskaya, M Räsänen *Inorg. Chem.* **51** 4398 (2012)
293. G Najafpour *Biochemical Engineering and Biotechnology* (Amsterdam: Elsevier, 2007)
294. A Takeda, H-S Andrei, M Miyazaki, S Ishiuchi, M Sakai, M Fujii, O Dopfer *Chem. Phys. Lett.* **443** 227 (2007)
295. M Schmies, A Patzer, M Fujii, O Dopfer *Phys. Chem. Chem. Phys.* **13** 13926 (2011)
296. Q Cao, N Andrijchenko, A-E Ahola, A Domanskaya, M Räsänen, A Ermilov, A Nemukhin, L Khriachtchev *J. Chem. Phys.* **137** 134305 (2012)
297. N N Andriichenko, A Yu Ermilov *Zh. Fiz. Khim.* **87** 1348 (2013) [d]
298. T Weber, E Riedle, H J Neusser, E W Schlag *Chem. Phys. Lett.* **183** 77 (1991)
299. A Sethy, B M Deb *Indian J. Chem., Sect. A* **46** 1565 (2007)
300. P Antoniotti, E Bottizzo, L Operti, R Rabezzana, S Borocci, F Grandinetti *J. Phys. Chem. Lett.* **1** 2006 (2010)
301. L Operti, R Rabezzana, F Turco, S Borocci, M Giordani, F Grandinetti *Chem.–Eur. J.* **17** 10682 (2011)
302. S Borocci, M Giordani, F Grandinetti *J. Phys. Chem. A* **118** 3326 (2014)
303. C Cheng, L Sheng *Comput. Theor. Chem.* **989** 39 (2012)
304. Q Wang, X Wang *J. Phys. Chem. A* **117** 1508 (2013)
305. J-L Chen, C-Y Yang, H-J Lin, W-P Hu *Phys. Chem. Chem. Phys.* **15** 9701 (2013)
306. Y-L Sun, J-T Hong, W-P Hu *J. Phys. Chem. A* **114** 9359 (2010)
307. C J Evans, A Lesarri, M C L Gerry *J. Am. Chem. Soc.* **122** 6100 (2000)
308. D S Brock, M J Hughes, G L Smith, J J C de Pury, H P A Mercier, G J Schrobilgen, in *Book of Abstracts of 16th European Symposium on Fluorine Chemistry* (Ed. T Skapin) (Ljubljana, Slovenia: Jožef Stefan Institute Publ., 2010) p. 95
309. M W Justik *Annu. Rep. Prog. Chem., Sect. A: Inorg. Chem.* **104** 134 (2008)
310. M Lozinšek, E Goreshnik, M Tramšek, B Žemva, in *Book of Abstracts of 16th European Symposium on Fluorine Chemistry* (Ed. T Skapin) (Ljubljana, Slovenia: Jožef Stefan Institute Publ., 2010) p. 97
311. Y Wang, Y Ma *J. Chem. Phys.* **140** 040901 (2014)
312. M Ozima, F A Podosek *J. Geophys. Res.* **104** 25493 (1999)
313. D Nishio-Hamane, T Yagi, N Sata, T Fujita, T Okada *Geophys. Res. Lett.* **37** L04302 (2010)
314. X Liu, Q Li, R Li, W Li, J Cheng *Spectrochim. Acta, Part A* **84** 68 (2011)
315. N N Andriichenko, Candidate Thesis in Physical and Mathematical Sciences, Moscow State University, Moscow, 2014
316. S Li, R B Gerber *J. Chem. Phys.* **124** 231103 (2006)
317. R Haiges, M Gerken, A Iuga, R Bau, K O Christe *Inorg. Chem.* **45** 7981 (2006)
318. K O Christe, D A Dixon, D J Grant, R Haiges, F S Tham, A Vij, V Vij, T-H Wang, W W Wilson *Inorg. Chem.* **49** 6823 (2010)
319. B M Rice, E F Byrd, W Mattson *High Energy Density Mater., Ser. Struct. Bond.* **125** 153 (2007)
320. D B Lempert, G N Nechiporenko, S I Soglasnova *Fiz. Goren. Vzryva* **45** 58 (2009)
321. M I Eremets, I A Trojan, A G Gavriliuk, S A Medvedev, in *Static Compression of Energetic Materials* (Eds S M Peiris, G J Piermarini) (Berlin, Heidelberg: Springer, 2008) p. 75
322. D M Badgujar, M B Talawar, S N Asthana, P P Mahulikar *J. Hazard. Mater.* **151** 289 (2008)
323. K O Christe, R Haiges, W Wilson, J Boatz *Inorg. Chem.* **49** 1245 (2010)
324. R Haiges, S Schneider, T Schroer, K O Christe *Angew. Chem., Int. Ed.* **43** 4919 (2004)
325. *Applications of Physical Methods to Inorganic and Bioinorganic Chemistry* (Ed. R A Scott) (New York: Wiley, 2007)
326. D W H Rankin, N Mitzel, C Morrison *Structural Methods in Molecular Inorganic Chemistry* (New York: Wiley, 2013)
327. Y-S Lee *Principles of Terahertz Science and Technology* (Berlin, Heidelberg: Springer, 2008)
328. X C Zhang, J Xu *Introduction to THz Wave Photonics* (New York: CRC Press, 2009)
329. Sh Sh Nabiev, D B Stavrovskii, L A Palkina, V L Zbarskii, N V Yudin, V L Vaks, E G Domracheva, M B Chernyaeva *Russ. J. Phys. Chem. B* **7** 203 (2013) [*Khim. Fiz.* **23** 13 (2013)]
330. V L Vaks, E G Domracheva, Sh Sh Nabiev, M B Chernyaeva, A M Babakov *Athmos. Ocean Opt.* **26** 1 (2013) [*Opt. Atmos. Okeana* **26** 659 (2012)]
331. *Handbook of Computational Chemistry* (Ed. J Leszczynsky) (Dordrecht: Springer, 2012)
332. *Combining Quantum Mechanics and Molecular Mechanics. Some Recent Progresses in QM/MM Methods* (Eds S Canuto, J R Sabin) (New York: Academic Press, 2010)

[a] — *At. Energ. (Engl. Transl.)*
[b] — *Dokl. Phys. (Engl. Transl.)*
[c] — *Russ. Chem. Bull., Int. Ed. (Engl. Transl.)*
[d] — *Russ. J. Phys. Chem. A (Engl. Transl.)*
[e] — *Russ. J. Phys. Chem. B, Focus on Physics (Engl. Trans.)*
[f] — *Russ. J. Inorg. Chem. (Engl. Transl.)*
[g] — *Comb. Expl. Shpck Waves (Engl. Transl.)*